CORRELATING SELF-CONSOLIDATING CONCRETE MIXTURE COMPOSITION TO ITS RHEOLOGICAL PROPERTIES

CORRELATING SELF-CONSOLIDATING CONCRETE MIXTURE COMPOSITION TO ITS RHEOLOGICAL PROPERTIES

By
JOUD ODEH, B.Sc.

Faculty of Engineering
Department of Civil Engineering

A Thesis
Submitted to the School of Graduate studies In Partial Fulfillment of the requirements
for the Degree of
Master of Applied Science

McMaster University

MASTER OF APPLIED SCIENCE (2018) McMaster University

(Department of Civil Engineering) Hamilton, Ontario

TITLE: Correlating Self-Consolidating Concrete mixture composition to its rheological properties

AUTHOR: Joud Odeh
B.Sc. (Civil Engineering)
Balamand University, Lebanon

SUPERVISOR: Professor Samir E. Chidiac, PhD PEng FCSCE

NUMBER OF PAGES: viii, 115

Abstract

Self-Consolidating concrete (SCC), a highly flowable concrete, is gaining wide acceptance in the concrete industries due to a higher productivity, lower energy consumption, improved working environment, and increase quality. SCC is susceptible to segregation and therefore a balance between flow-ability and stability is required. The absence of a comprehensive SCC mixture composition design guidelines merits investigating the effects of SCC mixture variables on the properties affecting its performance, namely flow and stability.

An experimental and analytical study were carried out to study the influence of 5 design variables, namely water to binder ratio (w/b), percent addition of silica fume (SF), percent addition of Ground Granulated Blast Furnace Slag (GGBFS), bulk volume of coarse aggregates, and binder content, on the workability and rheology of SCC. Workability measurements, specifically the slump flow, T_{50}, L-Box and segregation column, and rheological properties, namely plastic viscosity, yield stress, and thixotropy were measured to evaluate SCC's performance. A revised modified Bingham model was proposed to adequately account for the linear and non-linear responses of the concrete flow. It postulates that the flow is divided into a linear and non-linear part. The revised model is found to provide more consistent and precise estimates of the rheological properties. Using regression analyses, yield stress and plastic viscosity models that account for the statistically significant variables were derived from experimental test data. Yield stress is found to depend on the bulk volume fraction of the coarse aggregate, Silica Fume content, High Range Water Reducing Agent (HRWRA), and Viscosity Modifying Agent (VMA), and plastic viscosity on w/b, HRWRA, and Average Paste Thickness (APT).

Acknowledgements

First and foremost, I cannot express enough gratitude to my supervisor, Dr. Samir Chidiac for his continuous encouragement, guidance, and patience throughout my time as his student.

I also would like to thank the Natural Sciences and Engineering Research Council of Canada and McMaster University for the financial support, and Lafarge Canada and BASF for supplying the material needed to carry out the experimental part of this research.

My completion of this project could not have been achieved without the unwavering assistance and support of my colleagues Mehdi Shafikhani, Saeed Moharrami, Michael Meier, and of course staff at the Applied Dynamics Laboratory, particularly Kent Wheeler and Paul Heerema. Their co-operation is very much appreciated.

Finally, and above all, to my caring, loving and supportive family: my deepest gratitude.

Publication List

This thesis consists of the following paper:

Chidiac, S.E., Odeh, J., and Shafikhani, M. Correlating Self-Consolidating Concrete mix design to its rheological properties. To be submitted June 2018.

Co-Authorship

This thesis has been prepared in accordance with the regulations for a 'Sandwich' thesis format or as a compilation of papers stipulated by the Faculty of Graduate Studies at McMaster University and has been co-authored.

Chapter 2: Correlating Self-Consolidating Concrete mix design to its rheological properties.
by: S.E. Chidiac, J. Odeh and Shakikhani, M.
The experimental program was developed by the three authors. The experiments were conducted by J. Odeh and M. Shafikhani and the data analyses were carried out by J. Odeh directed by Dr. S.E. Chidiac. Chapter 2 was written by J. Odeh and edited by Dr. S.E. Chidiac.

Table of Contents

List of Figures

List of Tables

1 Thesis Summary

1.1 Introduction

Sustainable development and durable structures are becoming standard requirements for the construction industry. These requirements have evolved from the observed ecological and environmental changes mostly caused by man's past practices including those of the construction industry. Societal drive has been to reduce the use of energy and raw materials by reducing, reusing and recycling. For concrete, sustainability requirements also mandate an increase in service life and a decrease in the occurrences of premature failure; both are achievable by controlling the quality and improving the durability. Self-Consolidating Concrete (SCC), originally developed in the 80's to address Japan's shortage of skilled labour, has remedied some of the traditional concrete shortcomings. SCC, a highly workable and structurally stable concrete, self-consolidates under its own weight and self-fills the formwork without segregation. The removal of workers from placing and consolidating fresh concrete significantly improves its quality control provided it possesses the proper rheological properties. Therefore, the measurement and control of SCC's rheological properties are paramount to the quality and properties of concrete.

1.2 Impetus and Objective of Research

Standardized ASTM test methods such as the slump flow, T_{50}, L-Box, and segregation column, are empirical tests used in the concrete industries to measure workability. However, they do not provide a fundamental insight into the concrete behaviour in its fresh state. Having the tools to quantify the rheological properties based on the composition is a pivotal step to control the quality and optimize the mixture composition of SCC. The findings will lead to a more sustainable concrete.

This study aims to investigate the correlation between SCC mixture composition and its rheological properties. The thesis, a sandwich format, includes two chapters. The aim, motivation, and scope of the study are first presented. Subsequently, chapter 1 presents a review of a) SCC chronological development including design methodologies and guidelines, b) theoretical background governing the flow of fresh

concrete including the corresponding material models and rheological properties, c) test methods for evaluating the performance and properties of SCC, d) postulated relationship between SCC mixture and the rheological properties reported in the literature, and e) proposed models in the literature to characterize the rheological properties of concrete. Lastly, a brief on the experimental and analytical work performed and corresponding findings are presented. Chapter 2 presents in detail the experimental program, experimental results, analyses carried out and findings.

1.3 Background

1.3.1 Self-Consolidating Concrete

Self-Consolidating concrete was introduced by the Japanese in the late 1980's to address the shortage of skilled labour (Okamura & Ouchi, 2003). Since the beginning of 1983, poor construction quality was a major concern in Japan due to the reduced number of skilled labourers. The concepts of concrete with workable properties that can flow and consolidate under its own self-weight without any need for mechanical vibration and compaction seemed to provide the solution to the problem. To achieve these properties, chemical and mineral admixtures became key ingredients to produce high workable and stable concrete mixtures. The advantages listed below and wide applications of SCC were quickly realized by many countries and concrete associations (American Concrete Institute, 2007):

- Superior strength and durability
- Minimize voids in highly reinforced areas
- Flow easily into complex forms
- Reduce labor and equipment cost
- Faster placement without vibration or mechanical consolidation
- Reduce the need for skilled labor
- Reduce noise on the job site.

1.3.2 Design and Proportioning of SCC mixtures

Owing to its high flowability, SCC is more susceptible to particles separation, referred to as segregation, compared to normal slump concrete. As such, SCC mixture

composition and proportioning are crucial to controlling its flow and stability. Moreover, the addition of chemical and mineral admixtures to the composition has rendered concrete mixture design guidelines (Cement Association of Canada, 2002) obsolete as these design guidelines do not account for the admixtures required for SCC. A typical SCC mixture composition and corresponding parts are shown in Figure 1.1.

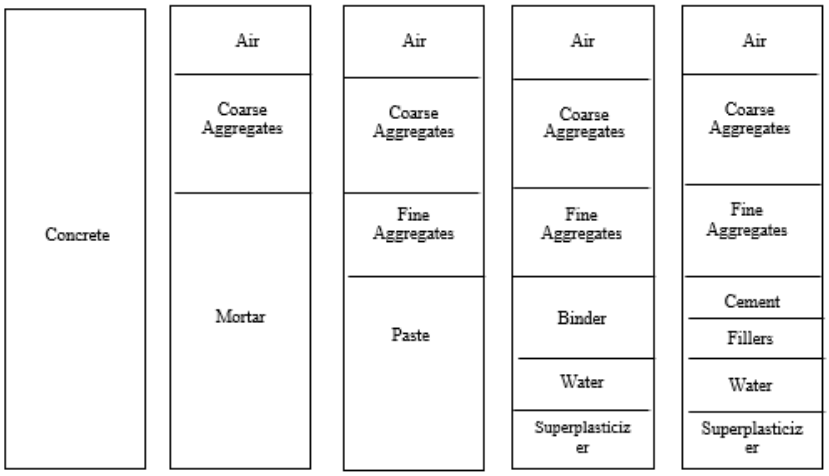

Figure 1.1: Schemetic SCC composition

Several methods have been proposed to design SCC mixes. The initial Japanese mix design followed the traditional concrete mixture proportioning while adjusting the ratio of the cementitious and superplasticizer content to meet the desired flow properties (Okamura & Ouchi, 2003). Subsequently, SCC mix design evolved by considering concrete as a solid aggregate phase suspended in a liquid paste or by optimizing the particles distribution based on packing considerations (Wu & An, 2013).

The first SCC mix design procedure was developed by Ozawa and Okamura (1995). They proposed a simple design method for SCC in which the coarse aggregates are set to 50% of the solid volume and the mortar volume to 40% to quantify the amount of fine aggregates. The water to binder (cement and supplementary cementitious materials) (w/b) ratio and superplasticizer dosages are then obtained through an iterative process by running slump flow tests on the mortar to get to the desired self-compatibility. Accordingly, the first proposed design method is iterative and requires trial mixes to

obtain the optimal mixtures proportions. Following the same methodology, modifications to the design method were proposed by the American Concrete Institute (ACI) (American Concrete Institute, 2007):

1. Determine the slump flow based on performance requirements
2. Select coarse aggregate maximum nominal size and proportioning to fine aggregate
3. Estimate binder and water content
4. Calculate the volume of paste and mortar
5. Select chemical admixtures
6. Mix a trial SCC batch
7. Test the fresh properties of trial SCC batch (Slump Flow, J-Ring, L-Box, Column Segregation Test)
8. Adjust the mixture proportion of SCC batch and continue the iterative process until the desired performance properties are achieved.

ACI's guidelines included design tables to assist the user with the design of SCC. Prior to proportioning SCC mixtures, an initial estimate of the slump flow is established based on the required application as shown in Table 1.1.

Table 1.1: Slump flow targets based on the design specifications (Daczko & Constantiner, 2001)

		Slump flow	
Design specifications		<550 mm	550 to 650 mm
Reinforcement level	Low		
	Medium	x	
	High	x	
Element shape intricacy	Low		
	Medium	x	
	High	x	x
Element depth	Low		
	Medium		
	High		
Surface finish importance	Low		
	Medium	x	
	High	x	x
Element length	Low		
	Medium	x	
	High	x	x
Wall thickness	Low	x	
	Medium	x	
	High		
Coarse aggregate content	Low		
	Medium		
	High		
Placement energy	Low	x	x
	Medium	x	
	High		

Selection of coarse aggregates is based on economics and is not considered a crucial step in designing and proportioning traditional concrete mixtures. However, with SCC's high flowability and its prone to segregation, proportioning coarse aggregates becomes a critical step in designing SCC mixtures, as their properties (the maximum aggregate size and volume) have a great influence on the stability, filling ability and passing ability

of SCC (ACI, 2007). It was recommended by ACI (2007), that an absolute volume range of 0.28 to 0.32 with a 12 mm nominal maximum size as a suitable range for SCC mixtures. Nonetheless, factors such as the clearance between the reinforcing bars, texture and the gradation of the coarse aggregates also influence the type of aggregates selected (ACI, 2007).

Unlike traditional concrete, the compressive strength becomes a less influencing factor when selecting the cementitious powder and water content for SCC mixtures (ACI, 2007). Instead, the cementitious paste composition should be selected to be able to support the aggregates. Typically in SCC production, materials such as silica fume, viscosity modifying agents (VMA) and increased fine aggregate content enrich the paste matrix by enhancing the particle size distribution of the particles. However, over-incorporating these materials in SCC mixtures can sacrifice SCC's filling and passing ability, and therefore a balance between stability and flow-ability should be maintained. The filling ability of SCC is controlled by the cementitious paste content. In this context, ACI (2007) has put forward guidelines relating the workability of SCC, namely the slump flow measurements, to the binder content of SCC as shown in Table 1.2.

Another important SCC mix design parameter is the water to binder ratio. Typically, this parameter is relatively lower than traditional concrete due to incorporating dispersing chemical admixtures i.e. high range water reducing agents (HRWRA). These types of admixture lead to increased strength by reducing the water to binder ratio and flow by dispersing the cement particles. Okamura and Ouchi (2003) originally proposed a water to binder ratio of 0.35.

Table 1.2: Suggested powder content for SCC (ACI, 2007)

	Slump flow (mm)		
	<550	550 to 600	>650
Binder content, (kg/m^3)	355 to 385	385 to 445	458+

The American Concrete Institute (2007) has recommended target ranges of 34% and 40% for paste volume percentage and 60% to 70% for the mortar volume percentage. Table 1.3, shown below, summarizes the SCC material proportioning.

Table 1.3: Proportioning SCC mixtures design (ACI, 2007)

Absolute volume of coarse aggregate	28 to 32% (12 mm nominal max size)
Paste fraction (by volume)	34 to 40% (Total mixture volume)
Mortar fraction (by volume)	68 to 72% (Total mixture volume)
w/b	0.32 to 0.45
Cement (powder content)	386 to 475 kg/m^3 (lower with VMA)

In the process of SCC production, workability requirements must be met. In 2002, the first European guidelines, EFNARC, was published for SCC (EFNARC, 2002). For a mix to be considered SCC, it needs to meet the requirements for filling ability, passing ability and stability summarized in Table 1.4.

Table 1.4: Acceptance criteria for SCC (EFNARC, 2002)

Test Methods	Typical range of values	
	Minimum	Maximum
Slump Flow (mm) (EFNARC, 2002)	650	800
T_{50} Slump Flow (s) (EFNARC, 2002)	2	5
J-Ring (mm) (EFNARC, 2002)	0	10
V-Funnel (s) (EFNARC, 2002)	6	12
Time Increase, V-Funnel at T_{50} (s) (EFNARC, 2002)	0	3
L-Box H2/H1 (EFNARC, 2002)	0.8	1
U-Box (H2-H1) (mm) (EFNARC, 2002)	0	30
Fill Box (%) (EFNARC, 2002)	90	100
GTM Screen Stability Test (%) (EFNARC, 2002)	0	15
Orimet (s) (EFNARC, 2002)	0	5

Optimizing the particle size distribution (PSD) is important in the development of SCC mixtures since it determines the packing density of aggregates. A higher packing density of aggregates would typically require less amount of paste to fill the voids and any excess in the paste content would be available for lubrication. Owing to SCC fluid-like nature, investigating the packing density is crucial. In this regard, Su et al. (2001) and Su and Miao (2003) proposed a mix design method, referred as the Chinese method, based on establishing an optimal packing factor for the aggregates; i.e., ratio of the mass of the aggregates in the densely packed state to the mass of the aggregate in the loosely packed state to meet the requirements of SCC properties. Upon determining this factor, the amount of paste required to fill in the voids between the aggregate voids can be evaluated. Their mix design methodology is easy to carry out and the amount of cement paste used is lower when compared to the Japanese method, making it more economical. Meanwhile, to compensate for the low binder content, they increased the amount of fine

aggregates to ensure passing ability. Comparing it to the Japanese method, Su et al. (2001) suggested a maximum cement content of 424 kg/m^3 compared to 500 kg/m^3 and volume of sand to mortar of 54%-60% compared to 40% proposed by Okamura and Ouchi (2003). In 2014, Kwan and Huen concluded that increasing the packing density of aggregates by incorporating more fine aggregates (to fill in the voids between the aggregates) is not entirely favorable since its higher surface area increases the paste content demand and decreases workability. Recognizing that the packing density by itself is not sufficient to develop proper SCC mixtures, Li and Kwan (2013) suggested that the particle size distribution, which is known to influence both the packing density and surface area of the particles, should be incorporated in the mix design. Owing to the many complications faced in determining the PSD of particles, Li and Kwan (2013) found that both the water film thickness (WFT) and paste film thickness (PFT), indirectly linked to the PSD, are the key factors governing the deformability, flowability, and strength of concrete. In their development of WFT and PFT parameters, they considered the combined effects of packing density, excess paste and water ratios and solid surface area of particles.

Overall, these design methods provide insights into the requirements to generate SCC mixes. Owing to the complex flow behavior and requirements of SCC, dependency on the type of material available and to the many admixtures available on the market, the development of a universal mix design method for SCC has yet to be realized.

1.3.3 SCC workability tests

For traditional concrete, measuring the workability by means of the slump test (ASTM C1611/C1611M, 2014) had been used worldwide to control the quality of the concrete. For SCC, the workability requirements are extended to include passing ability, filling ability and stability. ASTM standard test methods have been developed to evaluate the workability of SCC as summarized in Table 1.5. A brief description of relevant tests for filling ability, passing ability, and static stability is given next.

Table 1.5: Workability standard test methods for SCC (ACI, 2007)

Test Method	Category	Characteristic	Measurement
Slump flow (ASTM C1611/C1611M, 2009)	Free flow	Filling ability	Flow distance
Visual stability index (VSI) (ASTM C1611/C1611M, 2009)	Static condition	Resistance to segregation	Visual stability of the mixture
T_{50} (ASTM C1611/C1611M, 2009)	Free flow	Filling ability	Rate of flow
J-ring (ASTM C1621/C1621M, 2009)	Confined flow	Passing ability	Flow rate
L-box (EFNARC, 2002)	Confined flow	Passing and filling ability	Flow rate and distance
Column segregation test (ASTM C1610/C1610M, 2010)	Confined flow	Resistance to segregation	Segregation of aggregates

1.3.3.1 Filling ability

Filling ability is the ability of a mixture to flow into all spaces in the formwork without any need for vibration. Standard test methods such as the slump flow (ASTM C1611/C1611M, 2009) and/or V-funnel (EFNARC, 2002) are often used to determine the filling ability of fresh concrete. For a flowable concrete, like SCC, the slump test is not applicable, instead the spread which is referred to as slump flow of SCC mixtures is measured (Chidiac et al., 2006). The test procedure is conducted in a similar way to the standard test, however, the average diameter of the concrete sample after the cone is lifted as shown in Figure 1.2, is measured rather than the drop of the concrete sample. While conducting the test, the flow time for the concrete to reach a certain diameter is also measured and recorded. T_{50} is often recorded. It represents the time that it takes the concrete flow to reach a diameter of 50 cm. There are several papers that have related T_{50} results to the mixture's plastic viscosity (Koehler & Fowler, 2009; Utsi et al., 2003).

The V-funnel test (Ozawa et al., 1995) shown in Figure 1.3 is another test that evaluates the filling ability of SCC mixtures. The V-funnel test is conducted by filling the funnel with concrete, followed by a 1-minute pause, opening the gate, and measuring the time for all the concrete to flow through the funnel. The V-funnel results, i.e. time, were found to correlate well with the mixture's plastic viscosity and yield stress for a homogeneous fluid with no sign of segregation (Khayat et al., 2004). As for mixtures exhibiting similar yield stress, this correlation was shown to be more related to the plastic viscosity. On the other hand, Koehler and Fowler (2009) have shown that the V-funnel tests do not provide well-defined results since the V-funnel seems to be affected by the rheology and segregation resistance, while T_{50} gives a better relative measurement of viscosity.

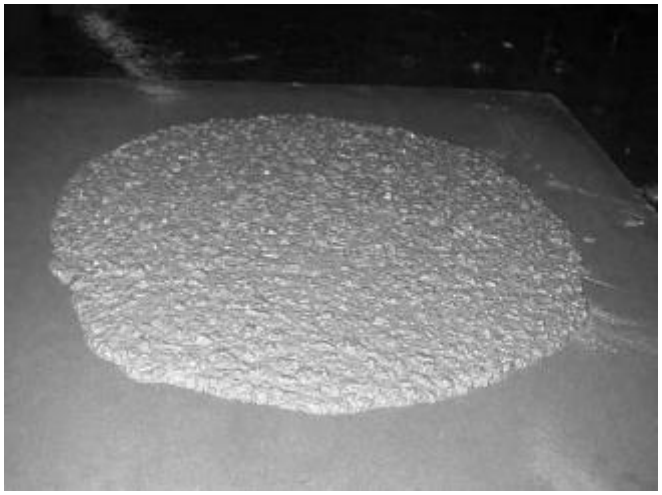

Figure 1.2: Slump flow (ASTM C1611/C1611M, 2014)

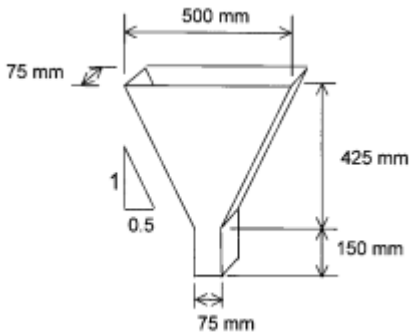

Figure 1.3: V-funnel apparatus (Khayat et al., 2004)

1.3.3.2 Passing ability

The passing ability is the ability of SCC to flow through tight openings under its own weight. It can be evaluated using standard test methods such as the J-Ring (ASTM C1621/C1621M, 2009), U-box or the L-box tests (EFNARC, 2002). The J-Ring, shown in Figure 1.4, is conducted the same way as the slump flow with the exception that the flow must pass through a ring of reinforcing bars fitted around the slump cone prior to starting the test. The U-box and L-box tests, shown in Figure 1.5 and Figure 1.6, respectively, are also used to evaluate the filling ability of SCC. The two tests are very similar in nature. In both tests, fresh concrete is filled from one compartment of the apparatus allowing it to sit for a predetermined time. A sliding gate, simulating reinforcement, is then opened, allowing the concrete to flow into the other compartment. The ratio of the concrete heights in the two compartments is subsequently determined. The closer the ratio is to 1 the higher the passing ability. With regard to correlating the empirical test results to more fundamental properties, Benaicha et al. (2013) found a correlation between the L-Box and U-Box results with the plastic viscosity of concrete.

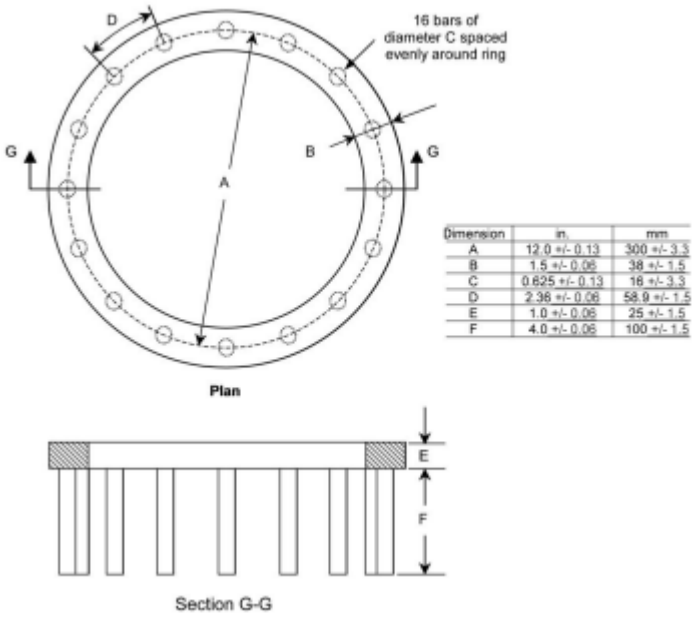

Dimension	in.	mm
A	12.0 +/- 0.13	300 +/- 3.3
B	1.5 +/- 0.06	38 +/- 1.5
C	0.625 +/- 0.13	16 +/- 3.3
D	2.36 +/- 0.06	58.9 +/- 1.5
E	1.0 +/- 0.06	25 +/- 1.5
F	4.0 +/- 0.06	100 +/- 1.5

Figure 1.4: Top and side view of the J-ring apparatus (ASTM C1621, 2009)

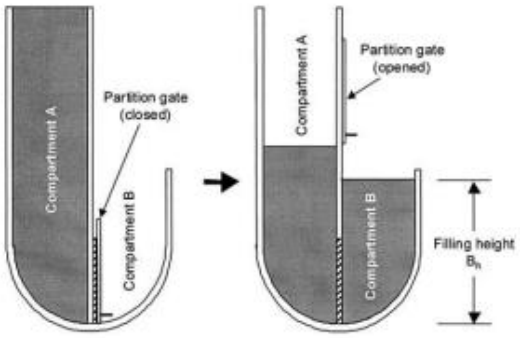

Figure 1.5: U-box test apparatus (Khayat et al., 2004)

Figure 1.6: L-box apparatus (Khayat et al., 2004).

1.3.3.3 Static Stability

Conducting the filling and passing ability tests successfully, requires a uniform concrete composition throughout the whole process. Owing to the flowable nature SCC, segregation under both static and dynamic conditions are more likely to occur. Dynamic stability depends on the concrete performance during the casting process and is related to the energy input; while static stability describes the concrete behaviour after the casting process until it sets in the formwork. To evaluate the static segregation potential of a mixture, various standard methods have been proposed, although these tests do not guarantee that a concrete is dynamically stable since the static segregation mechanism is different when the concrete flows. In practice, applications that require higher placing energy or from a great depth might cause the materials to separate. Unfortunately, there is no standard test method at the present to assess a mixture's resistance to dynamic segregation. Moreover, the mixture composition plays a crucial role in the mixture's

stability. Table 1.6 summarizes the influence of the mixture variable along with the applications performed on the site on the stability of concrete.

Table 1.6: Variables influencing stability (ACI, 2007)

Applications	Influence
Placement technique	High placement energy can cause materials to separate
Reinforcement level	If concrete falls or flows through reinforcement, separation of materials can occur
Element height	The depth of an element is proportional to its potential for aggregate settlement and bleed
Mixture variables	
Fluidity (slump flow) level	All other things being equal, as fluidity level increases, stability decreases
Viscosity level	As viscosity increases, stability increases

Tests methods such as the column segregation test, shown in Figure 1.7, measures the concrete's static segregation resistance (ASTM C1610, 2010). In this test, concrete is placed into a column without compaction. The device has three removable sections. After a period of 15 minutes, concrete's aggregates in the top and bottom layer are separated through a 4.75mm sieve. Upon completing the test, the segregation index is determined using Eq. 1.1 (ASTM C1610, 2010).

$$\mathrm{SI} = \begin{cases} \frac{2(\mathrm{CA_B}-\mathrm{CA_T})}{(\mathrm{CA_B}+\mathrm{CA_T})} * 100 & \text{if } \mathrm{CA_B} > \mathrm{CA_T} \\ 0 & \text{if } \mathrm{CA_B} < \mathrm{CA_T} \end{cases} \qquad \text{Equation 1.1}$$

where SI is the segregation index (%), CA_T denotes the mass of coarse aggregate in the top section of the column, and CA_B refers to the mass of coarse aggregate in the bottom section.

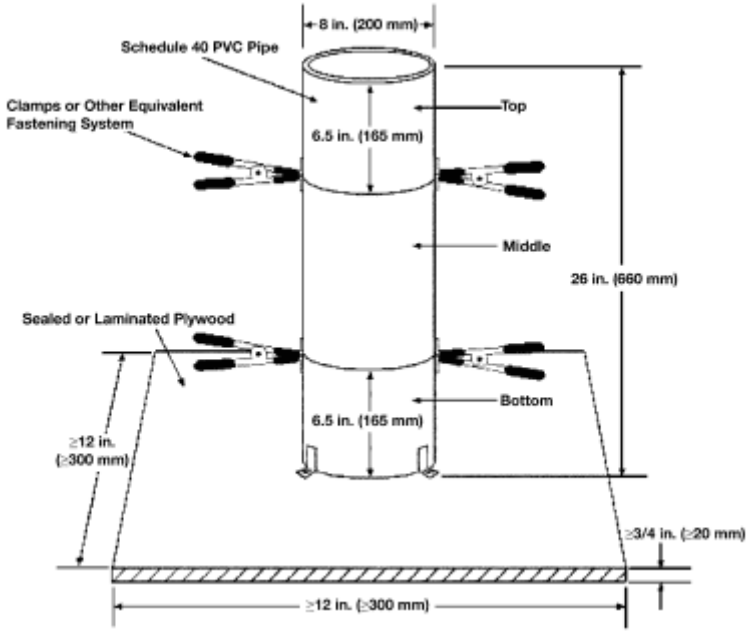

Figure 1.7: Static Segregation Column Test (ASTM C1610, 2010)

The penetration test, a standard test method shown in Figure 1.8 (ASTM C1712, 2014), is also used to assess the mixture's resistance to segregation but in a faster manner (Bui et al., 2002). The apparatus is used in conjunction with the slump flow test. A cylinder with a given weight is dropped into the fresh SCC sample in a slump cone after it has sat for 1 minute. The penetration depth is measured after a pre-given time limit, describing the degree of static segregation. In a segregated mix, the cylinder will penetrate deeper due to the lower amount of aggregates in the upper layer.

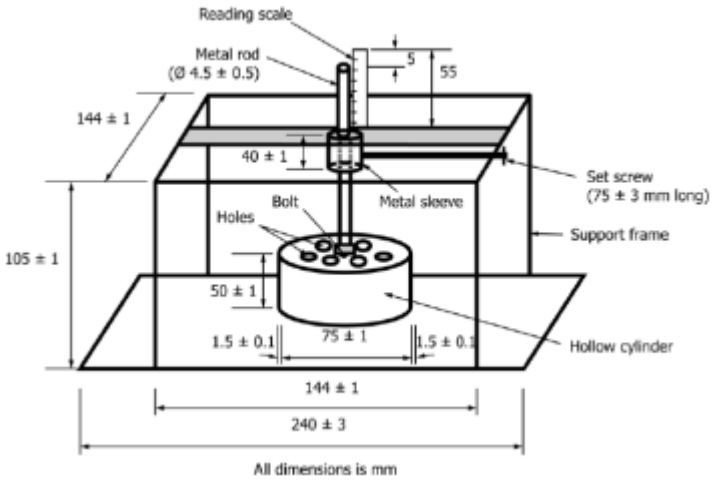

Figure 1.8: Static segregation penetration resistance test (ASTM C1712, 2014)

SCC stability can also be approximated using visual stability index (VSI) (ASTM C1611/C1611M, 2009). In this procedure, the concrete sample is visually inspected after performing the slump flow test to check any sign of segregation. Signs such as grouping of aggregates or bleeding water are indicators of segregation (Daczko, 2012). VSI is often reported as an integer between a minimum score of 0 to a maximum score of 3, with 3 has a higher risk of segregation. The results, however greatly depend on the experience of the test operator.

1.3.4 Rheological behavior of SCC

Characterizing the rheological behaviour of SCC in terms of the fresh rheological properties provides a quantification of its flow behaviour. Recognizing that the workability tests stated above only provide qualitative measures, this section provides a theoretical background on rheology, the rheological material models, and the tests developed to characterize the flow of SCC.

1.3.4.1 Rheology - a theoretical background

Rheology is defined as the science of flow and the material's resistance to deformation (Banfill, 1994). This flow behaviour can be characterized based on the interaction between shear stress and shear strain rate (Banfill, 1994). Many constitutive equations

have been proposed in the literature to study the rheology of various types of material. The simplest of all, the Newtonian model, is a straight line passing through the origin having a constant viscosity. It needs one measurement to sufficiently characterize the flow behaviour. Many materials, which exhibit more complex interactions, are referred to as non-Newtonian fluids. Power-law, or pseudoplastic, liquids obey Eq. 1.2

$$\tau = K\dot{\gamma}^n \qquad \text{Equation 1.2}$$

where K is the consistency index τ the shear stress, $\dot{\gamma}$ the shear strain rate and n the behaviour index, where a negative number represents shear- thinning and a positive index represents shear-thickening. A behaviour index of one leads to the Newtonian model (Rubio-Hernandez et al., 2013).

As for materials exhibiting yield stress, they behave as a rigid body at low stresses but flow as a viscous fluid once that yield stress is exceeded. For normal slump concrete, research has successfully used the Bingham model to simulate the flow behaviour of this material as represented by Eq. 1.3 (Tattersall & Banfill, 1983). Two intrinsic parameters are required to define the flow, i.e. plastic viscosity (μ) and yield stress (τ_o).

$$\tau = \tau_o + \mu\dot{\gamma} \qquad \text{Equation 1.3}$$

SCC, being a more fluid like material with higher amounts of fine particle, is found to exhibit for most mixes a nonlinear material response. Accordingly, SCC flow behaviour is described using a non-linear model such as the Herschel-Buckley model given in Eq. 1.4. It is an exponential relation that captures shear thinning when $n<1$, shear thickening when $n>1$, and degenerate to Bingham material model when n=1.

$$\tau = \tau_o + K\dot{\gamma}^n \qquad \text{Equation 1.4}$$

where K is the consistency factor ($Pa.s^n$).

Shear thickening was found to dominate in SCC mixtures (Feys et al., 2009). Therefore, it should be taken into account to avoid damaging equipment, especially at high shear

rates (Feys et al., 2008). One of the theories behind this behaviour phenomena is the formation of hydro-clusters, temporary assemblies of small particles (Feys et al., 2008). These particles have shown to pull together at a critical shear stress at which an increase in the viscosity is seen at increasing shear rates. Some authors have shown that the modified Bingham model, an extension of the Bingham model with a second-order term, is preferred to the Herschel–Bulkley as shown in Eq. 1.5 (Feys et al., 2007). From a mathematical point of view, they have revealed that the modified Bingham model parameter c/μ is linked to the flow index n in Herschel–Bulkley (Feys et al., 2007).

$$\tau = \tau_o + \mu\dot{\gamma} + c\dot{\gamma}^2 \qquad \text{Equation 1.5}$$

where "c" is the second order parameter (Pa.s^2). Figure 1.9 shows the most commonly used flow curves to describe the flow behaviour of fluids.

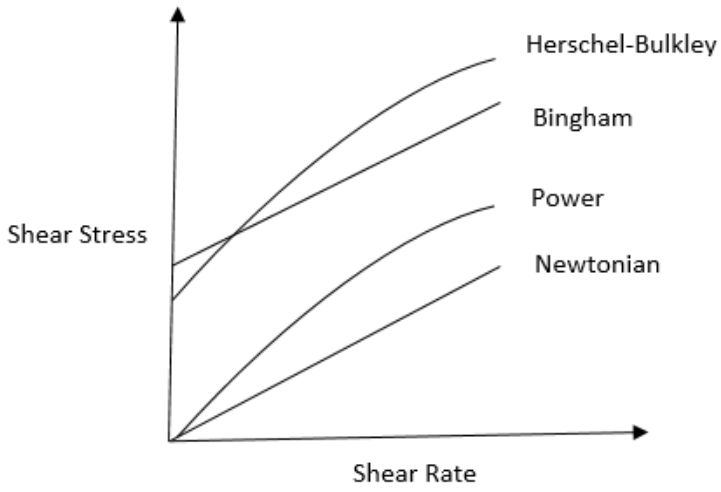

Figure 1.9: Rheological Models.

1.3.4.2 Rotational Rheometers

In order to study the flow behavior of concrete, rheometers have been developed to measure the relationship between rotational speed and torque; i.e. measuring the resistance of the sample at varying rotational speeds. While traditional rheometers have been shown to successfully characterize suspensions consisting of fine particles, concrete presents some challenges due to its heterogeneous composition, large

variations in particle size, ongoing chemical reactions and tendency to segregate. Nonetheless, many attempts have been made to adapt the traditional rheometers to concrete. One of the first attempts to develop a rheometer to characterize concrete as a Bingham fluid is the Tattersall Two Point Rheometer shown in Figure 1.10 (Tattersall, 1976). The apparatus was first developed using a food mixer while attaching a wattmeter. To further improve the instrument, a hydraulic drive motor was implemented to turn the impeller in the immersed concrete sample and the resistance due to the material; i.e. torque is measured.

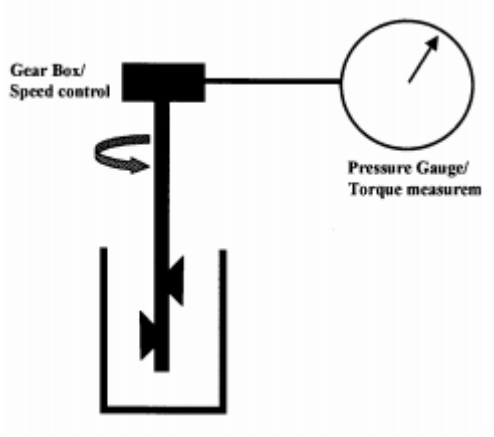

Figure 1.10: Tattersall two-point rheometer (Ferraris, 1999)

Since then, several rotational rheometers have been developed with different geometrical configurations, including coaxial cylinders (Couette) and parallel plate depicted in Figure 1.11. The main difference between these geometries lies in the shearing plane of the fresh concrete.

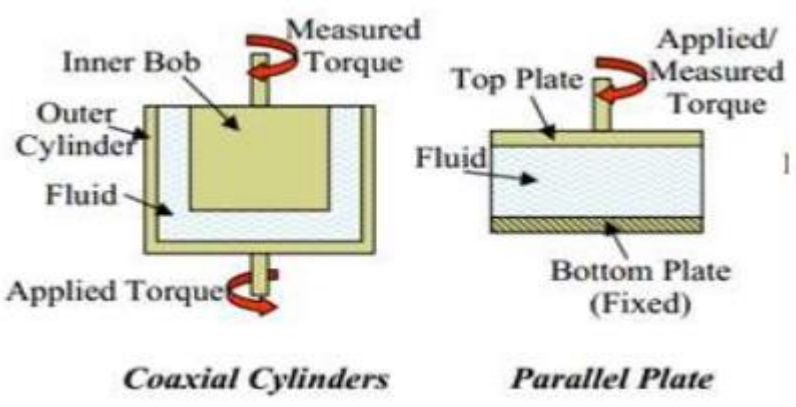

Figure 1.11: Types of rotational rheometers (Koehler & Fowler, 2004)

1.3.4.2.1 Coaxial Rheometer

The most common type of fluid rheometer is the coaxial cylinder. In this type of rheometer, the material is sheared between two cylinders with either the inner or the outer cylinder being stationary while the other is rotating. Since the material between the cylinders is the only part that is being sheared, the end effects at the top and bottom of both the cylinder and concrete are typically neglected (Koehler & Fowler, 2004). To be able to easily characterize the rheological properties, the material is assumed to have laminar flow, inertial effects are ignored, and the velocity of the material in contact with the surface is equal to the velocity of the rotating cylinder. These assumptions are often valid for rheometers with narrow gap cylinders (Koehler & Fowler, 2004). Adopting this type of rheometer to concrete would force the apparatus to have a wider gap. Moreover, for fluids with a yield stress, the range of shear stress imposed may not be sufficient to cause all the material to flow, and thus forming a plug flow as shown in Figure 1.12 (Koehler & Fowler, 2004). To achieve a linear flow gradient, Ferraris (1999) stated that the difference between the outer and inner radii should be at least five times the diameter of the maximum aggregate size and the ratio between the radii is held between 1.00 and 1.10.

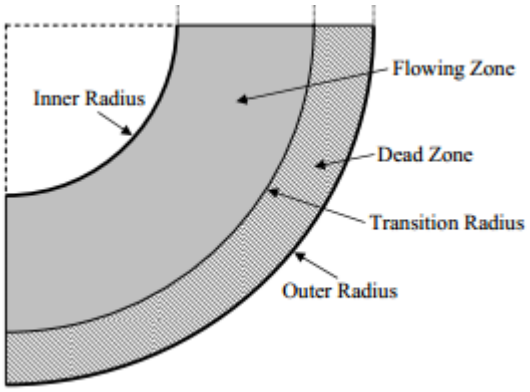

Figure 1.12: Flow of a Bingham Material in a Coaxial Cylinder Rheometer- Plug flow i.e. Dead zone (Koehler & Fowler, 2004)

BML viscometer, shown in Figure 1.13, is an updated version of the Tattersall two-point rheometer. This coaxial rheometer consists of two cylinders with an outer cylinder rotating at a predetermined angular velocity and an inner stationary cylinder. To avoid any slippage of the material, both the inner and outer cylinders are fitted with protruding vanes. Moreover, to avoid the end effects, the top portion of the inner cylinder measures the torque as the outer cylinder rotates (Wallevik, 2008).

Figure 1.13: BML viscometer (left) with an enlarged view of inner blades (right) (American Concrete Institute, 2008)

The RheoCAD shear rheometer shown in Figure 1.14 is an impeller type rheometer developed in France by CAD instruments. It consists of a ribbed cage mounted into a stationary bowl to prevent any material slippage, with an impeller mounted at the center.

Several bowl capacities are available along with several mobile geometries such as vane and double helical impellers. The torque measured represents the force required to rotate the mobile at the imposed rotational speed. RheoCAD shear rheometers are mainly intended to characterize building materials such as mortars, concrete, and SCC. However, one of the equipment's disadvantages experienced in this study, was with exceeding the maximum torque tolerated by RheoCAD 500, while testing SCC mixtures with a water to binder ratio of 0.32 with the double helical impeller. The problem was solved by implementing the vane impeller instead (both impellers are shown in Figure 1.15). In practice, vane tests are easy to perform, however at high shear rates and for a heterogeneous material like concrete with large coarse aggregates, the rotating vane have the tendency to push the large particles away from the center.

Because of the complexity of obtaining the rheological properties of SCC using mixer type rheometers, these types of rheometers are often assumed to follow Couette geometry i.e. a coaxial cylinder. In doing so, the material is considered to be sheared along a cylindrical surface defined by the vane height and diameter D, with the stress being uniform across the cylindrical sheared surface (Estellé et al., 2008)

Figure 1.14: RheoCAD 500 rheometer (CAD Instruments)

Figure 1.15: Double helical (left) and Vane impellers (right) (CAD Instruments)

1.3.4.2.2 Parallel Plate Rheometers

BTRHEOM, shown in Figure 1.16, is a parallel plate rheometer developed at the Laboratoire Central des Ponts et Chaussées (LCPC) in France by de Larrard et al. (1997). The rheometer consists of a cylindrical container with blades mounted on the lower and upper plates. The bottom plate is fixed while the upper plate rotates. The test is conducted by imposing different speeds to the top blade while recording the torque. All operations are inputted by the user prior to starting. The apparatus allows for measurements under vibration (ACI, 2008). However, this device is not designed for stiff materials. It is also costly and requires recalibration each time to account for the seal resistance (ACI, 2008).

Figure 1.16: BTRHEOM rheometer apparats (American Concrete Institute, 2008)

In practice, the use of rheometers is costly and impractical. In this regard, Chidiac at al. (2000) put forward a new approach to characterize the rheological properties of normal concrete based on workability measurements. In the development of their models, an automated slump rate machine (SLRM-I), shown in Figure 1.17, was developed to measure the slump, slump flow and rate of slump. Using continuum mechanics, they developed analytical models to predict the yield stress and plastic viscosity of fresh concrete given in Eqs. 1.6 and 1.7, respectively. Based on their experimental results using the BTRHEOM and the SLRM, a trend has been observed between the results of the two apparatuses revealing the ability of the SLRM to characterize the effects of the mixture composition on the rheological properties of SCC.

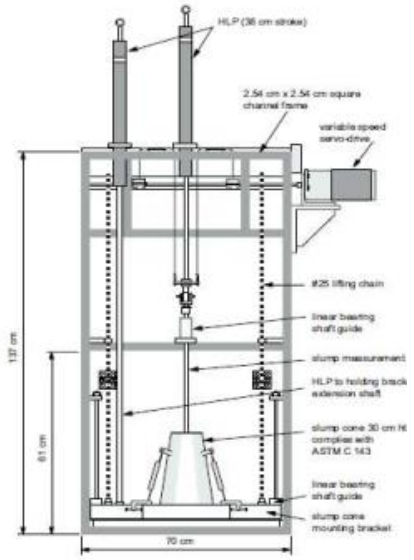

Figure 1.17: Slump Rate Machine 1st generation (Chidiac et al., 2000)

$$\tau o = \frac{4gV\rho}{\sqrt{3\pi}Sf^2} = 0.0703\left(\frac{\rho}{Sf^2}\right) \qquad \text{Equation 1.6}$$

$$\eta = \frac{\rho gHV}{150\pi SlSf^2}t_{slump} \qquad \text{Equation 1.7}$$

in which g is the gravitation constant (9.81 m/s^2), Sf the slump flow, Sl the slump, V the concrete volume, ρ the density of concrete and t_{slump} the slump time.

1.3.4.3 Thixotropy

Thixotropy is another important term in rheology. Barnes et al. (1989) described thixotropy as the "gradual decrease of the viscosity under shear stress followed by a gradual recovery of structure when the stress is removed". The process is time dependent and the viscosity is reversible. From a practical point of view, thixotropy can be seen in a concrete mixing truck. The different rheological behavior that concrete exhibits when at rest and flowing is due to thixotropy. Roussel (2006) stated that concrete is called a thixotropic material if it seems to flocculate quickly at rest and becomes more fluid while flowing.

1.3.4.3.1 Quantification of thixotropy

One of the approaches to quantify thixotropy is to perform the hysteresis loop test. During the rheometer test, the rotational velocity is stepwise increased from zero to a pre-determined maximum velocity then decreased back to zero. The corresponding torque is recorded. A schematic representing the up and down shear stress and shear strain rate is shown in Figure 1.18. When the material is sheared, the microstructure continuously breaks down as the rate increases. When the material is sheared at a decreasing rate, a gradual build-up occurs. One way to quantify thixotropy is by measuring the area enclosed in the hysteresis loop. This area provides a measure of the energy necessary to break down the initial structure to pass from the initial state to an equilibrium state (Erdem et al., 2009). Although the hysteresis is relatively simple, it greatly depends on the testing protocol and equipment.

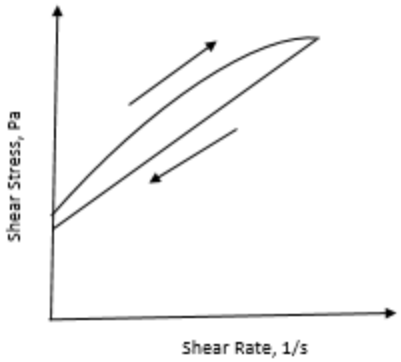

Figure 1.18: Thixotropy measurement - hysteresis loop

Thixotropy is reported to be influenced by the composition of SCC mixtures. Petkova and Samichkov (2007) suggest that an increase in thixotropy is attributed to the increase in the particle specific surface area in the paste matrix. Salem (2002) give a more in-depth explanation and propose that the pozzolanic reaction and the transformation of ettringite to monosulfate are responsible for the increase in thixotropy. Concrete with silica fume is shown to also be thixotropic as it exhibits a viscous behaviour at rest and tends to become more fluid once an external pressure is applied to it (Benaicha et al., 2015). Like silica fume, the VMA is also seen to increase the thixotropic behaviour due to its stabilizing nature which aids in rebuilding the structure (Phan et al., 2006). On the other hand, HRWRA works in an opposite fashion. Its implementation in concrete mixes reduces the flocculation between the cement particles which reduces thixotropy (Ur'ev et al., 1997).

1.3.5 Mineral and Chemical Admixtures

The composition and proportioning of SCC mixtures greatly affect the rheological properties of SCC. Like conventional concrete, SCC mix composition contains coarse, fine aggregates, water, chemical admixtures and mineral admixtures. However, in the design and production of SCC, achieving high workability and high resistance to segregation are key performance requirements. Towards achieving these requirements, incorporating more fine particles such as mineral admixtures and chemical admixtures

are the most crucial and distinct parameters required to attain SCC's flowability and stability.

1.3.5.1 Chemical Admixtures

1.3.5.1.1 High range water reducing agent (HRWRA)

HRWRA is typically employed in SCC mixtures to increase the flow of concrete by dispersion mechanism and more specifically by electrostatic repulsions and/or steric hindrance shown in Figure 1.19 (b) and (d) respectively (Uchikawa et al., 1997; Flatt et al., 2000). New studies have shown that steric forces, induced by the polymer chains adsorbing and a non- adsorbing side chains stretching out into the solution, are thought to be the stabilization mechanism responsible for keeping the solid particle apart (Flatt et al., 2000). Additional dispersion mechanisms of HRWRA, include: reducing the surface tension of the mixing water and decreasing the frictional resistance due to the lubrication properties produced by the low molecular weight polymers shown in Figure 1.19 (c) and (a) respectively (Piekarczyk, 2014).

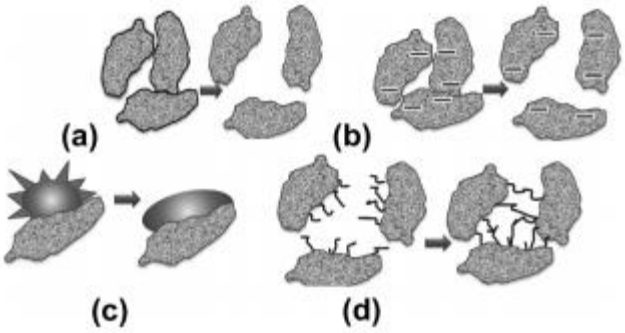

Figure 1.19: Types of dispersion actions: (a) lubricating properties of the polymers, (b) electrostatic repulsion due to negative charge, (c) decreasing of surface water tension, (c) steric repulsion by the adsorbing chains (Piekarczyk, 2014)

Owing to the above dispersion mechanisms, the yield stress is lowered without increasing the water to cement ratio. Several authors have studied the effect of HRWRA on yield stress by investigating the slump flow. Smeplass (1994) found that the use of

high water reducing agent mainly reduces the yield stress but has little impact on the plastic viscosity. Faroug et al. (1999) investigated the effect of naphthalene and melamine-based high range water reducers in concrete on the rheological properties. They found out that the effects of these two types of HRWRA are most pronounced at low w/c ratios, resulting in a decrease in both the yield stress and plastic viscosity. However, for mixes with w/c ratio greater than 0.4, the plastic viscosity is not affected; and the effect on the yield stress diminishes for mixes with w/c ratio of 0.5 (Faroug et al., 1999).

The current practice for adding HRWRA, also referred to as superplasticizer, is based on recommendations put forward by the manufacturer. It provides guidance on the amount of HRWRA to be added based on the cement content and the slump flow. It does not account for the total composition of the mixture. Excessive use of HRWRA leads to segregation and accordingly trial mixes are always required to study the effect of HRWRA dosages on the flow and stability of the SCC mixes. However, when all the cement particles are dispersed, also referred as the saturation point, adding more HRWRA does not result in an increase in the slump flow.

1.3.5.1.2 Air entraining agent (AEA)

AEA is used to increase the material resistance to freeze-thaw cycles. This admixture introduces microscopic bubbles that relieve some of the hydraulic pressure caused by expansion of water at freezing temperatures. AEA is also shown to improve workability. Chia and Zhang (2004) reported that AEA provides lubrication between the cement particles which causes a reduction in the plastic viscosity without causing any change in the yield stress. Similarly, Struble and Jiang (2004) came to the same finding but also found an increase in the yield stress. AEA is reported to reduce segregation and bleeding (Whiting, 1983).

1.3.5.1.3 Viscosity Modifying Agents (VMA)

VMA, a chemical admixture that is often used in SCC mixes, is added to increase the resistance to flow by increasing the viscosity. It is added to SCC mixes to reduce

segregation, bleeding and surface settlement by increasing the plastic viscosity. The reasoning behind its effectiveness stems from the strong Vander Waals attractive forces between the polymer chains that block the passage of free water and hence yield an increase in the mixture plastic viscosity (Benaicha et al., 2015).

Sonebi (2006) revealed that VMA results in high apparent viscosity at low shear rates due to the intertwining of VMA polymer chains. This behaviour is advantageous for concrete, since at low shear rate, a high viscosity prevents segregation while the relatively low viscosity at higher shear rates ensures deformability during mixing, pumping and placing. Similarly, El Barrak et al. (2009) showed that VMA impacts the static stability more than the dynamic stability.

1.3.5.2 Mineral Admixtures

Mineral admixtures, referred to material that possess pozzolanic properties, are also labelled supplementary cementitious materials (SCMs). Replacing a percentage of Portland cement with SCMs, such as Granulated Ground Blast Furnace Slag (GGBFS), fly ash, silica fume and limestone, are widely used to improve stability, strength, and durability of SCC. SCMs are mostly industrial by-products and hence they can reduce the cost and improve concrete sustainability. However, introducing a high volume of SCMs in SCC is limited due to the undesirable effects they have on the water demand which will negatively impact the strength for a constant HRWRA dosage (Elyamany et al., 2014).

1.3.5.2.1 Limestone

Limestone filler is regularly used as a mineral addition in SCC. Incorporating limestone as part of cement results in an economical and more environmentally friendly concrete since it reduces the cement content (Ghezal & Khayat, 2002). In terms of workability, these fillers are generally intended to enhance the particle size distribution of the binder skeleton and as a result, improve the packing density. By filling the spaces between the coarser particles, they can effectively enhance the mixture's cohesiveness and improve both mechanical and transport properties of the hardened material. These mineral admixtures reduce the amount of superplasticizer required to secure a given

deformability (Mehdipour & Khayat, 2016). Elyamany et al. (2014) emphasized that the amount of superplasticizer needed to secure a given property depends highly on the particle size distribution, particle shape and surface characteristics of the mineral admixtures.

1.3.5.2.2 Silica Fume

Silica fume, also known as condensed silica fume, is a very fine non-crystalline powder produced in electric furnaces as a by-product of silicon or silica-alloys. It is well known that silica fume has a high surface area and therefore, is very active in reacting with Calcium Hydroxide (CH) promoting the formation of calcium silicate hydrate (C-S-H) during the hydration process. This compound binds the cementitious matrix together, resulting in a compact and dense structure (Benaicha et al., 2015). Concrete mixes with silica fume blended as part of cement, result in a more viscous paste, as it significantly increases the surface area that must be wetted. Its effectiveness, in enhancing the viscosity, increases with the concentration of silica fume added. Benaicha et al. (2015) investigated the influence of using VMA and silica fume on the fresh properties of SCC mixes and found out that they influence the rheology (stability and filling capacity) in a very similar way. They both increase the plastic viscosity and the yield stress. Tattersal (1991) concluded that there is a threshold value after which silica fume causes an increase in both the yield stress and plastic viscosity. However, little change was observed for the yield stress below this threshold value. Nehdi et al. (1998) investigated the effect of two very fine fillers with a similar surface area, on the superplasticizer demand. Ground silica, with a surface area of 10,000 m^2/kg, didn't increase the superplasticizers demand as much as silica fume. Thus, they concluded that the high surface area is not the only parameter influencing the superplasticizer demand, but rather silica fume's strong affinity for multi-layer adsorption of superplasticizers molecules (Nehdi et al., 1998).

The addition of silica fume to concrete mixes increases the compressive strength. This is attributed to its high fineness and pozzolanic properties which increases the reactivity with the calcium hydroxide produced during cement hydration (Benaicha et al., 2015).

1.3.5.2.3 Granulated Ground Blast Furnace Slag (GGBFS)

Granulated ground blast furnace slag is a by-product obtained during the manufacture of pig iron in the blast furnace by combining earthy constituents of iron ore with limestone flux. GGBFS, another SCM, has a chemical composition very close to that of cement and its particle sizes are relatively constant. Khayat et al. (2008), explained the low HRWRA adsorption degree with grout made with 40% slag, due to the glassy morphology of slag particles. Boukendakdji et al. (2009) studied the effect of GGBFS on the workability of SCC mixes. For a constant water to binder (w/b) ratio and superplasticizer content, an increase in the slump flow was observed up to 20% slag content. However, at higher slag content, an increase in segregation was observed. A similar observation was noted with the flow time T_{50}. Beyond 15% percent addition, the flow time starts to increase with observed segregation. Sethy et al. (2016) studied the effect of industrial slag on the rheological properties of SCC using the ICAR rheometer. Plastic viscosity and T_{50} were both shown to decrease with increasing the slag addition, unlike the slump flow.

1.3.6 Rheological models

From a theoretical perspective, concrete can be referred to as concentrated suspensions. Accordingly, a brief review of some the rheological models developed for diluted, semi concentrated and concentrated suspensions and their relevance to concrete is presented. Relevant parameters are highlighted along with the assumptions made to develop these rheological models.

1.3.6.1 Suspensions

Suspensions refer to particles that are suspended throughout the bulk of a medium. Einstein (1906) reported that for diluted suspensions, i.e., with low particle concentration $\varphi < 10\%$, the interaction between particles can be neglected and that the viscosity of the suspensions becomes primarily a function of the volume fraction of the particles. Einstein model is given by

$$\eta = \eta_s(1 + [\eta]\varphi) \qquad \text{Equation 1.8}$$

where φ is the volume fraction of solids (%), η the viscosity of the suspension (Pa·s), η_s the viscosity of suspending fluid (Pa·s) and [η] the intrinsic viscosity. According to

Einstein, the intrinsic viscosity, given by Eq. 1.9, takes a value of 2.5 for infinitely diluted suspensions of spherical particles.

$$[\eta] = \lim_{\varphi \to 0} \frac{\eta - \eta_0}{\eta_0 \varphi} \quad \text{Equation 1.9}$$

where η_0 is the viscosity of the solvent.

Mooney (1950) extended Einstein's model to account for semi-concentrated suspensions. Upon approaching his objective, he realized that the viscosity follows an exponential function, which also depends on the volume fraction. To account for the increased particle interactions occurring at higher concentration, he introduced the "crowding factor" (k) which is based on the packing densities of the particles, where

$$\eta = \eta_s \exp\left(\frac{2.5\varphi}{1 - k\varphi}\right) \quad \text{Equation 1.10}$$

Recognizing that the volume fraction isn't enough to describe the flow of concentrated suspensions, Krieger-Dougherty (1959) incorporated the maximum packing density (φ_m) as shown in Eq. 1.11.

$$\eta = \eta_s \left(1 - \frac{\varphi}{\varphi_m}\right)^{-[\eta]\varphi_m} \quad \text{Equation 1.11}$$

Toutou and Roussel (2006) attempted to extend these models to cement paste, and noted that the Krieger-Dougherty (1959) relation is suitable to describe the viscosity of cement paste but not for the yield stress.

1.3.6.2 Concrete

Unlike liquid suspensions and cement paste, characterizing concrete's behaviour from its components is much more challenging because of the complex composition of this material. Nonetheless, several empirical or semi-empirical approaches have been proposed to capture the flow of concrete.

The compressible packing model (CPM), developed by de Larrard (1999), is considered a significant contribution to characterizing the rheological properties of concrete from its composition. CPM uses the packing density to characterize the granular skeleton of

the mixture while accounting for the packing process, distribution and shape of grains and the degree of agglomeration (de Larrard, 1999). The final model isn't only related to the volume fraction, but also to the particle properties and characteristics, including the shape, amount, aspect ratio and surface texture, which is reflected collectively by the maximum packing density (Chang & Powell, 1994). Taking the above arguments into account, Ferraris and de Larrard (1998) found that the relative concentration of solids $\frac{\varphi}{\varphi_m}$ has a significant effect on the viscosity as shown in the empirical Eq. 1.12.

$$\eta = \eta_s exp\left[26.75\left(\frac{\varphi}{\varphi_m} - 0.7448\right)\right] \quad \text{Equation 1.12}$$

where η and η_s are the viscosities of concrete and suspending fluid, respectively, φ and φ_m are the particle volume concentration and the maximum packing factor of particles, respectively.

For the yield stress, Ferraris and de Larrard (1998) came to the conclusion that the yield stress is more related to the linear combination of all the components' volume fraction versus the close-packing ratios. The following equations were developed for concrete with and without HRWRA respectively.

For mixtures without HRWRA,

$$\tau_o = \exp(2.537 + 0.540K_g + 0.854K_s + 1.134K_c) \quad \text{Equation 1.13}$$

For mixture with 1% HRWRA,

$$\tau_o = \exp(2.537 + 0.540K_g + 0.854K_s + 0.224K_c) \quad \text{Equation 1.14}$$

In this equation, τ_o is the yield stress (Pa) of concrete, and the indices *g*, *s* and *c* refer to gravel, sand, and cement, respectively. The compaction index K_x is calculated from $(1-\varphi_x)/\varphi_{x,max}$.

Some studies consider fresh concrete as a two-phase material with solid aggregate particles dispersed in a cement paste matrix. Kurokawa et al. (1996) developed a concrete rheological model based on the two-phase theory approach. They stated that the yield stress of fresh concrete could be expressed by taking the sum of the mortar

yield stress and the contribution of the friction caused by the coarse aggregates, while the viscosity could be expressed by taking the sum of the mortar viscosity, volume fraction and the frictions of the coarse aggregates

Kennedy (1940) stated that the rheology of concrete doesn't only depend on the rheology of paste, but also on the amount of excess paste filling the voids between the aggregates. The excess paste theory states that any addition to the compacted paste, which fills in between the aggregates as shown in Figure 1.20, will be used as excess paste for lubrication. Oh et al. (1999) found that the thickness of the excess paste is crucial in dictating concrete's rheology and that both the plastic viscosity and yield stress decreases when the thickness of the related excess paste (Γ) increases. The related excess paste thickness is defined as the excess paste thickness divided by the average diameter of aggregate. The regression models shown by Eqs. 1.15 and 1.16 reveal the independence of the mixture composition.

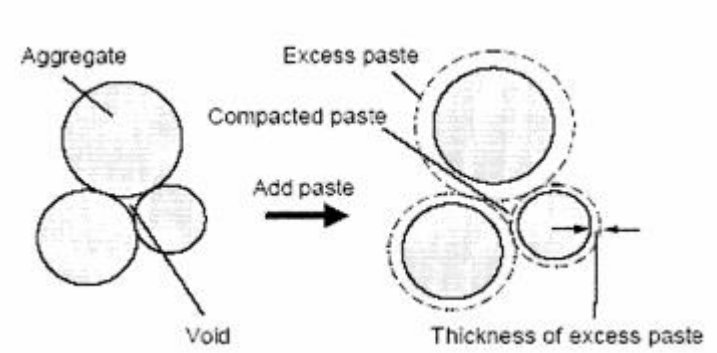

Figure 1.20: Excess paste theory (Oh et al., 1999)

$$\tau = 0.0525\Gamma^{-2.22} + 1 \qquad \text{Equation 1.15}$$

$$\eta = 0.0705\Gamma^{-1.69} + 1 \qquad \text{Equation 1.16}$$

The excess paste thickness theory can also be used to explain the packing of aggregates. An increase in the amount of excess paste is generally generated by decreasing the volume of voids between the aggregates, achieved from higher packing density. Smith and Collis (2001) stated that an optimum gradation has the lowest possible surface area and void content per unit weight.

Recognising that most of the models proposed in the literature are empirical and semi-empirical, Chidiac and Mahmoodzadeh (2009) employed the cell method, geometric model, to predict the rheological properties of mortar and fresh concrete. The cell method has been widely employed in various scientific fields to characterize the plastic viscosity of concentrated suspensions. It postulates that at a microscopic level, the representative volume of a suspension consists of a solid particle surrounded by a viscous fluid where interactions are taking place as shown in Figure 1.21. Solving such problem requires certain assumptions to the cell size and boundary conditions to come up with a suitable cell description. The relative viscosity (η_r) is then computed by applying energy conservation principles.

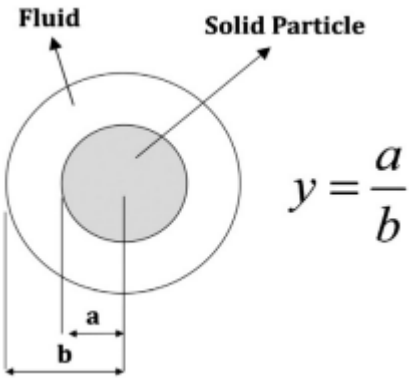

Figure 1.21: Definition of a cell (Mahmoodzadeh & Chidiac, 2013)

Chidiac and Mahmoodzadeh (2009) successfully extended the cell description proposed by Frankel and Acrivos (1967) due its ability to capture the maximum packing density, and Zholkovskiy et al (2006) by eliminating the effects of the cell boundary conditions, and accounting for the lubrication due to cement paste (K) as shown in Eqs. 1.17 to 1.21.

$$y(\varphi) = \left(\frac{\varphi}{\varphi_{max}}\right)^{\frac{1}{3}}(1 - K) \quad \text{Equation 1.17}$$

$$K = 0.006x\ \frac{Cement}{Water}\ \text{Without HRWRA} \quad \text{Equation 1.18}$$

$$K = 3.8x\frac{HRWRA}{Cement}x\frac{Water}{Cement+Fine\ Sand+Sand}\ \text{With HRWRA} \quad \text{Equation 1.19}$$

$$\lambda = y^3\frac{4(1-y^7)}{4(1+y^{10})-25y^3(1+y^4)+42y^5}\ \text{Using Zholkovskiy et al (2006)} \quad \text{Equation 1.20}$$

$\eta_r \cong \eta_i \lambda$ Equation 1.21

where η_i is the intrinsic plastic viscosity, and *K* a function of the concrete mixture.

Since both the plastic viscosity and yield stress are controlled by the excessive paste thickness, Chidiac and Mahmoodzadeh (2009) extended the plastic viscosity formulation by analogy to the yield stress (τ_0) as shown in the equations below.

$\tau_0 \cong \tau_i \lambda$ Equation 1.22

$y(\varphi) = \left(\frac{\varphi}{\varphi_{max}}\right)^{\frac{1}{3}} (1 - C_y \frac{m_G}{m_w})$ Equation 1.23

where τ_i is the intrinsic yield stress, m_G the mass of the aggregate, and C_y a fitting parameter.

1.4 Summary of Paper

Correlating SCC mix design to the rheological properties of Self-Consolidating Concrete (SCC) (to be submitted)

This paper reports on the experimental and analytical studies carried to correlate between SCC mix composition and the rheological properties. Using a fractional factorial statistical design of experiments with the following variables: water to binder ratio (w/b), percent addition of silica fume (SF), percent addition of GGBFS, bulk volume of coarse aggregates and binder content, a total of 16 SCC mixes were developed. Both the workability and rheological properties of the mixes were measured and correlated to the mixture composition. Using regression analyses, the relationship between SCC mix composition and rheological properties were derived.

Shear stress and shear strain rate curves were derived from the torque-rotational velocity measurements by assuming that the concrete flow is laminar and obeys Couette's flow model. By assuming that the shear stress and shear strain rate follow the modified Bingham model, the rheological properties of SCC were obtained. A two-step approach was developed for the modified Bingham model to capture the non-linear response of SCC which is found to provide a better estimate of the flow as well as the rheological properties of SCC.

1.5 Concluding remarks

The experimental and analytical investigations were carried out to correlate SCC mixture composition with workability and rheological properties. The workability test results of SCC mixtures revealed the followings:

1. The average paste thickness (APT) is a crucial parameter to consider since it takes into account the combined aggregate gradation, by incorporating the maximum packing density, as well as the aggregate proportioning. It is also shown that it was inversely related to the volume of fine aggregates.
2. HRWRA demand is shown to be influenced by the APT, silica fume, and GGBFS addition. Increasing the APT decreases the HRWRA demand for mixtures with the same binder composition.
3. The addition of SF and GGBFS are shown to increase/decrease the HRWRA demand respectively.
4. The w/b ratio, APT and the HRWRA affect the flow time, $T_{50.}$
5. For a given range of APT, the addition of silica fume is shown to increase the mixture's resistance to flow.
6. The flow time, $T_{50,}$ corresponding to the high water to binder ratio mixtures are all below the minimum target flow time indicating stability concerns.
7. Incorporating silica fume results in decreasing the passing ability for the low w/b ratio mixtures.
8. Results from the slump flow and the L-Box of the low w/b mixtures correlate well.
9. All the high w/b mixtures revealed no signs of segregation, proving VMA's effectiveness in maintaining the mixtures' resistance to static segregation. However, their effectiveness under dynamic conditions is yet uncertain.
10. The workability measurements (T_{50} and slump flow) are shown to correlate with the rheological properties of SCC (plastic viscosity and yield stress) respectively with a higher coefficient of determination between T_{50} and the plastic viscosity.

The observed relationship between rheological properties are SCC mixtures are as follow:

1. The plastic viscosity and thixotropy are found to correlate. They are shown to be mainly affected by the water to binder ratio (w/b), the average paste thickness, and the amount of HRWRA added.
2. The yield stress is impacted by the silica fume addition and the amount of coarse aggregate (bulk volume of coarse aggregates and the ratio of coarse to fine aggregate ratio, by mass, for the low and high w/b mixtures respectively).
3. From the experimental program conducted, set of rules were derived to relate the mix composition and the chemical admixtures used to achieve a certain range of the rheological properties.
4. Anti-thixotropic behaviour is found to be exhibited by the majority of the w/b = 0.4 mixtures raising stability concerns under high shearing regimes. Moreover, these mixtures might be problematic in cast in place applications since higher lateral pressure might be exerted on the formwork.
5. Statistical models developed to relate the rheological properties to the mixture design composition revealed that the plastic viscosity and yield stress can be estimated with 95% confidence from w/b, HRWRA, and APT and from volume fraction of the coarse aggregate, Silica Fume content, HRWRA and VMA respectively.
6. Validation of the models shows that the models are not complete as the standard errors are found larger than the experimentally measured ones, indicating other missing parameters.

Analyses of the data obtained using the concrete rheometer revealed the followings:

1. A concrete rheometer, although providing fundamental data, is found to be sensitive to the type of vane, mix design, loading and unloading procedure.
2. Use of concrete rheometer requires expertise in rheology and concrete. Moreover, the use of concrete rheometer is found to be physically demanding.
3. The thickness of the plug is found to vary depending on the w/b ratio, or specifically on the plastic viscosity.
4. A revised procedure for the Modified-Bingham model, to account for the linear and non-linear response separately, provides a better estimate of the plastic viscosity and yield stress.

1.6 Suggestions for Future Work

1. The effect of HRWRA and VMA on thixotropy needs to be further investigated.
2. Revised modified Bingham model needs to be evaluated using a wider range of SCC mixes.
3. Simple test methods to estimate the rheological properties such as the slump flow and T_{50} merit further investigation.
4. Develop an SCC mix design based on specified rheological properties.

References

American Concrete Institute. (2007). ACI 237R-07 (Self-Consolidating Concrete).

American Concrete Institute. (2008). ACI 238.1R-08 (Report on Measurements of Workability and Rheology of Fresh Concrete).

ASTM C1610. (2010). Standard Test Method for Static Segregation of Self-Consolidating Concrete Using Column Technique.

ASTM C1611/C1611M. (2014). Standard Test Method for Slump Flow of Self-Consolidating Concrete.

ASTM C1712. (2014). Standard Test Method for Rapid Assessment of Static Segregation Resistance of Self-Consolidating Concrete Using Penetration Test

Banfill, P. (1994). Rheological methods for assessing the flow properties of mortar and related materials. *Construction and Building Materials*, 43-50.

Barnes, H. A., Hutton, J. F., & Walters, K. (1989). *An introduction to rheology* (Vol. 3). Elsevier.

Benaicha, M., Jalbaud, O., Alaoui Hafidi, A., & Burtschell, Y. (2013). Rheological Characterization of Self-Compacting Concrete: V-Funnel and Horizontal Plexiglas Channel. *International Journal of Engineering Science and Innovative Technology*, 416-425.

Benaicha, M., Roguiez, X., Jalbaud, O., Burtschell, Y., & Alaoui, A. H. (2015). Influence of silica fume and viscosity modifying agent on the mechanical and rheological behavior of self compacting concrete. *Construction and Building Materials*, *84*, 103-110.

Boukendakdji, O., Kenai, S., Kadri, E. H., & Rouis, F. (2009). Effect of slag on the rheology of fresh self-compacted concrete. *Construction and Building Materials*, *23*(7), 2593-2598.

Bui, V. K., Montgomery, D., Hinczak, I., & Turner, K. (2002). Rapid testing method for segregation resistance of self-compacting concrete. *Cement and Concrete Research*, *32*(9), 1489-1496.

Cement Association of Canada, 2002, Design and Control of Concrete Mixture, Seventh Edition, Cement Association of Canada, Ottawa.

Chang, C.; and Powell, R. L., (1994). "Effect of particle size distributions on the rheology of concentrated bimodal suspensions", *Journal of Rheology,* Vol. 38, No. 1, pp. 85-98.

Chia, K. S., & Zhang, M. H. (2004). Effect of chemical admixtures on rheological parameters and stability of fresh lightweight aggregate concrete. *Magazine of Concrete Research*, *56*(8), 465-473.

Chidiac, S. E., Maadani, O., Razaqpur, A. G., & Mailvaganam, N. P. (2000). Controlling the quality of fresh concrete--A new approach. *Magazine of Concrete Research*, *52*(5), 353-364.

Chidiac, S. E., Habibbeigi, F., & Chan, D. (2006). Slump and Slump Flow for Characterizing Yield Stress of Fresh Concrete. *ACI Materials Journal*, 413-418.

Chidiac, S. E., & Mahmoodzadeh, F. (2009). Plastic viscosity of fresh concrete–A critical review of predictions methods. *Cement and Concrete Composites*, *31*(8), 535-544.

Collis, L., & Smith, M. R. (Eds.). (2001). Aggregates: sand, gravel and crushed rock aggregates for construction purposes. Geological Society.

Daczko, J. A., & Constantiner, D. (2001, August). Rheodynamic concrete. In *Proceedings of the 43rd Congresso Brasileiro Do Concreto*.

Daczko, J. A. (2012). Fresh Properties and Test Methods. In J. A. Daczko, *Self-Consolidating Concrete: Applying What We Know* (pp. 41-58). New York: Spoon Press.

De Larrard, F., Hu, C., Sedran, T., Szitkar, J. C., Joly, M., Claux, F., & Derkx, F. (1997). A new rheometer for soft-to-fluid fresh concrete. *Materials Journal*, *94*(3), 234-243.

De Larrard, F., (1999). "Concrete mixture proportioning - A scientific approach", E & FN Spon.

Faroug, F., Szwabowski, J., & Wild, S. (1999). Influence of superplasticizers on workability of concrete. *Journal of materials in civil engineering*, 11(2), 151-157.

Ferraris, C. F., & de Larrard, F. (1998). Testing and Modelling of Fresh Concrete Rheology.

Ferraris, C. F. (1999). Measurement of the rheological properties of high performance concrete: state of the art report. *Journal of research of the national institute of standards and technology*, *104*(5), 461.

Feys, D., Verhoeven, R., & De Schutter, G. (2007). Evaluation of time independent rheological models applicable to fresh self-compacting concrete. *Applied rheology*, *17*(5), 56244-57190.

Feys, D., Verhoeven, R., & De Schutter, G. (2009). Why is fresh self-compacting concrete shear thickening? *Cement and concrete Research*, *39*(6), 510-523.

Flatt, R. J., Houst, Y. F., Bowen, P., Hofmann, H., Widmer, J., & Sulser, U. (2000). Electrosteric Repulsion Induced By Superplasticizers between Cement Particles-An Overlooked Mechanism? *ACI SPECIAL PUBLICATIONS*, *195*, 29-42.

Frankel, N. A., & Acrivos, A. (1967). On the viscosity of a concentrated suspension of solid spheres. *Chemical Engineering Science*, *22*(6), 847-853.

El Barrak, M., Mouret, M., & Bascoul, A. (2009). Self-compacting concrete paste constituents: hierarchical classification of their influence on flow properties of the paste. *Cement and Concrete Composites*, *31*(1), 12-21.

Elyamany, H. E., Elmoaty, A. E. M. A., & Mohamed, B. (2014). Effect of filler types on physical, mechanical and microstructure of self compacting concrete and Flow-able concrete. *Alexandria Engineering Journal*, *53*(2), 295-307.

EFNARC. (2002). Specification and Guidelines for Self-Compacting Concrete. Farnham: Association House.

EINSTEIN, **A .** Ann. Phys., Lpz., **19,** p. 289 (1906); **34,** p. 591 (1911).

Erdem, T. K., Khayat, K. H., & Yahia, A. (2009). Correlating rheology of self-consolidating concrete to corresponding concrete-equivalent mortar. *ACI Materials Journal*, *106*(2), 154.

Estellé, P., Lanos, C., Perrot, A., & Amziane, S. (2008). Processing the vane shear flow data from Couette analogy. *Applied Rheology*, *18*(3), 34037.

Ghezal, A., & Khayat, K. H. (2002). Optimizing self-consolidating concrete with limestone filler by using statistical factorial design methods. *Materials Journal*, *99*(3), 264-272.

Kennedy, C. T. (1940). The design of concrete mixes. In *Journal Proceedings* (Vol. 36, No. 2, pp. 373-400).

Khayat, K. H., Assaad, J., & Daczko, J. (2004). Comparison of field-oriented test methods to assess dynamic stability of self-consolidating concrete. *Materials Journal*, *101*(2), 168-176.

Khayat, K. H., Yahia, A., & Sayed, M. (2008). Effect of supplementary cementitious materials on rheological properties, bleeding, and strength of structural grout. *ACI Mater. J*, *105*(6), 585-593.

Koehler, E. P., & Fowler, D. W. (2004). Development of a portable rheometer for fresh portland cement concrete.

Koehler, E. P., & Fowler, D. W. (2009). Comparison of Workability Test Methods for Self-Consolidating Concrete. *Journal of ASTM International*, *7*(2), 1-19.

Krieger, I. M., & Dougherty, T. J. (1959). A mechanism for non-Newtonian flow in suspensions of rigid spheres. *Transactions of The Society of Rheology (1957-1977)*, *3*(1), 137-152.

Kurokawa, Y.; Tanigawa, Y.; Mori, H.; and Nishinosono, K., (1996). "Analytical study on effect of volume fraction of coarse aggregate on Bingham's constants of fresh concrete", *Transactions of the Japan Concrete Institute*, Vol. 18, pp. 37-44.

Piekarczyk-Łaźniewska, B. (2014). The methodology for assessing the impact of new generation superplasticizers on air content in self-compacting concrete. Construction and Building Materials, 53, 488-502.

Li, L. G., & Kwan, A. K. (2013). Concrete mix design based on water film thickness and paste film thickness. *Cement and Concrete Composites*, *39*, 33-42.

Mahmoodzadeh, F., & Chidiac, S. E. (2013). Rheological models for predicting plastic viscosity and yield stress of fresh concrete. *Cement and Concrete Research*, *49*, 1-9.

Mehdipour, I., & Khayat, K. H. (2016). Effect of Supplementary Cementitious Material Content and Binder Dispersion on Packing Density and Compressive Strength of Sustainable Cement Paste. *Materials Journal*, *113*(03), 361-372.

Mooney, M. (1951). The viscosity of a concentrated suspension of spherical particles. *Journal of colloid science*, *6*(2), 162-170.

Nehdi, M., Mindess, S., & Aıtcin, P. C. (1998). RHEOLOGY OF HIGH-PERFORMANCE CONCRETE: EFFECT OF ULTRAFINE PARTICLES. *Cement and Concrete Research*, *28*(5), 687-697.

Nielsson, I., & Wallevik, O. H. (2003). Rheological evaluation of some empirical test methods–preliminary results. In *Third international RILEM symposium, RILEM Pub. PRO* (Vol. 33, pp. 59-68).

Oh, S. G., Noguchi, T., & Tomosawa, F. (1999). Toward mix design for rheology of self-compacting concrete. In *proc. of First International RILEM Symposium on Self-Compacting Concrete (eds. Skarendahl,. Å. and Peterson, O.), Stockholm* (pp. 361-372).

Okamura, H., & Ouchi, M. (2003). Self-compacting concrete. *Journal of advanced concrete technology*, *1*(1), 5-15.

Öner, M., Erdoğdu, K., & Günlü, A. (2003). Effect of components fineness on strength of blast furnace slag cement. *Cement and Concrete Research*, *33*(4), 463-469.

Ozawa, K., & Okamura, H. (1995). Evaluation of self compactability of fresh concrete. JAPAN SOCIETY OF CIVIL ENGINEERS.

Petkova, V., & Samichkov, V. (2007). Some influences on the thixotropy of composite slag Portland cement suspensions with secondary industrial waste. *Construction and Building Materials*, *21*(7), 1520-1527.

Phan, T. H., Chaouche, M., & Moranville, M. (2006). Influence of organic admixtures on the rheological behaviour of cement pastes. *Cement and Concrete Research*, *36*(10), 1807-1813.

Roussel, N. (2006). A thixotropy model for fresh fluid concretes: theory, validation and applications. *Cement and Concrete Research*, *36*(10), 1797-1806.

Rubio-Hernandez, F. J., Velaquez-Navarro, J. F., & Ordonez-Belloc, L. M. (2013). Rheology of concrete: a study case based upon the use of the concrete equivalent mortar. *Materials and Structures*, 587-605.

Salem, T. M. (2002). Electrical conductivity and rheological properties of ordinary Portland cement–silica fume and calcium hydroxide–silica fume pastes. *Cement and Concrete Research*, *32*(9), 1473-1481.

Sethy, K. P., Pasla, D., & Sahoo, U. C. (2016). Utilization of high volume of industrial slag in self compacting concrete. *Journal of Cleaner Production*, *112*, 581-587.

Smeplass, S. (1994). Applicability of the Bingham model to high strength concrete. In *RILEM PROCEEDINGS* (pp. 145-145). CHAPMAN & HALL.

Sonebi, M. (2006). Rheological properties of grouts with viscosity modifying agents as diutan gum and welan gum incorporating pulverised fly ash. *Cement and Concrete Research*, *36*(9), 1609-1618.

Struble, L. J., & Jiang, Q. (2004). Effects of air entrainment on rheology. *ACI materials journal*, *101*(6), 448-456.

Su, N., Hsu, K. C., & Chai, H. W. (2001). A simple mix design method for self-compacting concrete. *Cement and concrete research*, *31*(12), 1799-1807.

Su, N., & Miao, B. (2003). A new method for the mix design of medium strength flowing concrete with low cement content. *Cement and Concrete Composites*, *25*(2), 215-222.

Tattersall, G. H. (1976). The workability of concrete.

Tattersall, G. H., & Banfill, P. F. G. (1983). *The rheology of fresh concrete* (Vol. 759). London: Pitman.

Tattersall GH. (1991). Workability and Quality Control of Concrete.London:E&FN Spon.

Toutou, Z., & Roussel, N. (2006). Multi scale experimental study of concrete rheology: from water scale to gravel scale. *Materials and Structures*, *39*(2), 189-199.

Uchikawa, H., Hanehara, S., & Sawaki, D. (1997). The role of steric repulsive force in the dispersion of cement particles in fresh paste prepared with organic admixture. *Cement and Concrete Research*, *27*(1), 37-50.

Ur'ev, N. B., Baru, R. L., Izhik, A. P., Choi, S. V., & Saskovets, V. V. (1997). Rheology and thixotropy of cement-water suspensions in the presence of superplasticizers. *Colloid journal of the Russian Academy of Sciences*, *59*(6), 773-779.

Utsi, S., Emborg, M., & Carlswärd, J. (2003). Relation between workability and rheological parameters. In *International RILEM Symposium on Self-Compacting Concrete* (pp. 154-164). RILEM Publications SARL.

Wallevik, J. E. (2008). Minimizing end-effects in the coaxial cylinders viscometer: Viscoplastic flow inside the ConTec BML Viscometer 3. *Journal of Non-Newtonian Fluid Mechanics*, 116-123.

Whiting, D., & Stark, D. (1983). Control of air content in concrete. *NCHRP report*, (258).

Wu, Q., & An, X. (2014). Development of a mix design method for SCC based on the rheological characteristics of paste. *Construction and Building Materials*, *53*, 642-651.

Zholkovskiy, E. K., Adeyinka, O. B., & Masliyah, J. H. (2006). Spherical cell approach for the effective viscosity of suspensions. *The Journal of Physical Chemistry B*, *110*(39), 19726-19734.

2 Correlating Self-Consolidating Concrete mixture to its rheological properties

Abstract

Self-Consolidating Concrete (SCC) is a special type of concrete that is able to flow and compact under its own weight. As such, its mixture composition and rheological properties are different from those of traditional normal slump concrete. This study, which includes an experimental and analytical part, is carried out to study the relationships between the mixture composition and the flow. Towards this objective, a half factorial design was used to design the experiment using the following 5 variables: water to binder ratio, silica fume as % replacement of cement content, ground granulated blast furnace slag as % replacement of cement content, bulk volume of coarse aggregate and binder content. The concrete workability measurements, specifically the slump flow, T_{50}, L-box ratio and static segregation column test were made, in addition to the rheological properties, namely plastic viscosity, yield stress and thixotropy. The effects of the design variables on the workability and rheology were analysed. Further, correlations between workability measures and rheological properties were investigated.

SCC flow behaviour is best characterized using non-linear models such as modified Bingham model or Herschel-Bulkley (H-B) model. A revised model based on the modified Bingham model is proposed in this study. It is postulated that the linear and non-linear flow can be decoupled and a new approach is put forward to determine the Bingham properties, plastic viscosity, and yield stress, based on the linear response and the 2^{nd} order nonlinear property using the nonlinear part of the curve. The results show that the proposed model yield more consistent and accurate properties when compared to the Modified Bingham model.

Statistical models were developed to correlate the rheological properties to the mixture composition. Using 95% level confidence, the yield stress is found to depend on the bulk volume fraction of the coarse aggregate, Silica Fume content, HRWRA and VMA,

and plastic viscosity on w/b, HRWRA and APT. Validation of the models shows that the models are not complete as the standard errors are larger than the experimentally measured ones, which can indicate other missing variables.

2.1 Introduction

Self-Consolidating Concrete (SCC), which consists of aggregates and cement paste, has the ability to flow, consolidate and pass through congested reinforcement under its own weight. These attributes accelerate the placement of concrete and reduce labour (Ghezal & Khayat, 2002). Accordingly, SCC has to meet certain workability measures, specifically, filling ability, passing ability and stability. Albeit, these workability measures provide a quantitative (pass/fail) assessment of the mixture, they do not provide a fundamental approach for quantifying the concrete flow behavior. Rheological properties namely, plastic viscosity and yield stress, afford the characterization of the concrete flow behavior (Chidiac & Mahmoodzadeh, 2009).

The rheology of concrete is dictated by the composition and proportioning of the mixtures. In comparison to normal slump concrete, SCC mixtures include a higher percentage of paste volume, a smaller maximum aggregate size, and higher dosage of chemical admixtures, namely High Range Water Reducing Agent (HRWRA) and Viscosity Modifying Agent (VMA) (Ghoddousi et al., 2014). The influence of material and mixture proportions on the rheological properties of concrete is captured in Figure 2.1 and Table 2.1 (Koehler and Fowler, 2007).

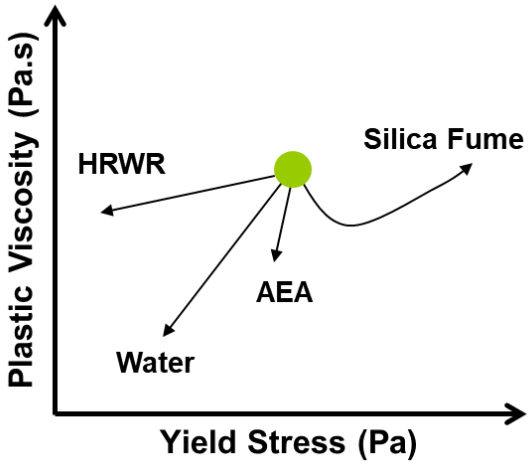

Figure 2.1: Effects of admixtures and water on rheological properties (Koehler & Fowler, 2007)

Table 2.1: Effects of Materials and Mixture Proportions on Rheology (Koehler & Fowler, 2007)

	Yield Stress	Plastic Viscosity
Aggregate max. size (increase)	↓	↓
Aggregate grading (optimize)	↓	↓
Aggregate angularity	↑	↑
Aggregate shape (equidimensional)	↓	↓
Paste volume (increase)	↓	↓
Water/powder (increase)	↓	↓
Fly ash	↓	↓
Slag	↑↓	↑↓
Silica fume (low %)	↑↓	↓
Silica fume (high %)	↑	↑
VMA	↑	↑↓
HRWRA	↓	↑↓
AEA	↑↓	↑

HRWRA increases the flowability of the mixture by dispersing the cement particles by steric and/or electrostatic repulsions (Uchikawa et al., 1997; Flatt et al., 2000). While

all the studies show that HRWRA reduces the yield stress (Smeplass, 1994), others (Faroug et al., 1999; Koehler and Fowler, 2007) have found that both the yield stress and plastic viscosity were impacted with a more pronounced effect reported for low w/b mixtures. HRWRA is found to reduce thixotropy due to a decrease in the flocculation between cement particles (Ur'ev et al., 1997).

VMA mitigates and/or eliminates segregation by increasing the plastic viscosity due to the attractive Van der Waals forces between the chains which blocks the passage of free water (Benaicha et al., 2015). El Barrak et al. (2009) reported that VMA influences the static stability more than the dynamic stability. Their results are similar to those of Phan et al. (2006) where VMA is found to aid in rebuilding the structure leading to an increase in thixotropic behaviour.

Replacing a percentage of Portland cement with SCMs, such as Granulated Ground Blast Furnace Slag (GGBFS), fly ash, silica fume, and limestone, is widely used to improve stability, strength and durability of SCC. Moreover, reducing the cement content by incorporating SCMs can effectively reduce the cost and improve concrete sustainability. By incorporating these fine materials, the grain size distribution and the particle packing are enhanced, thus ensuring greater cohesiveness (Khayat et al., 2000). Boukendakdji et al. (2009) studied the effect of GGBFS on the workability of SCC and found that the workability improves when 20% of the cementitious materials is replaced by GGBFS with an optimum content of 15%. Shi et al. (2002) pointed out that the addition of silica fume could either be beneficial or unfavorable on the rheology of high-performance concrete. They found that replacing 6% of total binder mass with silica fume led to a substantial reduction of the plastic viscosity and yield stress. However, with 12 % as partial substitution of silica fume, both the plastic viscosity and yield stress increased. Petkova and Samichkov (2007) suggested that an increase in the particle specific surface area in the paste matrix can lead to an increase in thixotropy.

The binder volume must suffice not only to fill in the voids between the aggregates but also to provide sufficient lubrication between the particles in order to achieve high workability. Towards achieving this objective, the excess paste theory, originally

proposed by Kennedy (1940), is widely used by researchers to determine the thickness of the paste coating each aggregate (Mebrouki et al., 2014; Chidiac et al., 2013). The theory postulates that any excess of the cement paste needed to fill the voids between the aggregates disperses the particles in the concrete mixture (Wong & Kwan, 2008). A better packing of granular materials results in a mixture with a lower amount of voids, and hence more excess paste is available for lubrication and therefore better workability.

The packing density of granular solids greatly impacts the fresh properties of SCC (Ghoddousi et al., 2014). This is attributed to its ability to capture the geometrical characteristics of the aggregates such as the shape, angularity, texture, particle size distribution, wall effect and method of compaction (Nanthagopalan & Santhanam, 2012). Taking into account the maximum packing density along with the excess water ratio, excess paste ratio and solid surface area, Li and Kwan (2013) evaluated the paste film thickness and water film thickness and found out that these two parameters are the keys factors governing the deformability, flowability and strength of concrete. Nanthagopalan and Santhanam (2012) investigated the effect of three different granular packing densities (0.64, 0.66 and 0.68) on the workability of SCC. They reported a significant increase in both the slump flow and the slump flow with the J-ring when the packing density increased from 0.64 to 0.68 for a constant paste volume and paste composition.

Fresh concrete, especially SCC, exhibits different rheological behavior when at rest than when flowing due to thixotropy. Thixotropy is defined as the reversible, isothermal, time-dependent decrease in the material viscosity when subjected to shearing stress or shearing strain (Mewis, 1979). When concrete is at rest, the cement particles flocculate forming a networked structure resulting in an increase in the viscosity, and when subjected to a shearing regime, the inter-particle links and flocculation are ruptured, resulting in a decrease in viscosity (Wallevik, 2003). Thixotropy is important, especially for high fluidity material such as SCC, because it increases the material resistance to segregation, reduces its hydrostatic pressure on the formwork, and enhances its pump ability, to name a few (Erdem et al., 2009; Billberg, 2003; Khayat et al., 2005; Ovarlez & Roussel, 2005).

This study aimed to examine the correlation between the mixture proportions and rheological properties of SCC. Fractional factorial design of the experiment was carried out using the following design variables: binder content, water to binder ratio (w/b), the volume fraction of coarse aggregate and percent additions of SF and GGBFS. Correlation included both the design variables as well as secondary variables such as packing density, maximum packing density and average paste thickness (Chidiac et al., 2013).

2.2 Rheology- theoretical background

Rheology, which refers to the science of flow and deformation of materials, has been applied to study the flow behaviour of suspensions such as concrete (Banfill, 1994). Numerous research has shown that Bingham model, given by Eq. 2.1, captures the flow behaviour of normal slump concrete and that two intrinsic parameters, namely plastic viscosity (μ) and yield stress (τ_0), are sufficient to define the flow (Tattersall, 2003; Banfill, 2006).

$$\tau = \tau_0 + \mu\dot{\gamma} \qquad \text{Equation 2.1}$$

where τ is the shear stress (Pa) and $\dot{\gamma}$ shear strain (s^{-1}). For SCC, the behaviour is found to be generally non-linear where shear thickening and thinning have been observed. Therefore, non-linear models are needed to capture the rheological behaviour of the material (De Larrard et al., 1998). The most common model has been the Herschel-Bulkley (H-B) model given by Eq. 2.2. The non-linearity is introduced to the Bingham model through the exponent "*n*". This power relationship reveals shear thinning when $n < 1$ and shear thickening when $n < 1$.

$$\tau = \tau_0 + K\dot{\gamma}^n \qquad \text{Equation 2.2}$$

$$\frac{d\tau}{d\dot{\gamma}} = nK\dot{\gamma}^{n-1} \qquad \text{Equation 2.3}$$

where *K* is the consistency index ($Pa.s^n$).

Feys et al. (2007) state that the H-B model has two major disadvantages when describing a non-linear material. They indicate that upon deriving Eq. 2.2 with respect

to the shear rate given by Eq. 2.3, the curve has the tendency to approach '0' at very low shear rates in case of shear thickening, resulting in overestimating of the yield stress. The latter interpretation was also experimentally verified in Feys et al. (2007) work, where the fitted H-B curve was positioned above the data points at low shear rates. Moreover, the parameter, *K*, lacks physical interpretation, since it is a variable with the dimension $Pa.s^n$. They further postulate that the Modified-Bingham model, given by Eq. 2.4, is a more suited model for describing the rheological behaviour of SCC,

$$\tau = \tau_0 + \mu\dot{\gamma} + c\dot{\gamma}^2 \qquad \text{Equation 2.4}$$

This model is regarded to be an extension of the Bingham model with a second-order term (*c*)). From their experimental results, the parameter c/μ (modified-Bingham) linked to *n* (H-B), can be applied to describe the non-linear behaviour, indicating shear thinning ($c/\mu < 0$), shear thickening ($c/\mu > 0$) and the linear Bingham model ($c/\mu = 0$) (Feys et al., 2007). It should be noted that the rheological properties are deduced by fitting the experimental data obtained using a concrete rheometer to a material model.

2.3 Experimental Program

An experimental program was designed and carried out to study the relationships between the mixture design and the rheological properties. Towards this objective, the design of experiment method using fractional factorial design (Box et al., 2005) was adapted to statistically account for the design variables. The experimental program included testing and measurement of SCC fresh properties, specifically the flow properties, segregation resistance and rheological properties.

2.3.1 Design of experiment

A statistical modeling approach has been used to identify the relative significance of key mixture variables and their coupled effects on the properties of SCC (Khayat et al., 1999). For this study, a statistical partial factorial design is adapted to investigate the influence of five SCC variables on the flow and rheological properties. A is equal to the bulk volume of coarse aggregate (V_{ca}), B and C equal to the ground granulated blast

furnace slag (GGBFS) and silica fume (SF), two supplementary cementing materials, used as percent replacement of cement content, respectively. D equals to the water to binder ratio (w/b), and E equals to the total binder content, which the sum of cement and supplementary cementing materials. The variables range and corresponding two-level codes, -1 and +1, are given in Table 2.2. Half fractional factorial design method with two levels yield the sixteen mixtures shown in Table 2.3. Moreover, a design corresponding to the center points was included to validate the models. Moreover, the mixtures had to meet SCC classifications set by ACI (ACI, 2007) namely, a slump flow of 650±50 mm, T_{50} between 2 and 5 s, L-Box ratio greater than 0.8, and a segregation index less than 10%. This was achieved by adjusting the amount of HWRA and VMA added to the mixture.

Table 2.2: Low and high values for the SCC design variables

Variable	Values	
	-1	+1
V_{ca} (m^3/m^3)	0.25	0.30
GGBFS (%)	0	30
SF (%)	0	8
w/b	0.32	0.40
Binder content (kg/m^3)	450	550

Table 2.3: Mixtures design adapted for the experimental program

Mix #	A	B	C	D	E	V_{ca} (m^3/m^3)	GGBFS (%)	SF (%)	w/b	Binder Content (kg/m^3)
1	-1	-1	-1	-1	1	0.25	0	0	0.32	550
2	1	-1	-1	-1	-1	0.3	0	0	0.32	450
3	-1	1	-1	-1	-1	0.25	30	0	0.32	450
4	1	1	-1	-1	1	0.3	30	0	0.32	550
5	-1	-1	1	-1	1	0.25	0	8	0.32	450
6	1	-1	1	-1	-1	0.3	0	8	0.32	550
7	-1	1	1	-1	-1	0.25	30	8	0.32	550
8	1	1	1	-1	1	0.3	30	8	0.32	450
9	-1	-1	-1	1	1	0.25	0	0	0.40	450
10	1	-1	-1	1	-1	0.3	0	0	0.40	550
11	-1	1	-1	1	-1	0.25	30	0	0.40	550
12	1	1	-1	1	1	0.3	30	0	0.40	450
13	-1	-1	1	1	1	0.25	0	8	0.40	550
14	1	-1	1	1	-1	0.3	0	8	0.40	450
15	-1	1	1	1	-1	0.25	30	8	0.40	450
16	1	1	1	1	1	0.3	30	8	0.40	550
17	0	0	0	0	0	0.275	15	4	0.36	500

2.3.2 Material properties

SCC was prepared using a mixture of crushed limestone, siliceous sand, General Use and Portland-Limestone cement (GUL), SF, GGBFS, AEA, HRWRA, VMA, and water. The coarse aggregate (CA), "14-5MM CONC ST GRVL WSHD-AG8686" meeting the specifications of OPSS 13.2 mm concrete stone, was supplied by Lafarge North America's Cambridge plant located in Cambridge, Ontario. Nominal maximum CA size of 14 mm was used throughout the whole experimental program with specific gravity, absorption, and bulk density of 2.74, 1.58% and 1544 kg/m^3, respectively. The sand, "Concrete Sand Washed-AG2719" meeting the specifications of OPSS concrete sand, was supplied by Lafarge North America's Cambridge plant located in Cambridge, Ontario.

The sand fineness modulus, specific gravities, absorption, and bulk density are respectively, 2.88, 2.71, 1.28% and 1746 kg/m^3. The bulk density, specific gravity, and absorption for CA and sand were determined in accordance with ASTM C127-12 (ASTM, 2012) and ASTM C128-12 (ASTM, 2012), respectively. The CA and sand gradation curves were measured in accordance with CSA test method A23.2-2A (2009) and ASTM C136-06 (ASTM, 2006). The results, shown in Figures 2.2 and 2.3, show that the particles size and distribution lie within CSA limits. The characteristic CA and sand diameters, which correspond to 63.2 % passing, are respectively, 10 ± 0.260 mm and 1.26 ± 0.07 mm (Goltermann et al., 1997). The diameters corresponding to 50% passing are 8.37 mm ± 0.201 mm and 0.911 ± 0.049 mm for CA (D_{ca}) and sand (D_s) respectively. The maximum oven-dried packing densities for CA and sand, measured according to ASTM C29-97 (ASTM, 1997) are 0.564 ± 0.00516 and 0.649 ± 0.00519. The corresponding maximum packing density for each mixture was computed using the compressible packing model (CPM) developed by de Larrard (1999).

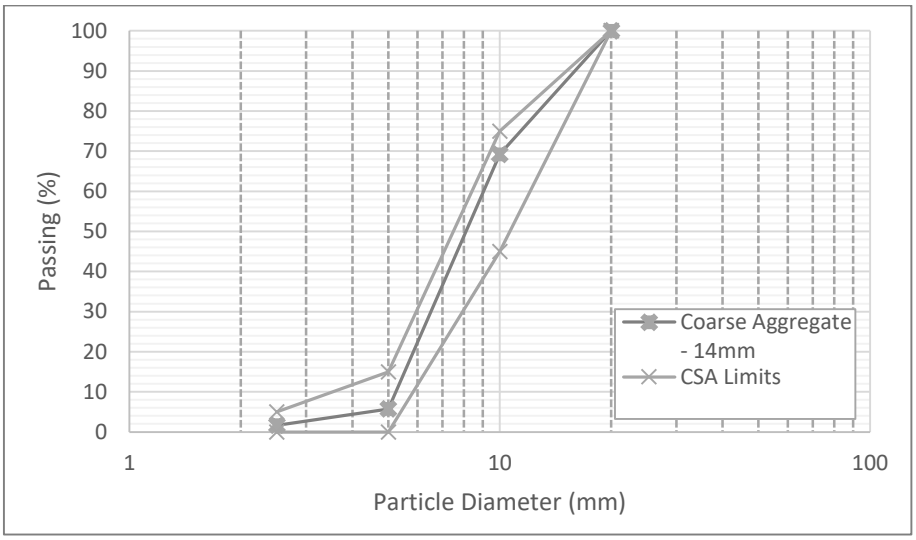

Figure 2.2: 14 mm coarse aggregates particle size distribution curve

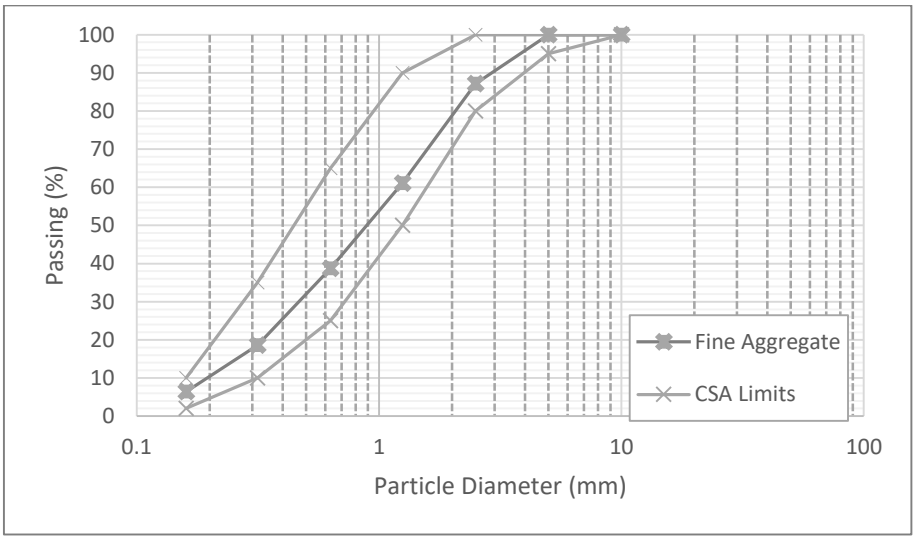

Figure 2.3: Fine aggregate particle size distribution curve

GUL was supplied by St. Marys Cement, GGBFS type NewCem Grade 80 BS was supplied by Lafarge North America, and MasterLife© SF 100 by BASF Construction Chemicals. The specific gravity of the GUL, GGBFS, and SF is 3.15, 2.93 and 2.2, respectively, and the corresponding Blaine fineness values are 468, 475 and 12000 m^2/kg. The chemical and physical properties of the GUL, GGBFS, and SF are given in Table 2.4.

Table 2.4: Chemical and physical properties of GUL, GGBFS and SF

	GUL	GGBFS	SF
SiO_2 (%)	18.00	36.15	99
Fe_2O_3 (%)	2.80	0.64	
Al_2O_3 (%)	4.4	10.4	
CaO (%)	61.3	36.9	
Free CaO (%)	1.1	-	
MgO (%)	2.90	0.46	
SO_3 (%)	3.55	2.66	
K_2O (%)	0.48	0.51	
Na_2O (%)	0.24	0.41	
TiO_2 (%)	0.27	1.11	
Loss on Ignition (%)	5.5	-	
Total Alkali as Na_2O (%)	0.56	-	
Specific Surface Area (Blaine-m^2/kg)	468	475	12000
% retained (45um)	-	1.5	
% retained 325	1.8	-	
Time of Setting-Initial (min)	105	-	
Compressive Strength - 28 Day (MPa)	41.7	38.7	

HRWRA, AEA, and VMA, specifically Glenium© 7700, MasterAir© AE 200 and MasterMatrix© VMA 362, used in this experimental program, were supplied by BASF's Construction Chemicals. Glenium© 7700 admixture meets ASTM C 494 (ASTM, 2005) requirements for Type A, water-reducing, and Type F, high-range water-reducing, admixtures (BASF, 2014). MasterAir© AE 200 admixture meets the requirements of ASTM C 260 (ASTM, 2006). MasterMatrix© VMA 362 admixture meets ASTM C 494 requirements for Type S, Specific Performance, admixtures (BASF, 2014). According to the manufacturer, the specific gravity of Glenium 7700, MasterAir AE 200 and MasterMatrix VMA 362 admixtures are 1.064, 1.010 and 1.002, respectively. The solid content of Glenium 7700 and MasterMatrix VMA 362 admixtures is 33% and 1% by mass, respectively.

2.3.3 Mixing and Placement Procedure

The experimental procedure developed for the mixing, placing and consolidating was consistent for all SCC mixtures. Mixing was carried out using a vertical- axis pan mixer. The mixing procedure was as follow:

a) Pour 70 % of the total water, AEA and VMA admixtures in the same bucket and mix them for 30 s.
b) Place in the loading pan the CA followed by the cementing material and then the sand.
c) Load the dry material into the pan mixer and mix it for 2 min.
d) Add 70% of the mixed liquid (water with AEA and VMA admixtures) and continue mixing for 2 min.
e) Mix remaining 30% of the liquid with HRWRA for 30 s.
f) Add the remaining liquid to the mix and continue mixing for 5 min.
g) Rest for 2 min then mix for 1 minute before testing the slump flow.
h) If the slump flow is less than the specified limit, add more HRWRA and mix for 2 min.
i) Go to step g) and repeat until the required slump flow is achieved.

The SCC mixes are then placed and allowed to flow under its own weight. There were no mechanical or other external tools used to consolidate the concrete.

2.3.4 Testing Procedure

The testing protocol was developed to evaluate the workability and rheology properties of SCC. Workability provides a qualitative measure of the mixture ability to flow under its own weight, pass through reinforcement bars and resist segregation. Rheology provides a theoretical approach to quantify the flow by means of rheological properties.

2.3.4.1 Workability

For workability, the slump flow, T_{50}, static segregation column test, L-Box test, air content test, and density were measured in accordance with ASTM C1611 (2009), ASTM C1611 (2009), ASTM C1610 (2010), ACI A237 (2007), CSA A23.2-4C (2009), and CSA A23.2-4C (2009), respectively. The slump flow and T_{50}, measured using the

slump rate machine, SLRM, provide a measure of the concrete ability to flow as shown in Figure 2.4. The static segregation column test, shown in Figure 2.5, measures the mixture ability to resist segregation. The L-Box test, shown in Figure 2.6, assess the mixture's passibility.

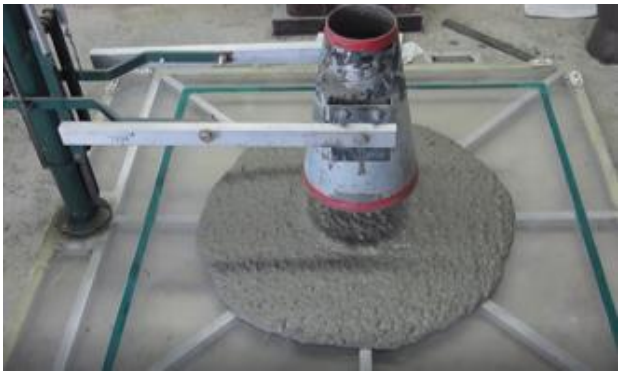

Figure 2.4: Slump flow and T_{50} measurements using SLRM

Figure 2.5: Static Column Segregation column

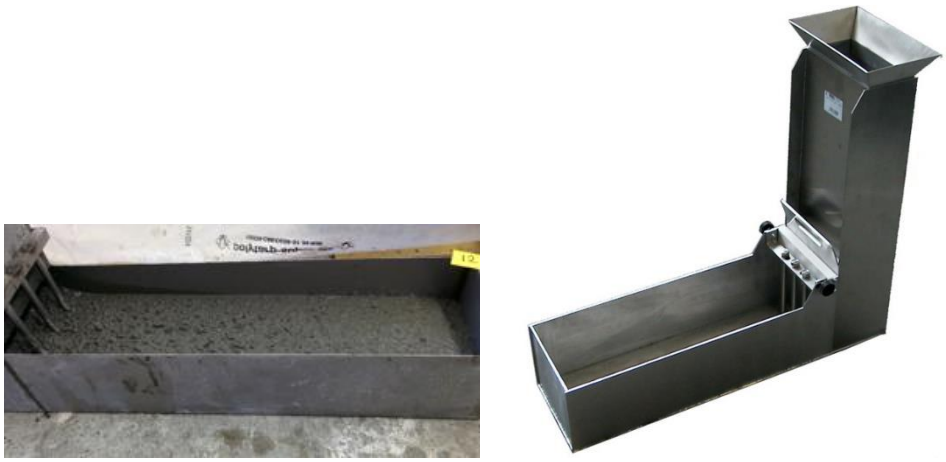

Figure 2.6: L-Box

2.3.4.2 Rheology

Rheology is the study of the flow and deformation of a viscous material employing the interaction between shear stress and shear strain rate (Banfill, 1994). The most common use of rheology in concrete is to characterize the rheological properties of the mixture. Using a concrete rheometer, the relationship between torque and rotational speed is first established. By assuming that the concrete flow in the rheometer obeys a Couette flow and that the material response obeys a predefined rheological model, the corresponding shear stress-shear strain rate for the concrete is established. Subsequently, the rheological properties, being the yield stress and plastic viscosity for Bingham rheological model, are estimated. In this study, RheoCAD 500, a concrete rheometer developed by CAD Instruments, France is shown in Figure 2.7, was used to estimate the rheological properties.

The RheoCAD consists of a container with a series of vertical rods around the perimeter to prevent any material slippage, a drive unit control system, and a vane impeller with a height and radius of 250 mm and 60 mm, respectively. The vane impeller, shown in Figure 2.8, was used to measure the torque versus rotational speed.

Figure 2.7: RheoCAD 500 rheometer (CAD Instruments)

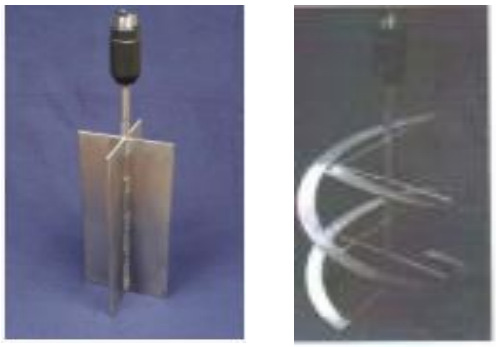

Figure 2.8: Impeller geometries: vane impeller (left) and double helical impeller (right) (CAD Instruments)

A ramp-up and ramp-down test protocol were implemented. The ramp-up consisted of a gradual increase of the rotational speed from 2 rpm to 62 rpm with an increment of 6 rpm resulting in 10 steps. Ramp-up is intended to break down the structure. Subsequently, the vane speed is reduced to the initial speed using the same increment of 6 rpm per step. For each step, the steady-state rotational speed and torque are recorded. The duration of each step is 10 s however the actual test time varies depending on when steady state condition is established. The test protocol is shown in Figure 2.9.

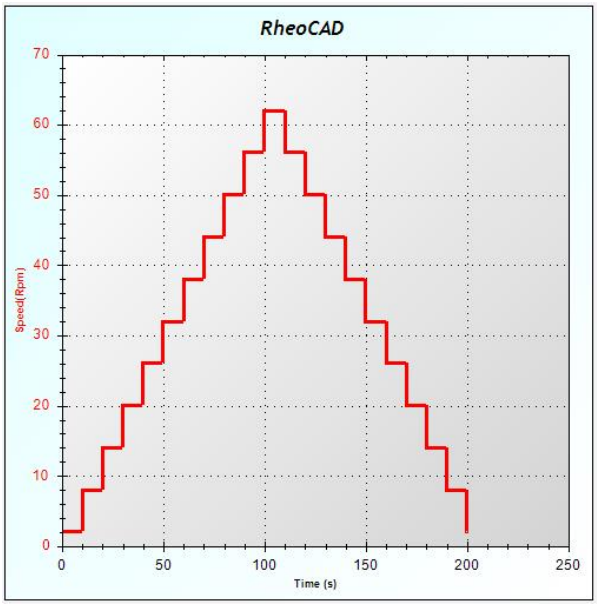

Figure 2.9: Experimental program testing protocol

By adopting the Couette analogy, and assuming that a) the flow is laminar, steady and incompressible, b) the flow is sheared along a cylindrical surface defined by the vane height h and diameter D, and c) the stress distribution is uniform along the cylindrical sheared surface (Estellé, 2012), the corresponding shear stress and shear strain rates are obtained (Nehdi and Rahman, 2004) and used in this study,

$$\tau = \frac{R_o^2+R_i^2}{4\pi h R_o^2 R_i^2} T \qquad \text{Equation 2.5}$$

$$\dot{\gamma} = \frac{R_o^2+R_i^2}{R_o^2-R_i^2} 2\pi N \qquad \text{Equation 2.6}$$

Where R_0 is the outer radius of the stationary cylinder, R_i is the inner radius of the rotating cylinder (vane radius), T is torque measured by the rheometer, and N is the rotational speed of the rotating impeller. During the test, a plug state was observed with the sheared region being affected by the mixture plastic viscosity. Accordingly, two different radii for the two w/b ratio mixtures were generally observed. The flow boundary, R_c, was measured to be about 0.130 m for w/b =0.32 and 0.115 m for w/b=0.4. To reflect the actual sheared region, these measurements are substituted in place of the outer radius in Eqs. 2.5 and 2.6. To illustrate, Figure 2.10 shows a schematic

view of a concentric cylinder with the radii (R_o, R_i, and R_c) and Figures 2.11 and 2.12 shows the relative R_c position for both w/b ratios mixtures.

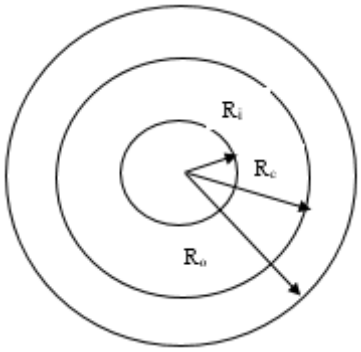

Figure 2.10: Schematic view of a concentric cylinder

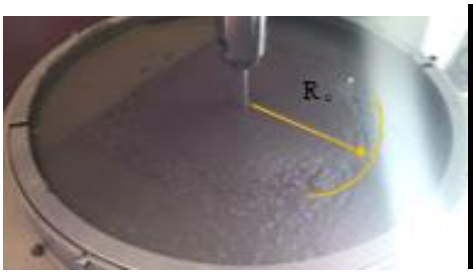

Figure 2.11: RheoCAD – Mix #14, w/b=0.4, Rc = 0.115 m

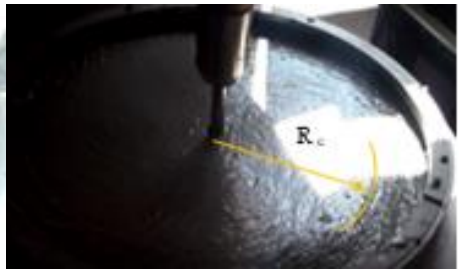

Figure 2.12: RheoCAD – Mix # 4, w/b=0.32, Rc = 0.13m

2.4 Experimental Results and Analyses

2.4.1 SCC Mixtures Proportion

The final mixtures proportions for the 17 SCC mixes including the chemical admixtures are given in Table 2.5. The amount of chemical admixtures were adjusted to ensure that the slump flow meets SCC requirements without causing any segregation.

Table 2.5: SCC mixtures proportion

Mix#	w/b	Water	GUL	GGBFS	SF	CA	FA	AEA	VMA	HRWRA
		(kg/m^3)						(mL/100kg binder)		
1	0.32	176	550	0	0	684	915	15	0	693
2	0.32	144	450	0	0	821	952	15	0	786
3	0.32	144	315	135	0	684	1079	15	0	647
4	0.32	176	385	165	0	821	769	15	600	650
5	0.32	144	414	0	36	684	1075	15	0	1127
6	0.32	176	506	0	44	821	764	15	0	827
7	0.32	176	341	165	44	684	889	15	0	649
8	0.32	144	279	135	36	821	931	15	0	837
9	0.4	180	450	0	0	684	992	15	393	487
10	0.4	220	550	0	0	821	663	15	400	328
11	0.4	220	385	165	0	684	787	15	477	302
12	0.4	180	315	135	0	821	848	15	401	376
13	0.4	220	506	0	44	684	781	15	400	489
14	0.4	180	414	0	36	821	843	15	400	679
15	0.4	180	279	135	36	684	969	15	400	527
16	0.4	220	341	165	44	821	636	15	400	469
17	0.36	180	405	75	20	753	867	15	400	599

2.4.2 Workability of SCC

The density, air content, slump flow, T_{50}, L-Box ratio, and static segregation index obtained for the 17 mixes are reproduced in Table 2.6. The results of mix #17, which was repeated three times, provides a reference to the variance in the measured values. Measured values of the density, air content, slump flow, T_{50}, L-box ratio and column test reveal a coefficient of variance (COV) (%) of 1, 21, 9, 42, 7 and 173 respectively. The error in the column test is high, however, the mean is almost equal to zero which amplifies the error. The error results reveal the vulnerability of the test to human error. T_{50}, which is mostly dependent on the reaction rate of the operator, has the highest coefficient of variance. A variance of 9% is calculated for the slump flow as it is not influenced by the operator, but rather by the characteristics of the aggregates, specifically the shape, angularity, and packing.

Table 2.6: Workability measurements

Mix #	Density (kg/m^3)	Air content (%)	Slump flow (mm)	T_{50} (s)	L-Box ratio (-)	Column static segregation (%)
1	2408	5.5	760	2.3	0.89	0.0
2	2451	4.0	638	6.3	0.64	0.0
3	2416	4.5	680	7.7	0.87	0.6
4	2370	5.4	720	1.6	0.93	0.5
5	2408	7.1	590	6.8	0.30	0.6
6	2399	5.5	560	3.5	0.44	0.0
7	2329	6.0	635	4.7	0.58	0.0
8	2372	6.0	610	4.1	0.59	0.4
9	2309	6.6	618	1.5	0.69	0.0
10	2341	3.0	613	0.4	0.76	1.3
11	2324	4.4	608	1.1	0.80	0.6
12	2287	6.4	665	1.3	0.75	0.0
13	2301	4.3	595	0.6	0.72	1.1
14	2318	6.4	605	1.8	0.81	1.0
15	2227	7.4	590	1.7	0.67	0.0
16	2361	3.6	545	1.5	0.54	0.0
17	2412±18	3.0±0.6	706±66	1.6±0.65	0.84±0.06	0.2±0.3

2.4.2.1 APT (Average Paste Thickness)

Recognizing the importance of packing density and paste thickness on the flow of fresh concrete, the packing density (ϕ), maximum packing density (ϕ_{max}), and average past thickness (APT) were computed for the 17 mixes using the CPM model (de Larrard, 1999) and Chidiac et al. (2013) model. Knowing the volume fraction of the fine aggregates and coarse aggregates from the mixtures, their characteristics diameters corresponding to 63.2 % passing, and their measured maximum packing densities, the CPM was employed to calculate ϕ_{max}.

The APT model is given by Eq. 2.7.

$$APT = -\frac{1}{2}\left(D_s + \frac{\phi_{ca}D_s^2}{\phi_s D_{ca}} + \frac{\phi D_s^2(1-\phi_{max})}{\phi_s \phi_{max} D}\right) + \frac{1}{2}\sqrt{\left(D_s + \frac{\phi_{ca}D_s^2}{\phi_s D_{ca}} + \frac{\phi D_s^2(1-\phi_{max})}{\phi_s \phi_{max} D}\right)^2 + \frac{4}{3}\frac{(\phi_{max}-\phi)}{\phi_{max}}\frac{D_s^2}{\phi_s}}$$ Equation 2.7

$$D = \left(\frac{{D_{ca}}^3\phi_{ca} + {D_s}^3\phi_s}{\phi_{ca}+\phi_s}\right)^{1/3}$$ Equation 2.8

where D, D_s and D_{ca} are the mean diameters of the total particles gradation, fine aggregate gradation and coarse aggregate gradation corresponding to 50 % passing respectively. ϕ,$\phi_{s,}$ ϕ_{ca} and ϕ_{max} are volume fraction of aggregates, fine aggregates, coarse aggregates, and maximum packing density of aggregates respectively. The volume fraction of fine and coarse aggregates, along with ϕ_{max},ϕ/ϕ_{max}, D (given by Equation 2.8), and APT for each mixture are reported in Table 2.7.

In terms of the mixture composition, increasing the paste layer can be accomplished by increasing the binder content for a given aggregate volume. Moreover, a further increase in the paste thickness could be achieved by increasing the coarse aggregates content compared to the fine aggregates. This is attributed to the coarse aggregate's smaller surface area, which would normally reduce the amount of paste needed to coat the surfaces leaving more paste in between the particles for lubrication. Therefore, for a given w/b ratio, the overall volume of both the coarse aggregates and the binder, could be captured by the amount of fine aggregates left in the mixture. Accordingly, one can relate the amount of fine aggregates to the average paste thickness as shown in Figure 2.13.

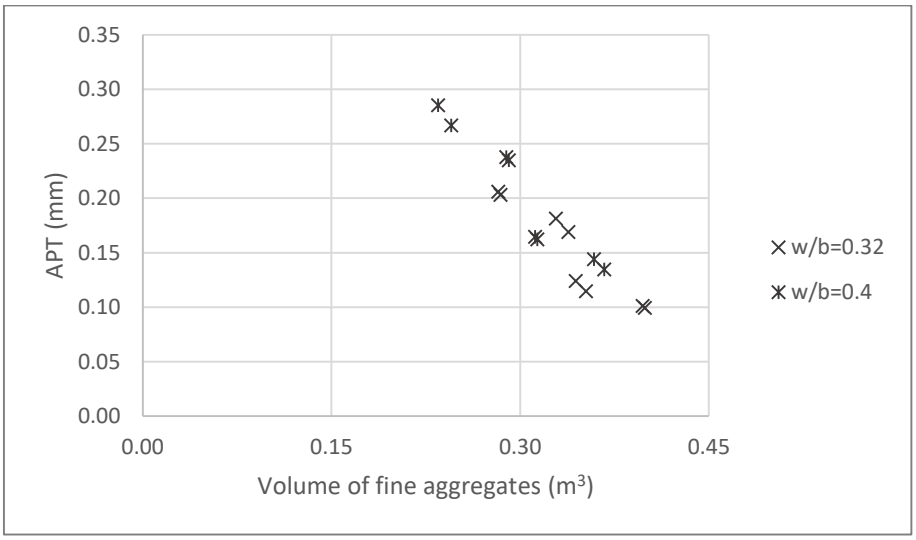

Figure 2.13: Relationship between the APT values (mm) and the volume of fine aggregtes (m^3) for both w/b ratios

Table 2.7: φmax and APT measurements

Mix #	ϕ_s	ϕ_{ca}	ϕ_{max}	ϕ/ϕ_{max}	D (mm)	APT (mm)
1	0.338	0.250	0.776	0.758	6.385	0.169
2	0.352	0.300	0.782	0.834	6.555	0.115
3	0.399	0.250	0.770	0.843	6.180	0.099
4	0.284	0.300	0.788	0.741	6.800	0.203
5	0.397	0.250	0.770	0.840	6.185	0.101
6	0.282	0.300	0.789	0.739	6.806	0.206
7	0.328	0.250	0.777	0.744	6.421	0.181
8	0.344	0.300	0.782	0.823	6.583	0.124
9	0.367	0.250	0.773	0.797	6.286	0.134
10	0.245	0.300	0.792	0.688	6.958	0.267
11	0.291	0.250	0.782	0.692	6.567	0.235
12	0.313	0.300	0.785	0.781	6.690	0.162
13	0.289	0.250	0.782	0.689	6.574	0.238
14	0.312	0.300	0.786	0.779	6.696	0.164
15	0.358	0.250	0.774	0.786	6.314	0.144
16	0.235	0.300	0.792	0.675	7.003	0.285
17	0.321	0.275	0.782	0.762	6.563	0.172

2.4.2.2 Chemical admixtures

Both HRWRA and VMA admixtures were used in this study to control the flow and segregation of the mixtures. In order to minimize/eliminate the risk of segregation, VMA was used in the high w/b mixtures with a fixed dosage of 400 mL/100 kg of binder. Even though VMA was only intended to be added to the high w/b mixtures, it was also used in one of the low w/b ratio mixtures, mix #4, due to observed segregation. Therefore, this mixture will be omitted from the analysis. In regards to the HRWRA, incremental dosages, based on the testing procedure stated in section 3.4, were added to all mixtures until the slump flow is within the targeted range. The recommended HRWRA and VMA dosage, mL/100kg of binder, by BASF (2014) were 130-975 and 130-910 respectively. The HRWRA dosages, mL/100 kg of binder, corresponding to the low w/b and high w/b ratio mixtures were in the range of 650-1127 & 300-680 respectively. It is important to note that the high w/b mixtures have VMA added to them, which explains the relatively high amounts of superplasticizers added to attain a slump flow value within the targeted range.

2.4.2.2.1 HRWRA demand and the composition of SCC

For a given range of slump flow values, the HRWRA demand for each mixture greatly depends on the mixture composition. Since VMA was used in only half of the experimental program, the effect of the mixture composition on the HRWRA demand will be investigated in each of the w/b ratios independently.

Table 2.8 illustrates the effect of the average paste thickness as well as the supplementary cementitious materials (SF and GGBFS addition) on the amount of HRWRA needed for both w/b ratio mixtures. It is important to note that the APT values are within a range and are not equal for precise comparison.

Results show that for mixtures with the same binder composition, i.e. same GGBFS and SF levels, the HRWRA dosages required to achieve the targeted slump flow range, for both w/b ratios, was shown to decrease as the APT increases as illustrated in Table 2.8. Moreover, for a given range of paste thickness, the amount of HRWRA increases when 8 % of binder content is replaced by silica fume due to its high fineness, while decreases,

when 30 % of cement is replaced by GGBFS due to its glassy texture, which is known to enhances the workability for a constant water content.

Table 2.8: HRWRA dosages, in mL/ 100 kg of binder, added to the low and high w/b mixtures when incoporating either 8% SF or 30 % GGBFS to mixtures with low and high APT (mm) ranges

	w/b =0.32		w/b = 0.4	
	Low APT (0.099–0.124)	High APT (0.169– 0.206)	Low APT (0.134– 0.164)	High APT (0.235- 0.285)
No SCMs	790	700	490	330
8% SF	1130	830	680	450
30% GGBFS	650	-	375	300

2.4.2.3 Workability tests (Slump flow, T_{50}, L-Box, Column Segregation Column) and mix composition

2.4.2.3.1 Slump flow using the SLRM

The slump flow measurements, reported in Table 2.6, were measured using the SLRM according to ASTM C1611 (2009). With the use of chemical admixtures, the majority of the mixtures reached the targeted slump flow range of 650 ± 50 mm except for few mixtures. The effect of the mix composition on the slump flow measurements, as well as the amount of chemical admixtures needed to obtain the measured slump flow values, are going to be investigated for each of the w/b ratios mixtures.

- Low w/b ratio (w/b =0.32)

Upon examining the slump flow values for the low w/b mixtures, one can note a wide range of the slump flow measurements i.e. 560 mm to 760 mm. Within these mixtures, the presence of SF as the only supplementary cementitious materials, resulted in slump flow less than 600 mm as illustrated in Table 2.9. In fact, high dosages of HRWRA i.e. 825 and 1126 mL/100 kg were added to these mixtures depending on their relative APT values, and yet the slump flow was below the minimum target i.e. 560 and 590 mm respectively. This is attributed to the increase in both the fineness and Pozzolanic properties of silica fume, which increases the inter-particle friction and therefore decreases the slump flow. As for the mixtures containing both supplementary

cementitious materials i.e. 8 % SF and 30% GGBFS, higher slump flow measurements was observed i.e. 610 mm and 635 mm with lower demand for HRWRA i.e., 840 and 650 mL/ 100 kg of binder for APT values of 0.124 mm and 0.181 mm respectively. This is attributed to the glassy texture of GGBFS which improves the workability without the need to increase the superplasticizer content. Moreover, higher slump flow values were witnessed for the mixtures containing no SF. Within these mixtures, even a higher slump flow was achieved for the mixtures containing GGBFS compared to the mixtures containing no supplementary cementitious materials. From the results reported in Table 2.9 and for a similar APT value, the mixture with GGBFS resulted in a higher slump flow i.e. 680 mm than the mixture with no GGBFS i.e. 638 mm, and yet required less HRWRA i.e. 650 mL/100 kg of binder, compared to a dosage of 785 mL/100 kg of binder. In other words, the addition of GGBFS to the low w/b mixtures was shown to increase the slump flow by 7 %, while decreasing the HRWRA demand by 18 % for low average paste thickness of around 0.110 mm.

Table 2.9: Slump flow measurements along with APT and HRWRA for the low w/b mixtures with supplementary cementitious materials and no supplementary cementitious materials

Supplementary Cementitious Material	Slump flow (mm)	HRWRA (mL/100 kg of binder)	APT (mm)
SF	560	825	0.206
	590	1125	0.101
SF & GGBFS	610	840	0.124
	635	650	0.181
GGBFS	680	650	0.099
-	638	785	0.115

- High w/b ratio (w/b=0.4)

In regards to the slump flow values corresponding to the high w/b ratio, a lower and a close range was witnessed, 545 mm to 665 mm, which was unexpected. This is mostly attributed to the VMA usage. With the increase in the cohesion within the binder paste, a decrease in the slump flow measurements was witnessed, compared to the low w/b ratio mixtures. The VMA dosage and the HRWRA range which were added to these

mixtures were 400 mL/ 100 kg of binder and 300 to 680 mL/ 100 kg of binder respectively. The slump flow corresponding to the mixtures containing SF exhibited a lower range i.e. 545-605 mm than the mixtures without SF i.e. 608 - 665 mm, which was achieved by adding HRWRA dosage of 470 - 525 mL/100 kg of binder for an APT range of 0.134 - 0.267 mm, and 301 – 490 mL/100 kg of binder for an APT range of 0.144 – 0.285 respectively. As expected, an increase in HRWRA was required by the mixtures with silica fume. Moreover, the relative amount of HRWRA added to each mixture, greatly depend on the APT value.

2.4.2.3.2 T_{50}

Similarly, a wide range of T_{50} measurements was recorded within the low w/b ratio mixtures, ranging as low as 2.3 s up to 7.7 s, revealing other important factors. One of the most significant variable affecting the flow time, T_{50}, is the w/b ratio shown in Figure 2.14. Moreover, the APT values of the low w/b ratio mixtures were also shown to negatively impact the T_{50} measurements as illustrated in Figure 2.15. Typically, as the paste thickness around the particles decreases, more friction would develop between the aggregates as they move past each other. Therefore, more resistance i.e. increase in viscosity is experienced as soon as the concrete starts to flow i.e. yield stress is exceeded.

Table 2.10: The effect of four ranges of APT values along with the added HRWRA, mL/100 kg binder, on T_{50} for the mixtures with and without silica fume

	Without SF		With SF	
APT (mm)	HRWRA	T_{50} (s)	HRWRA	T_{50} (s)
Low APT (0.099 - 0.115)	700	7	1125	6.75
Low/moderate APT (0.124)	-	-	840	4.13
Moderate/high APT (0.169-0.181)	690	2.28	650	4.72
High APT (0.206)	-	-	825	3.5

The table above illustrates the influence of four ranges of APT values (low, low/moderate, moderate/high and high), along with the added HRWRA, on the T_{50} measurements for mixtures with and without silica fume. From the results shown in Table 2.10, one can conclude that for a given range of APT values, the average paste thickness becomes a critical parameter when designing mixtures without SF compared to mixtures with SF. Due to silica fume's high fineness, which stabilizes the concrete volume, the mixture's resistance to flow increases as illustrated in Table 2.10.

As for the T_{50} measurements corresponding to the high water to binder ratio mixtures, they were all below the minimum target flow time of 2 s which could indicate stability concerns.

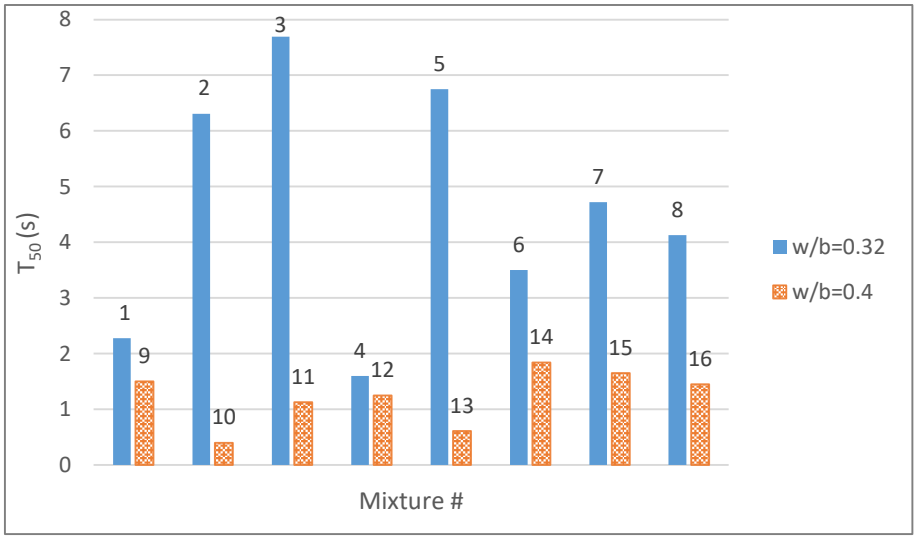

Figure 2.14: T_{50} results for w/b=0.32 and w/b=0.4 mixtures

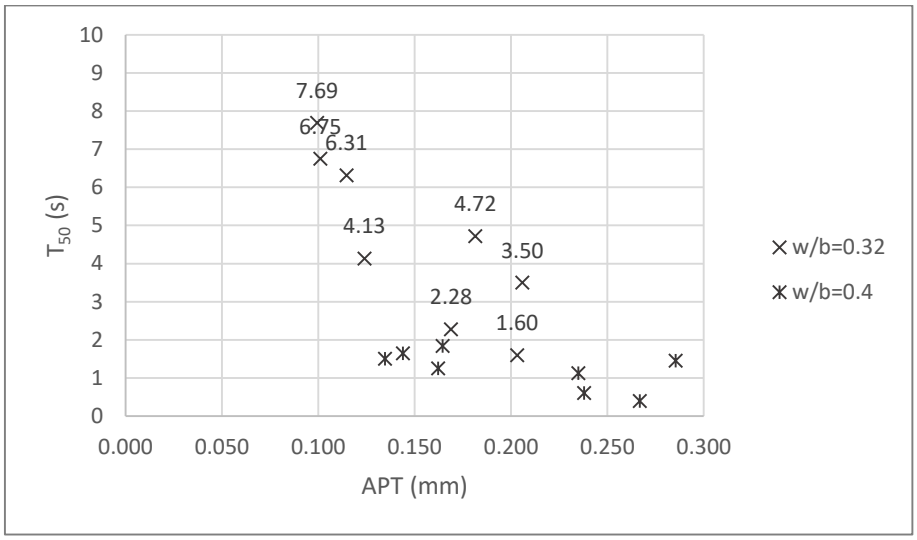

Figure 2.15: Relationship between T_{50} measurements and APT

2.4.2.3.3 L-Box

Regarding the L-Box ratios, all of the low w/b ratio mixtures with silica fume incorporated in them exhibited low passibility ratio (0.3-0.59). Within these mixtures, the presence of GGBFS improved the passing ratio, however, they were still below a ratio of 0.6. These mixtures can be problematic in applications where highly congested reinforcements are required. Moreover, mix # 16 from the high w/b mixtures resulted in a low passing ratio of 0.54 which was consistent with low measured slump flow. Figure 2.16 shows the relation between the confined and the free flow tests, L-Box and slump flow respectively, for both w/b ratios. A better correlation exists for the low w/b mixtures.

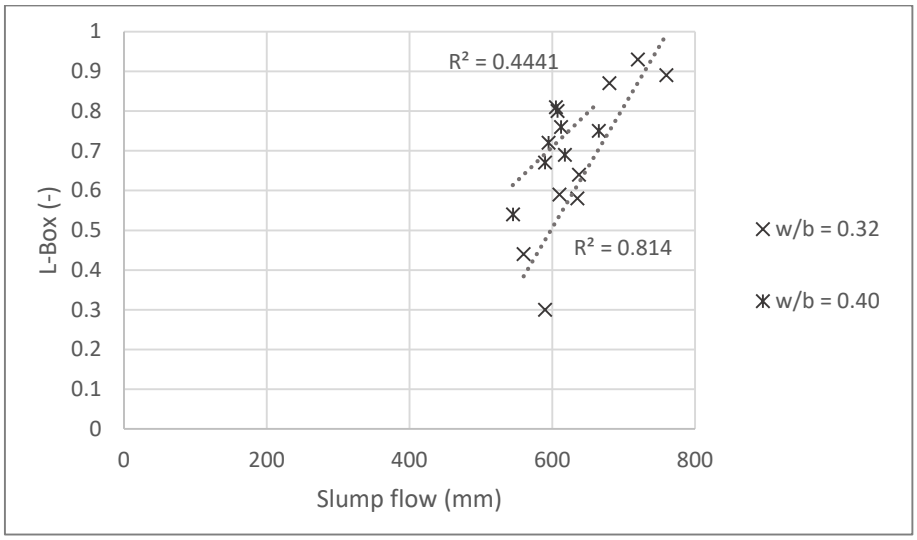

Figure 2.16: Relationship between L-Box ratio and Slump flow

2.4.2.3.4 Column Segregation Test

All of the SCC mixtures exhibited no sign of segregation based on the segregation index achieved by the column segregation test. However, these results do not give an indication of the mixture's stability under dynamic conditions, particularly the mixtures with low T_{50} values.

2.4.3 Rheological properties

To estimate the rheological properties of concrete, a rheological model is assumed as an a priori. The three rheological models most used in the literature for concrete are Bingham model, Herschel-Bulkley model and modified Bingham model which are represented by Eq. 2.1, Eq. 2.2 and Eq. 2.4, respectively. In this study, only the Bingham and modified Bingham model are used as they provide well-defined rheological properties, namely the yield stress and plastic viscosity.

The rheological data were fitted to the Bingham and the Modified-Bingham (M-B) models and the results are given in Table 2.11. In general, both models showed good coefficient of determination. However, a negative yield stress was obtained when fitting the experimental data of Mix # 3 to the Bingham model, which has no physical interpretation. For these cases, a non-linear model would be a better representative of

the material's response due to its ability to capture any non-linearity as shown in Figure 2.17 below.

Table 2.11: Bingham and Modified Bingham parameters along with R^2

	Bingham model			Modified-Bingham model			
Mix	Yield (Pa)	Viscosity (Pa.s)	R^2	Yield (Pa)	Viscosity (Pa.s)	c ($Pa.s^2$)	R^2
1	14	32	0.99	14	32	0.03	0.99
2	35	51	0.99	39	49	0.22	0.99
3	-11	88	0.99	32	62	2.46	0.99
4	39	23	0.99	31	28	0.47	0.99
5	73	37	0.99	59	45	0.79	0.99
6	72	23	0.99	66	26	0.32	0.99
7	60	41	0.99	52	45	0.44	0.99
8	79	42	0.99	66	50	0.79	0.99
9	79	13	0.97	68	19	0.50	0.99
10	82	5	0.98	79	6	0.11	0.99
11	70	7	0.99	66	9	0.18	0.99
12	78	14	0.97	66	20	0.56	0.99
13	87	6	0.99	88	5	0.04	0.99
14	90	11	0.98	80	16	0.44	0.99
15	98	13	0.98	86	19	0.54	0.99
16	108	6	0.99	105	7	0.10	0.99
17	47.3±7.6	16±1.7	0.99	41.3±8.77	19.3±1.55	0.29±0.07	0.99

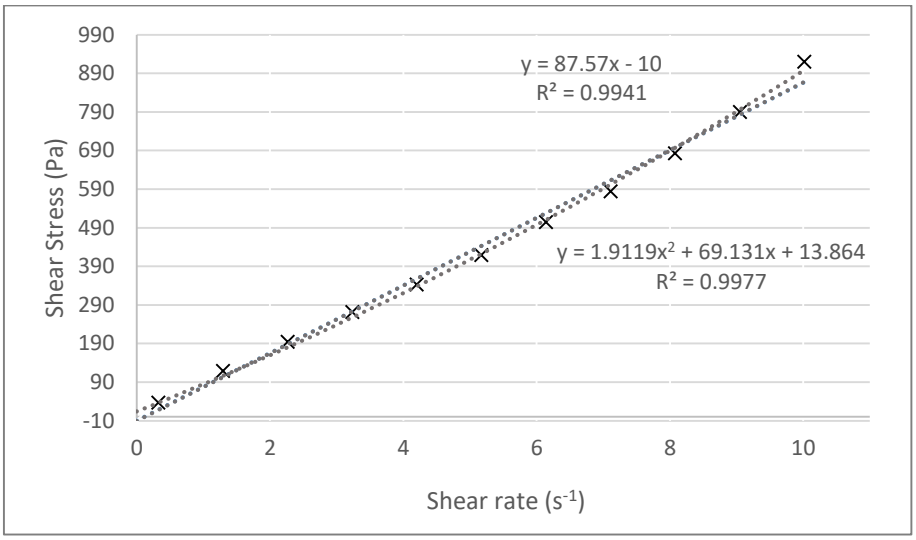

Figure 2.17: Flow curve of Mix #3 fitted with Bingham and Modified Bingham models

However, as this non-linearity increases, the differences in terms of the rheological parameters, between Bingham and M-B models increase. Table 2.12 reveals the percentage difference of the rheological properties for the mixes that exhibited shear thinning ($c < 0$), shear thickening ($c > 0$), and linear response ($c \approx 0$).

Table 2.12: % differences of τ_0 and μ using both the Bingham and Modified - Bingham for $c < 0$, $c = 0$, and $c > 0$

Mix #	c	|% difference of τ_0|	|% difference of μ|
13	0.04	1	8
2	0.22	11	4
5	-0.79	19	22
3	2.46	390	29

A new rheological model is proposed to distinguish between the linear and non-linear portion of the response due to shear thinning/ thickening phenomena, which is usually captured at higher shear rates. It is postulated that the flow regime can be decomposed into a linear and nonlinear part with the yield stress and plastic viscosity determined using the linear response; while c is determined from the non-linear part of the curve.

Linear response occurs when the shear rate ($\dot{\gamma}$) is less than the critical shear rate ($\dot{\gamma}_c$). The proposed approach is graphically illustrated in Figure 2.18.

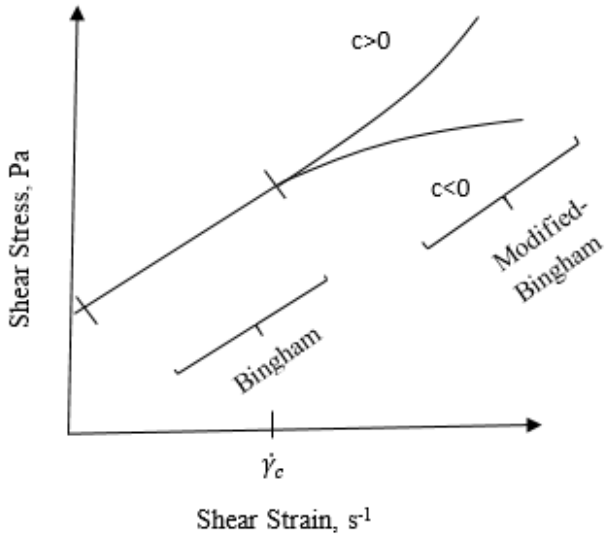

Figure 2.18: Illustration of the Revised Modified Bingham Model

$\dot{\gamma}_c$ is defined as the shear rate at which a deviation on the flow curve start to take place as shown in Figure 2.18.

$$\begin{cases} \tau = \tau_o + \mu\dot{\gamma} & , \ \dot{\gamma} < \dot{\gamma}_c \\ c = avg(\frac{\tau - \tau_o - \mu\dot{\gamma}}{\dot{\gamma}^2}), & \dot{\gamma} > \dot{\gamma}_c \end{cases}$$ Equation 2.9

To further illustrate the proposed model, Figure 2.19 shows the experimental data of mix # 12 when fitted to the Revised Modified-Bingham represented by the dotted line and the Bingham model fitted to the linear part of the curve where the rheological properties are obtained. The significant deviation between the two lines is due to the material response at higher shear rates from which c was calculated. This method will have the ability to capture the materials' properties more precisely at lower shear rates regardless of the behaviour of the mixture at higher shear rates, and yet capture the nonlinear part through the term "c" in a more precise manner.

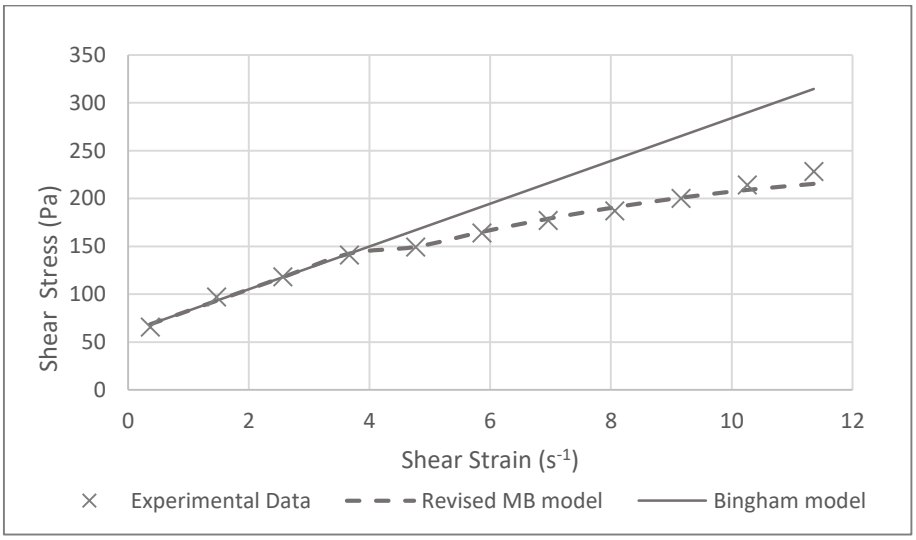

Figure 2.19: The Bingham model fitted to the first 4 experimental data points of mix #12; deviation from the Bingham is shown at high shear rates

Table 2.13: Revised M-B properties, differences in the rheological properties between the M-B and the proposed model along with thixotropy measurements

Mix	Yield Stress (Pa)	Viscosity (Pa.s)	R^2	$\dot{\gamma}_c$ (s^{-1})	c (Pa.s2)	Yield (%)	Viscosity (%)	Thixotropy (Pa.s-1)
1	16	31	0.999	9	0.1	14	3	344
2	40	49	0.997	8	0.17	3	0	1061
3	16	78	1	5.17	0.59	50	26	1972
4	34	25	0.991	6.14	-0.18	10	11	173
5	60	42	0.988	5.17	-0.48	2	7	638
6	61	29	0.984	3.23	-0.66	8	12	293
7	49	46	0.992	4.2	-0.53	6	2	586
8	66	48	0.984	5.17	-0.57	0	4	710
9	61	24	0.996	2.56	-1.06	10	26	61
10	79	6	0.988	5.86	-0.09	0	0	-106
11	66	8	0.991	4.76	-0.1	0	11	-28
12	60	22	0.991	3.66	-0.77	9	10	-8.6
13	87	6	1	n/a	0	1	20	-34
14	82	14	0.991	5.86	-0.22	3	13	0
15	86	17	0.991	4.76	-0.35	0	11	60
16	106	6	0.984	6.96	-0.05	1	14	-83
17	38±8	20±1	0.9797	4.76±1.10	0.39±0.16	7	5	198

*Negative area reveals anti-thixotropic behaviour.

Differences in the calculations of yield and viscosity using both the M-B and the proposed models are given in Table 2.13. Of significance are the values corresponding to mix #3 where the error is 50% and 26% for the yield stress and plastic viscosity respectively. These results indicate that separating the linear and nonlinear response of the flow provides a better characterization of the Bingham properties, as the former should not be affected by the degree of nonlinearity as is the case for mix #3. Moreover, the calculation of the plastic viscosity is more sensitive to the calculation method as 10 mixes showed a difference greater to or equal to 10% in comparison to the yield stress with only 4 mixes. Although this study possesses a small sample, the results are convincing to use the properties from the revised Modified Bingham model in the subsequent analyses.

2.4.4 Relationship between the empirical tests and the rheological properties

Historically, researchers have compared the rheological properties to workability measures as the latter is faster and easier to implement (Chidiac et al., 2000; Nielsson & Wallevik, 2003). Slump flow has been associated with the yield stress of the material as the spread of the concrete depends on the capacity of the material to support itself. Further, the resistance to flow represented by plastic viscosity has been associated with the travel time concrete needs to reach a spread of 50 cm, T_{50}.

Figure 2.20 shows a plot of yield stress versus slump flow. Results show that the yield stress is inversely proportional to the slump flow as is expected. Statistically, the fit shows that slump flow accounts for 69% of the yield stress variability where R^2 is equal to 0.69. Estimation of the error is calculated using the root square mean deviation (RSMD) which represents the sample standard deviation. RSMD is found equal 13.7 Pa.

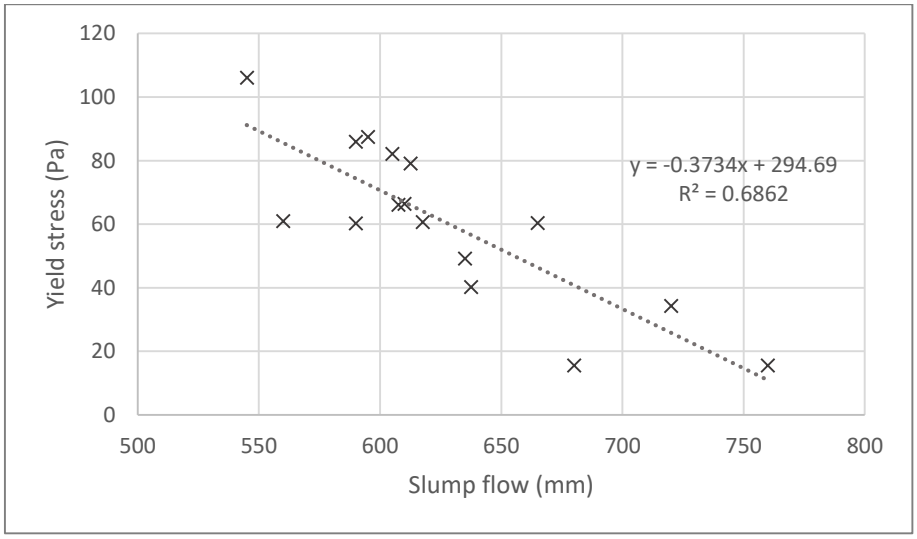

Figure 2.20: The correlation between the yield stress (dynamic yield stress) and the slump flow

Figure 2.21 shows a plot of plastic viscosity versus T_{50}. Results show that the viscosity is linearly proportional to the flow time as is expected. The higher the resistance to flow the longer it will take the material to reach a specified spread. Statistically, the fit

shows that T_{50} accounts for 84% of the plastic viscosity variability where R^2 is equal to 0.84. Estimation of the error is calculated using RSMD and is found equal 7.9 Pa.s.

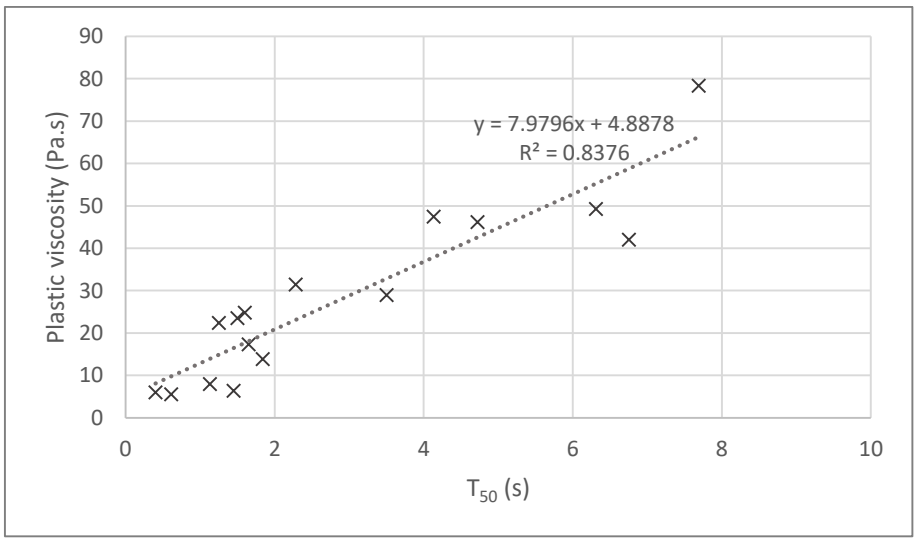

Figure 2.21: The correlation between plastic viscosity and T_{50}

2.4.5 Mix composition and rheological properties

The composition of the mixture is known to influence the flow characteristics of the material. However, the introduction of chemical admixtures, specifically HRWRA and VMA, the response is more influenced by the admixtures than the composition. Moreover, to achieve certain properties, the amount of admixtures added depends on the mixture composition. This effect is investigated.

2.4.5.1 Plastic viscosity vs mix composition

2.4.5.1.1 Water to Binder ratio (w/b)

Two w/b ratios (0.32 and 0.4) were investigated in this study. Typically, increasing the water to binder ratio increases the workability of concrete mixes, and hence reduces both the plastic viscosity and yield stress. As expected, the lower w/b ratio of 0.32 resulted in more viscous mixtures, which was also previously confirmed from the higher T_{50} measurements.

2.4.5.1.2 Average Paste Thickness & Volume of Fine aggregates

Since the plastic viscosity was shown to correlate well with the T_{50} measurements, the influence of the APT can also be related to the plastic viscosity as shown in Figure 2.22. This parameter gives a more comprehensive description, since it takes into account the combined aggregate gradation, by incorporating the maximum packing density, as well as the aggregate proportioning. Moreover, the APT was shown to be inversely related to the volume of fine aggregates. Therefore, one can also come to generalize that the volume of fine aggregates directly influences the plastic viscosity of the low w/b ratio mixtures as shown in Figure 2.23. By decreasing the APT (increasing the fine aggregate volume), the distance between the aggregates decreases, which in turn increases the inter-particle friction between the moving aggregates, and hence increasing the viscosity. To further illustrate, the mixture with the least APT value of 0.099 mm, (volume of fine aggregate of ≈ 0.4 m^3 per $1m^3$ of concrete), resulted in the most viscous mixture.

With regards to the high w/b ratio mixtures, an increase in the plastic viscosity was witnessed only when the volume of the fine aggregates exceeded 0.3 m^3 per $1m^3$ of concrete (APT < 0.164 mm). Below this volume (APT > 0.235 mm), mixtures exhibited a significantly low plastic viscosities measurements as shown in Figure 2.23. Adding VMA admixtures to these mixtures might have improved their stability under static conditions, however, they might be at risk under high shearing rates.

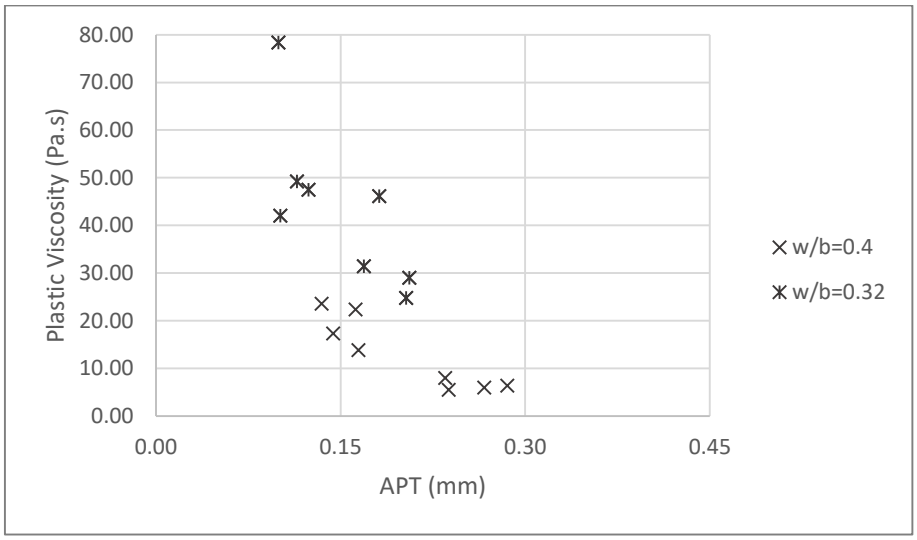

Figure 2.22: Relationship between the plastic viscosity (Pa.s) and APT (mm)

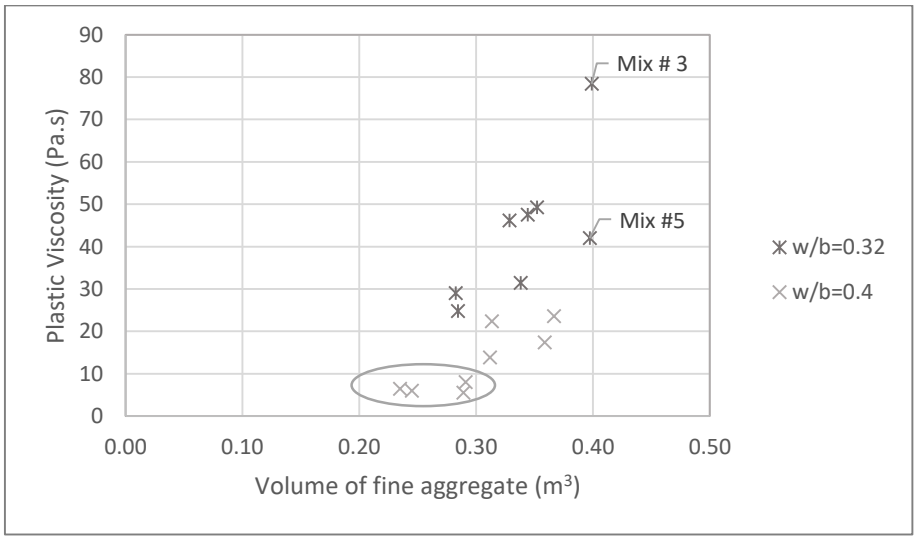

Figure 2.23: Correlation between the plastic viscosity (Pa.s) and the volume of fine aggregates (m^3) for both w/b ratios

2.4.5.1.3 Chemical admixtures

In terms of the binder and coarse aggregates levels, mix # 5 tend to be a similar mixture to mix # 3 with a similar APT value. However, it showed a much lower viscosity as shown in Figure 2.24. Owing to the incorporation of SF in that mixture, the amount of HRWRA that was needed to achieve the targeted slump flow, was significantly higher. Adding such a high amount of HRWRA was most likely the reason

as to the significant reduction in plastic viscosity. Figure 2.24 and 2.25 shows the effect of HRWRA on the plastic viscosity for both w/b ratios. The results reveal that by significantly increasing the amount of HRWRA, for mixtures within a given range of APT, the plastic viscosity decreases.

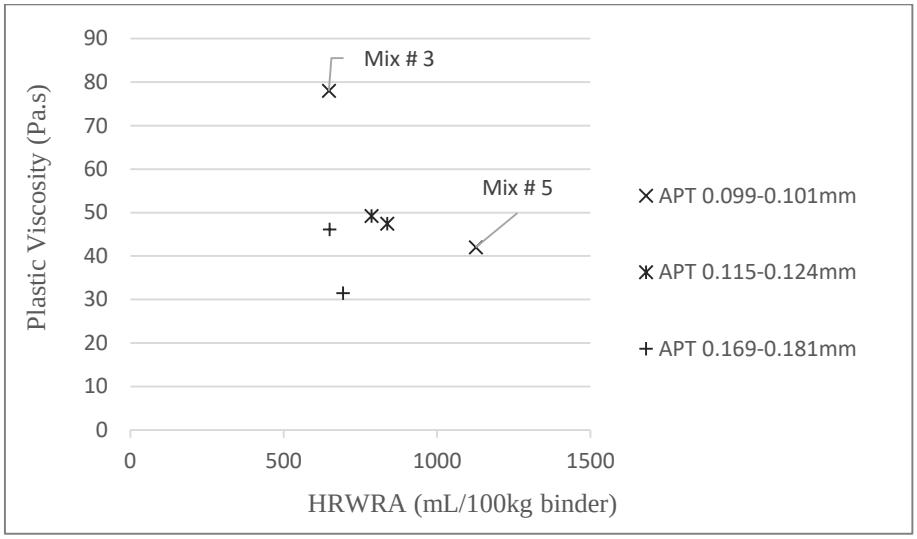

Figure 2.24: The effect of HRWRA dosages (mL per 100 kg of binder) on the plastic viscosity for w/b=0.32 for mixtures with similar APT values

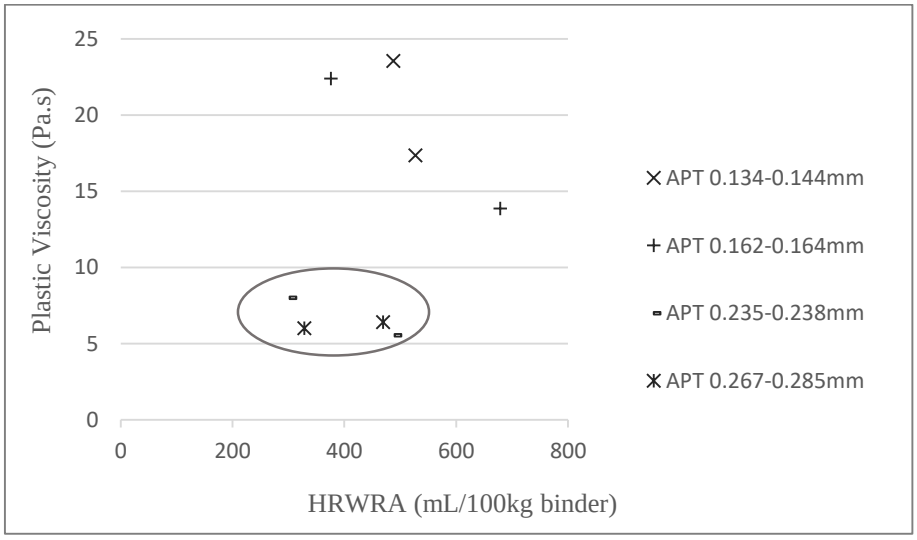

Figure 2.25:The effect of HRWRA dosages (mL per 100 kg of binder) on the plastic viscosity for w/b=0.4 for mixtures with similar APT values

For the mixtures with a high APT value > 0.235 mm (w/b =0.40), increasing the HRWRA dosages to 300 and 400 mL/100kg of binder for the mixtures with and without silica fume respectively, resulted in negligible plastic viscosity measurements of 6 - 8 Pa.s as shown in Figure 2.25. These mixtures are more prone to segregation under dynamic conditions.

Based on the above discussion, a set of rules were derived from the 16 mixtures to relate the mixture composition, as well the as the chemical admixtures needed to achieve a certain category for the plastic viscosity response (Very low, Low, low/moderate, moderate, high and very high) for each of the w/b ratios.

For w/b = 0.32 mixtures

1. **Moderate plastic viscosity (21 – 31 Pa.s):**

Without silica fume

Using mixtures with moderate/high APT of 0.169 mm and HRWRA dosage of 700 mL/ 100 kg of binder (from Table 2.10).

With silica fume

Using mixtures with high APT of 0.206 mm and HRWRA dosage of 830 mL/ 100 kg of binder.

2. **High plastic viscosity (40 – 50 Pa.s):**

Without silica fume

Using mixtures with low APT of 0.115 mm and HRWRA dosage of 790 mL/ 100 kg of binder.

With silica fume

Using mixtures with low APT of 0.101 mm and HRWRA of 1130 mL/ 100 kg of binder or using mixtures with low/moderate APT of 0.124 mm and HRWRA dosage of 850 mL/ 100 kg of binder

3. **Very high plastic viscosity (≈ 80 Pa.s)**

Without silica fume

Using mixtures with low APT of 0.099 mm and HRWRA dosage of 650 mL/ 100 kg of binder.

For the w/b =0.40 with VMA dosage of 400 mL/100 kg of binder

1. **Very low plastic viscosity (6 -8 Pa.s)**

Without silica fume:

Using mixtures with a high APT of 0.235 - 0.267 mm and HRWRA dosage of 301 - 328 mL/ 100 kg of binder.

2. **Low plastic viscosity (14 – 17 Pa.s)**

With silica fume:

Using mixtures with a moderate APT of 0.144 - 0.164 mm and HRWRA dosage of 530 - 680 mL/ 100 kg of binder.

3. **Low/Moderate plastic viscosity (22 – 24 Pa.s)**

Without silica fume:

Using mixtures with a moderate APT of 0.134 – 0.162 mm and HRWRA dosage of 490 - 380 mL/ 100 kg of binder.

2.4.5.2 Yield stress (dynamic yield stress) vs mix composition

2.4.5.2.1 Water to binder ratio (w/b)

Increasing the w/b ratio significantly increased the yield stress which was unanticipated. That could be attributed to the implementation of 400 mL of VMA admixtures per 100 kg of binder. Therefore, the impact of this variable by itself on the yield stress couldn't be investigated in this study.

2.4.5.2.2 Silica fume (SF)

Incorporating SF as partial replacement of cement was shown to increase the yield stress for both w/b ratio mixtures as shown in Figure 2.26 and 2.27. As expected, an increase in the SF content from 0% to 8%, led to an increase in the mixtures stiffness because of its high fineness. It is important to note that silica's fume effect on the yield stress, was more pronounced for w/b = 0.32 mixtures due to the increase in the particle concentration which in turn, increases the interactions in a given volume of fresh concrete.

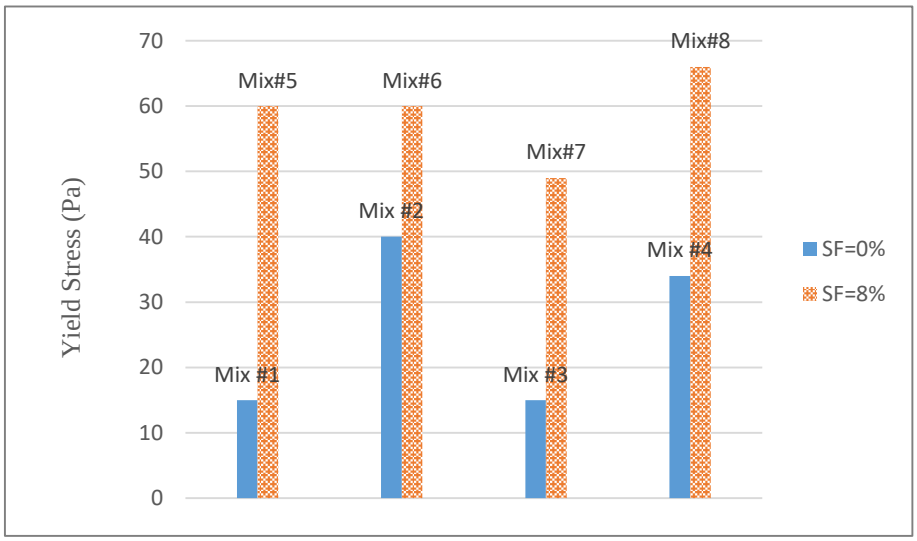

Figure 2.26: Influence of silica fume addition on the yield stress for w/b=0.32 mixtures

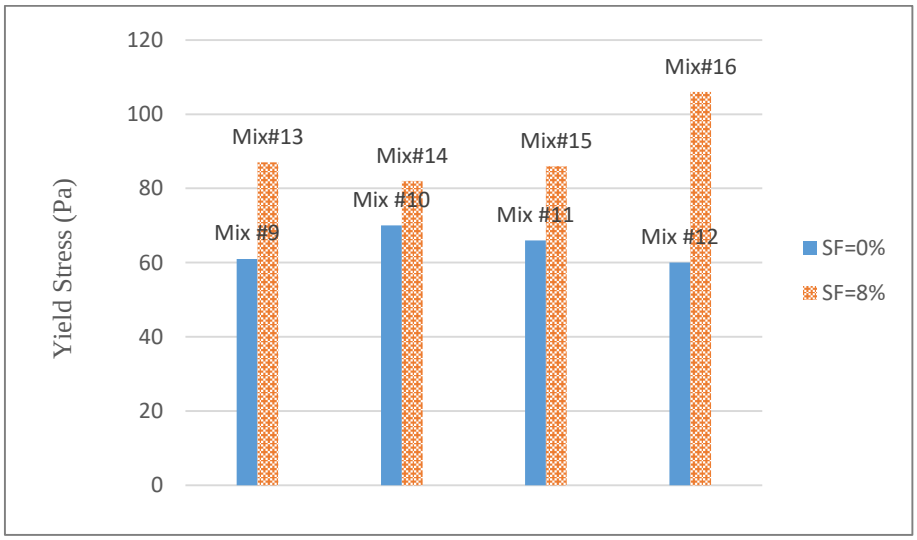

Figure 2.27: Influence of silica fume addition on the yield stress for w/b=0.4 mixtures

2.4.5.2.3 Coarse aggregates

When considering the yield stress of concrete, the inter-granular contact and aggregate interlocking become relevant. With that being said, the aggregate volume fraction could be an indicator of how close the particles are with respect to each other for a given paste

volume. In order to study the influence of the coarse aggregates content on the yield stress, silica fume which was shown to be a significant variable was kept constant. As expected, an increase in the volume of coarse aggregates from 0.25 to 0.30, while keeping both the SF and the binder content constant, increased the yield stress for w/b =0.32 mixtures as shown in Figure 2.28 and 2.29. However, this increase was more pronounced for the mixtures without silica fume.

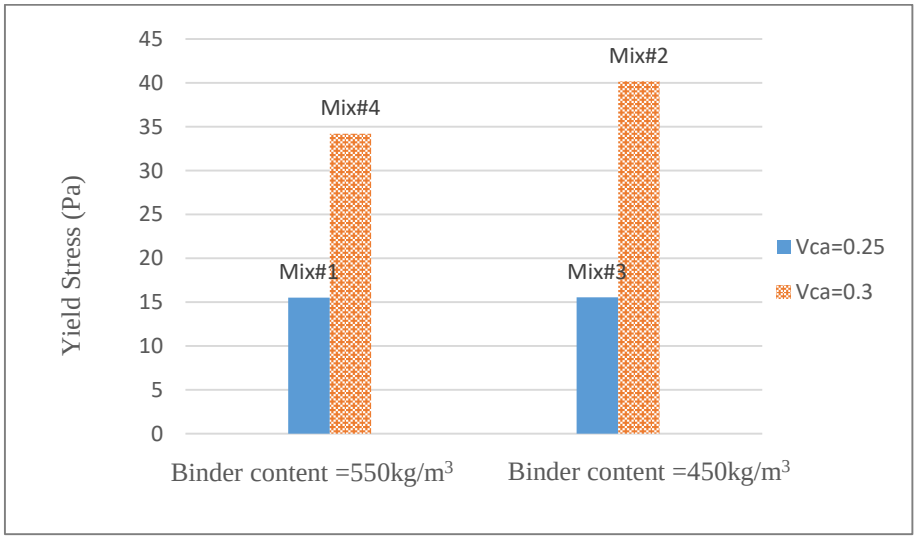

Figure 2.28: Effect of Vca on the yield stress for low w/b mixes without silica fume

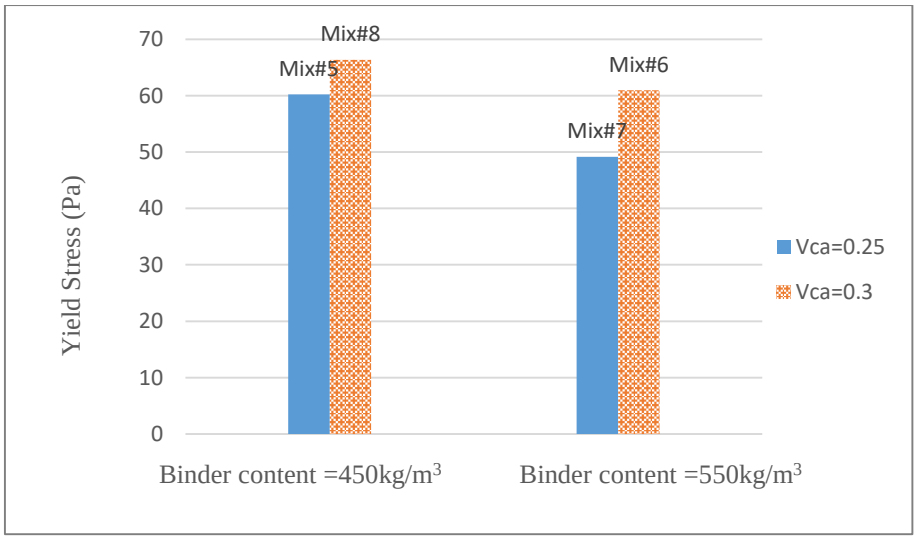

Figure 2.29: Effect of Vca on the yield stress for low w/b mixes with Silica fume

As for the high w/b ratio mixtures, a significant increase in the yield stress was witnessed only when the ratio of coarse to fine aggregates (CA/FA), by mass, exceeded a ratio of 1. With regards to the composition of these mixtures, both the coarse aggregates and the binder content level were set to (+1) leaving little room for the fine aggregates to occupy. Increasing this ratio to 1.22 and 1.27 (volume of fine aggregates 0.24 m^3) for mix # 10 and 16 respectively, resulted in 25 % increase in the yield stress. Below this ratio, the yield stress didn't seem to change much as shown in Figure 2.30.

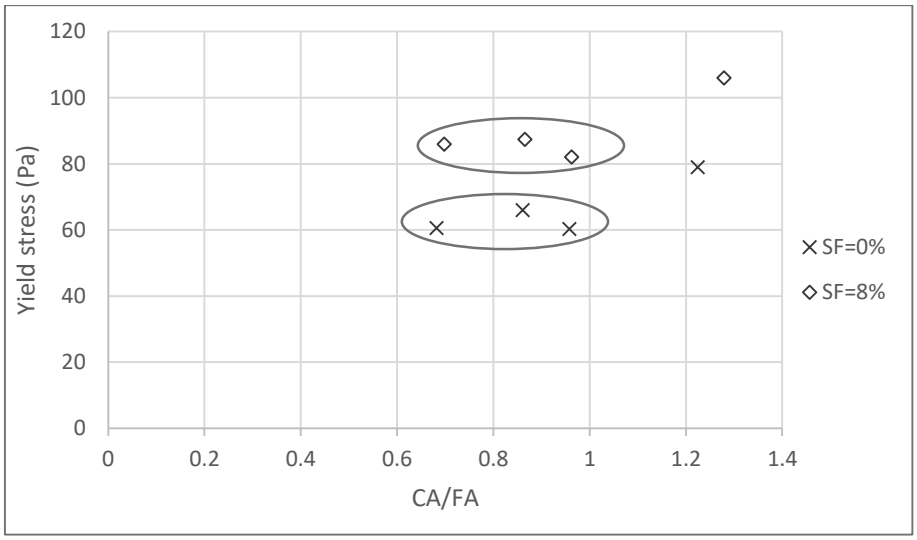

Figure 2.30: Effect of coarse aggregate to fine aggregate CA/FA ratio by mass on the yield stress for high w/b ratio mixtures

2.4.5.2.4 Chemical admixtures

The yield stress measurements corresponding to the high w/b ratio mixtures were, in fact, relatively higher (60-106 Pa) compared to the low w/b mixtures (15 – 66 Pa), which was also confirmed by the lower slump flow values.

As it has been previously mentioned, the yield stress is mainly affected by the addition of silica fume and the amount of coarse aggregates, bulk volume of coarse aggregates and CA/FA ratio for the low and high w/b ratio respectively. Furthermore, it is a well-known fact that the dispersion effect of superplasticizers decreases the yield stress, which was previously shown to be influenced by the mix composition (APT, SF and

GGBFS addition). Accordingly, rules have been derived from the 16 mixtures, in order to relate the mixture composition, as well the as the chemical admixtures needed to achieve a certain category for the yield stress response (Low, Low/moderate, moderate/high, High and Very High) for each of the w/b ratios.

For w/b = 0.32 mixtures

Without silica fume

1. **Low Yield stress (≈15 Pa):**

Using mixtures with APT of 0.099-0.169 mm and HRWRA dosage of 650 - 700 mL/ 100 kg of binder.

2. **Moderately low Yield stress (≈ 40 Pa):**

Using mixtures with low APT of 0.115 mm and HRWRA dosage ~ 800 mL/ 100 kg of binder.

With silica fume

3. **Moderately high Yield stress (50-66 Pa):**

Using mixtures with APT of 0.101 – 0.206 mm and HRWRA dosage of 650 -1125 mL/ 100 kg of binder, depending on the APT value and the GGBFS addition (HRWRA demand discussed in section 2.4.2.2.1).

For the w/b =0.40 with VMA dosage of 400 mL/100 kg of binder:

Without silica fume

1. **High Yield stress (60 -80 Pa):**

Using mixtures with APT of 0.134 – 0.267 mm and HRWRA dosage of 300-490 mL/ 100 kg of binder, depending on the APT value and GGBFS addition.

With silica fume

2. **Very high Yield stress (80- 106 Pa):**

Using mixtures with APT of 0.144 – 0.285 mm and HRWRA dosage of 470 -680 mL/ 100 kg of binder, depending on the APT value and GGBFS addition.

2.4.6 Thixotropy and Rheopexy

2.4.6.1 Thixotropy

Thixotropy is equal to the area between the up and down curve of the hysteresis loop. It is estimated using the trapezoidal rule. The area represents the stored energy required to overcome in order break down the structural built-up of the material. The more viscous the material is, the more energy is required to break down the structure and therefore increasing its thixotropic intensity. Figure 2.31 confirms that thixotropy correlates well with plastic viscosity for low w/b ratio mixes.

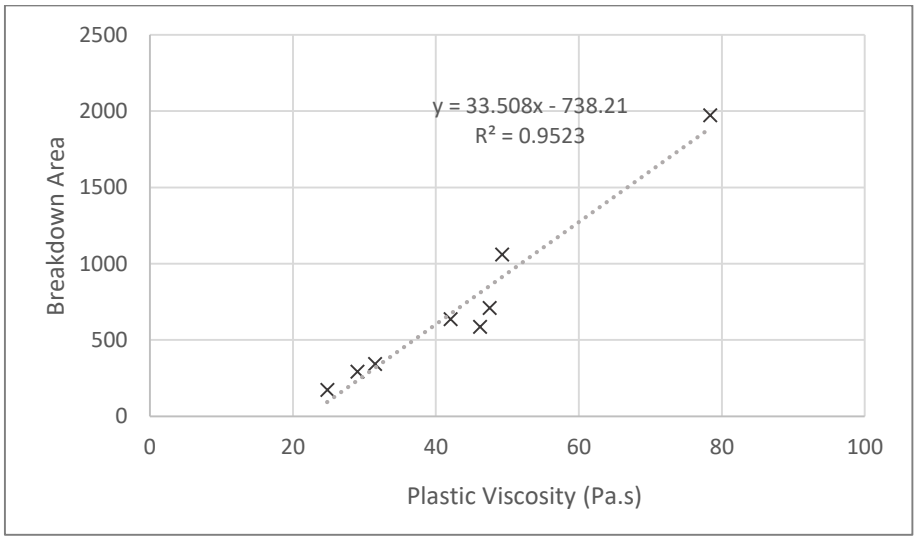

Figure 2.31: Relationship between breakdown area and thixotropy for w/b=0.32

Recognizing the correlation between thixotropy and plastic viscosity provides insight to controlling the flow of SCC. Decreasing APT by decreasing both the binder and coarse aggregates contents (or by increasing the fine aggregates), and by decreasing the HRWRA dosage lead to an increase in thixotropic intensity. Incorporating more fine aggregates seems to aid in rebuilding the structure as the mixture is subjected to shearing. Hence, requiring more energy to break down the structural built-up. With regards to cement paste, Ur'ev et al. (1997) related the flocculation rate of the cement particles to thixotropy. Due to the dispersion mechanism of HRWRA that keeps the cement particles apart due to the electrostatic repulsive forces and/or the steric hindrance (Flatt et al., 2000), the flocculation rate between the cement grains would

typically decrease. Consequently, the thixotropic behaviour is reduced. For most cases, VMA increases the viscosity and thus increases thixotropy.

2.4.6.2 Rheopexy

Rheopexic or anti-thixotropic materials generally exhibit lower viscosity when at rest than when flowing. Furthermore, its intensity increases as the material's viscosity is reduced. The behaviour is represented by a negative break down area i.e. positive build up area. In other words, the ramp down curve is located above the ramp up curve on the rheogram.

This response was observed for the majority of 0.4 w/b mixes. A closer look at the mixture composition shows that both HRWRA and VMA were added to assist with the flow and the stability of the mixture, respectively. The interaction has allowed the material to flow and provided the necessary resistance to segregation. If one compares the rheological properties of 0.32 and 0.4 mixes, one observes that the yield stress values for 0.32 mixes are lower than those for 0.4 mixes, whereas the plastic viscosity values are higher. As such, mixes with w/b equals 0.32 flows easily and possesses higher resistance to the flow. Although it is not possible to pinpoint the exact cause, the following observations can be made: 1) Mixes with 0.32 w/b need HRWRA to meet the slump flow target as they contain lower amount of water; 2) 0.4 w/b mixes contain more water, but still not sufficient to achieve the slump flow target, and thus required the addition of HRWRA which has or can compromise the stability of the mixtures; 3) VMA which tends to increase the viscosity and the thixotropy was added to the 0.4 w/b mixes, but the measured properties show that its effect was less significant in comparison to the addition of HRWRA and w/b; 4) Increasing the amount of VMA is found to negatively impact the concrete ability to meet the flow target. In brief, increasing the water content increases the thickness of the water layer around the cement particles and therefore increase the inter-particle distance. As a result, the particles flocculation decrease due to the decrease in the coagulation forces and hence resulting in a reduction in both the viscosity and thixotropy. Examination of the results shows that the mixes with the highest APT (highest binder and highest coarse aggregates content) exhibit the highest degree of anti-thixotropy. Furthermore, a small thixotropy

area was achieved when the binder and coarse aggregate content were set to the lower level (-1). Figures 2.32 and 2.33 show the combined effect of the mixtures composition (binder, and coarse aggregates content) and APT, respectively, on the structural breakdown/ buildup for high w/b mixes.

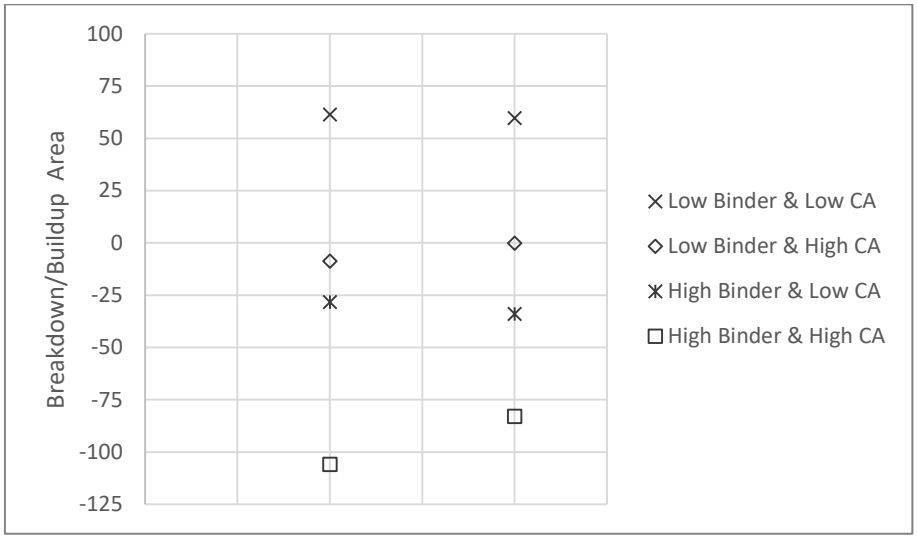

Figure 2.32: Relationship between breakdown/buildup area and the binder and the coarse aggregate levels for w/b = 0.4

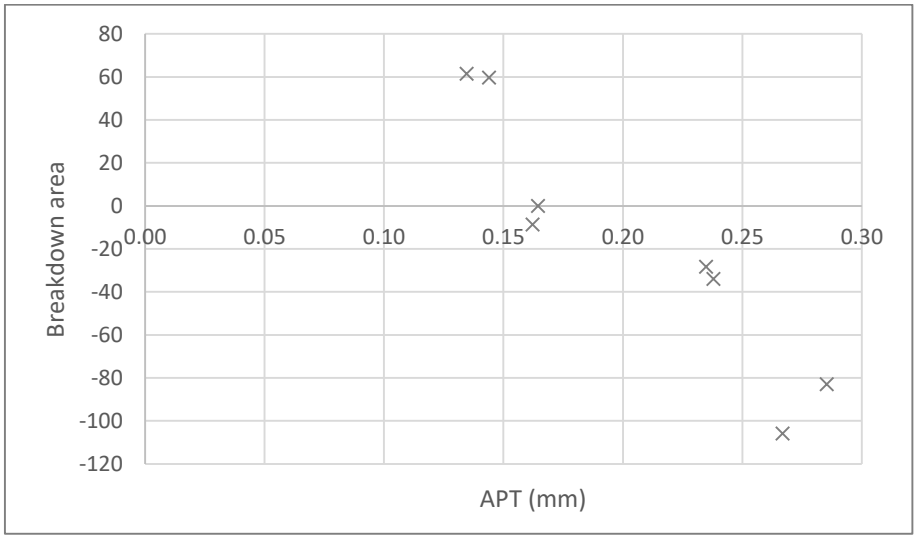

Figure 2.33: Relationship between breakdown/buildup area and the binder and the coarse aggregate levels for w/b = 0.4

2.4.7 Model Analyses

Analytical models were developed to statistically correlate the relationship between the response and the mixture composition. The models were derived using the coded units calculated using Eq. 2.10.

$$x_i = \frac{x_{i,actual} - x_{center}}{\Delta_i/2} \quad \text{Equation 2.10}$$

Where $x_{i,actual}$ and x_{center} are the actual value and the mean value, respectively, and Δ_i is the difference between the two levels.

A probability value of less than 0.05 was considered to be a significant evidence that the factor has a significant influence on the modeled response. Student tests, t-tests, were run to evaluate the significance of each of the main factors and their second order interaction on the response. However, to be able to use the t- distribution and later the confidence intervals, the responses must come from a normal distribution i.e. symmetric and unimodal (Dunn, 2010). In this investigation, Box-Cox transformation was used to normalize the plastic viscosity response using the equation below (Box and Cox, 1964).

$$y'_\lambda = \frac{y^\lambda - 1}{\lambda . \bar{g}_y^{\lambda-1}} \quad \text{Equation 2.11}$$

Where λ is the shift parameter; y'_λ is the new transformed data, and $\bar{g}_y$ is the geometric mean of the response variable. The optimal λ value, with the greatest correlation coefficient, was determined using the statistical software R. The tables below show the coefficient estimate for each of the factors, indicating the contribution of that factor to the modeled response.

Table 2.14: Parameter estimates of derived models for the transformed plastic viscosity response

Coefficients of the transformed Plastic Viscosity response at $\lambda = 0.414141$, $R^2 = 0.954$		
Parameter	Estimate	Pr > |t|
Intercept	48.453	< 0.0001
APT	-18.565	< 0.0001
w/b	-12.101	< 0.0001
HRWRA	-9.301	0.023

Table 2.15: Parameter estimates for the yield stress response

Coefficients of the yield stress response, $R^2 = 0.913$		
Parameter	Estimate	Pr > |t|
Intercept	43.611	< 0.0001
V_{ca}	4.617	0.059
Silica fume	20.397	< 0.0001
VMA*HRWRA	-38.507	0.001
HRWRA	-37.348	< 0.0001

The derived models are summarized as follows:

$$\eta(\mu)(\text{Pa.s}) = 48.453 - 18.565 * \text{APT} - 12.101 * \frac{\text{w}}{\text{b}} - 9.301 * \text{HRWRA}$$

Equation 2.12

$$\tau\ (\text{Pa}) = 43.611 + 4.617 * V_{ca} + 20.397 * \text{SF} - 37.348 * \text{HRWRA} - 38.507 * \text{VMA} * \text{HRWR}A$$

Equation 2.13

The plastic viscosity is mainly affected by the water to binder ratio, the average paste thickness, and the amount of super plasticizers added. An increase in any of these variable has a negative impact on the plastic viscosity. The experimental data showed

that increasing the water to binder ratio from 0.32 to 0.4 resulted in an unexpected increase in the yield stress although HRWRA was added. This was argued to be due to the addition of VMA and HRWRA to mitigate segregation while still achieving the desired flow. As expected, HRWRA is found to be a significant variable and to lower the yield stress significantly. The two-factor interaction, HRWRA*VMA was also found to be significant as postulated from the experimental results. Moreover, the impact of both the coarse aggregates volume and silica fume content on the yield stress are found statistically significant and conforming with previously reported findings.

2.4.8 Models Validation

The yield stress and plastic viscosity models were evaluated using the center point. The measured versus the predicted plastic viscosity and yield stress corresponding to the main 16 SCC data points and the three replicates of the center point are shown in Figures 2.34 and 2.35, respectively. The standard error of the models with 95 % confidence is shown by the solid line. The results indicate that the plastic viscosity has predictions that are within 95 % confidence level as opposed to the yield stress which showed less accuracy. The maximum absolute errors in predicting the plastic viscosity are 2.0 Pa.s, 1.4 Pa.s, and 5.6 Pa.s, and 24. 4 Pa, 9.3 Pa, and 23.0 Pa for the yield stress corresponding to mixes # 17, 17-R1 and 17-R2. These results show that the standard errors are larger than the testing standard errors of 4 Pa.s and 8 Pa for the plastic viscosity and yield stress, respectively.

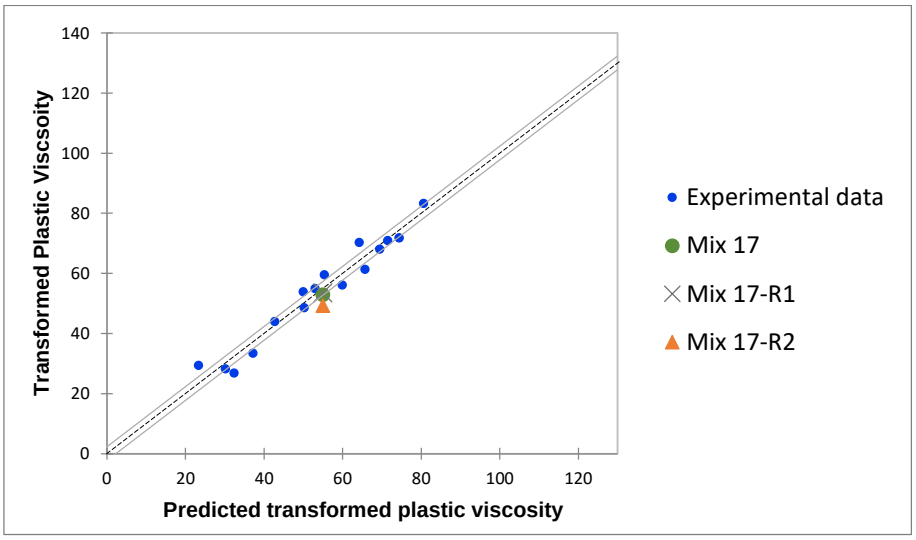

Figure 2.34: Transformed plastic viscosity versus predicted transformed plastic viscosity

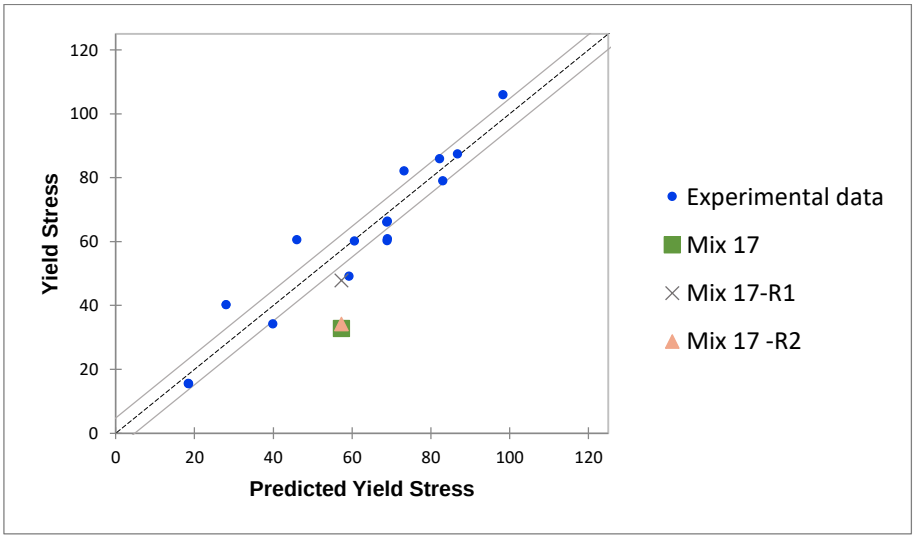

Figure 2.35: Measured yield stress versus predicted yield stress

2.5 Concluding remarks

The following conclusions are drawn from the present study:

1. The thickness of the plug flow depends on the w/b ratio.
2. Revised Modified-Bingham model put forward in this study provides a better estimate of the plastic viscosity, yield stress, and the second order parameter.
3. The average paste thickness (APT) gives a more comprehensive description compared to the individual mixture composition, since it takes into account the

combined aggregate gradation, by incorporating the maximum packing density, as well as the aggregate proportioning.

4. The APT is also shown to be inversely related to the volume of fine aggregates present in the mixture.
5. The HRWRA demand is shown to decreases as the APT increases for mixtures with the same SF and GGBFS levels.
6. For a given range of slump flow, the amount of HRWRA increases when 8 % of the binder content is replaced by silica fume due to its high fineness; whereas decreases when 30 % of the binder content is replaced by GGBFS due to its glassy texture.
7. The addition of GGBFS and SF are shown to increase/ decrease the slump flow respectively.
8. Incorporating both VMA and silica fume in the high w/b ratio mixtures, resulted in slump flow measurements < 600 mm, confirming their negative impact on the slump flow.
9. The w/b ratio, APT and the HRWRA affect the flow time, $T_{50.}$
10. For a given range of APT, the addition of silica fume is shown to increase the mixture's resistance to flow.
11. The flow time, T_{50} corresponding to the high water to binder ratio mixtures are all below the minimum target flow time < 2s, indicating stability concerns.
12. Incorporating silica fume results in decreasing the passing ability for the low w/b ratio mixtures.
13. A good correlation exists among the free flow tests, slump flow, and the confined flow test, L-box for the low w/b mixtures.
14. No signs of segregation in all the high w/b mixtures, indicating VMA's effectiveness in maintaining the mixtures resistance to static segregation. However, their effectiveness under dynamic conditions is questionable.
15. The Slump flow and T_{50} are found to correlate with the yield stress and plastic viscosity, respectively. A higher coefficient of determination between T_{50} and plastic viscosity is observed.

16. Plastic viscosity is found to correlate well with thixotropy. Accordingly, it can be concluded that both are equally influenced by the paste thickness, w/b, and HRWRA.
17. The yield stress is impacted by the silica fume addition and the amount of coarse aggregate (bulk volume of coarse aggregates and the ratio of coarse to fine aggregate ratio (CA/FA) by mass for the low and high w/b mixtures respectively).
18. From the experimental program conducted, a set of rules were derived to relate the mix composition and the chemical admixtures used to achieve a certain range of rheological properties.
19. Anti-thixotropic behaviour is found to be exhibited by the majority of the w/b = 0.4 mixtures. Its intensity increases when APT decreases (increase in both the binder and coarse aggregate contents).
20. Statistical models developed to relate the rheological properties to the mixture design composition revealed that:
    a) Plastic viscosity can be estimated with 95% confidence from w/b, HRWRA, and APT.
    b) Yield stress can be estimated with 95% confidence from volume fraction of the coarse aggregate, Silica Fume content, HRWRA, and VMA.
21. Validation of the models shows that the models are not complete as the standard errors are found larger than the experimentally measured ones.

References

American Concrete Institute. (2007). *ACI 237R-07 (Self-Consolidating Concrete).*

ASTM C1610. (2010). Standard Test Method for Static Segregation of Self-Consolidating Concrete Using Column Technique.

ASTM C1611/C1611M. (2014). Standard Test Method for Slump Flow of Self-Consolidating Concrete.

ASTM C494/C494M (2005). *Standard Specification for Chemical Admixtures for Concrete.*

ASTM C127 (2012). *Standard Test Method for Density, Relative Density (Specific Gravity), and Absorption of Coarse Aggregate.*

ASTM C128 (2012). *Standard Test Method for Density, Relative Density (Specific Gravity), and Absorption of Fine Aggregate.*

ASTM C136 (2006). *Standard Test Method for Sieve Analysis of Fine and Coarse Aggregates.*

ASTM, C. (2006). 260. *Standard Specification for Air-Entraining Admixture for Concrete.*

ASTM C29/C29M (1997). *Standard Test Method for Bulk Density (Unit Weight and Voids in Aggregate.*

Banfill, P. (1994). Rheological methods for assessing the flow properties of mortar and related materials. *Construction and Building Materials*, 43-50.

Banfill, P. F. G. (2006). Rheology of fresh cement and concrete. *Rheology reviews, 2006*, 61.

BASF. (2014). *MasterAir AE 200.*

BASF. (2014). *MasterGlenium 7700.*

BASF. (2014). RHEOMAC *SF* 100 *Densified Silica Fume Admixture.*

BASF. (2014). *MasterMatrix VMA 362.*

Benaicha, M., Roguiez, X., Jalbaud, O., Burtschell, Y., & Alaoui, A. H. (2015). Influence of silica fume and viscosity modifying agent on the mechanical and rheological behavior of self compacting concrete. *Construction and Building Materials, 84*, 103-110.

Billberg, P. (2003). Form pressure generated by self-compacting concrete. In *Proceedings of the 3rd international RILEM symposium on self-compacting concrete, RILEM PRO33 Reykjavik, Iceland* (pp. 271-280).

Boukendakdji, O., Kenai, S., Kadri, E. H., & Rouis, F. (2009). Effect of slag on the rheology of fresh self-compacted concrete. *Construction and Building Materials*, *23*(7), 2593-2598.

Box, G. E., & Cox, D. R. (1964). An analysis of transformations. *Journal of the Royal Statistical Society. Series B (Methodological)*, 211-252.

Box, G. E. P, Hunter, JS, and Hunter, WG 2005. Statistics for Experimenters: Design, Innovation, and Discovery.

Chidiac, S., Maadani, O., Razaqpur, A., & Mailvaganam, N. (2000). *Controlling the quality of fresh concrete-a new approach.* National Research Council.

Chidiac, S. E., & Mahmoodzadeh, F. (2009). Plastic viscosity of fresh concrete–A critical review of predictions methods. *Cement and Concrete Composites*, *31*(8), 535-544.

Chidiac, S. E., Moutassem, F., & Mahmoodzadeh, F. (2013). Compressive strength model for concrete. *Magazine of Concrete Research*, *65*(9), 557-572.

CSA A23.2. (2009). *Test methods and standard practices for concrete*

De Larrard, F., Ferraris, C. F., & Sedran, T. (1998). Fresh concrete: a Herschel-Bulkley material. *Materials and structures*, *31*(7), 494-498.

Dunn, K. (2010). Process Improvement Using Data. *online], http://learnche. org/pid*.

El Barrak, M., Mouret, M., & Bascoul, A. (2009). Self-compacting concrete paste constituents: hierarchical classification of their influence on flow properties of the paste. *Cement and Concrete Composites*, *31*(1), 12-21.

Erdem, T. K., Khayat, K. H., & Yahia, A. (2009). Correlating rheology of self-consolidating concrete to corresponding concrete-equivalent mortar. *ACI Materials Journal*, *106*(2), 154.

Estellé, P., Lanos, C., Perrot, A., & Amziane, S. (2008). Processing the vane shear flow data from Couette analogy. *Applied Rheology*, *18*(3), 34037.

Faroug, F., Szwabowski, J., & Wild, S. (1999). Influence of superplasticizers on workability of concrete. *Journal of materials in civil engineering*, 11(2), 151-157.

Feys, D., Verhoeven, R., & De Schutter, G. (2007). Evaluation of time independent rheological models applicable to fresh self-compacting concrete. *Applied rheology*, *17*(5), 56244-57190.

Flatt, R. J., Houst, Y. F., Bowen, P., Hofmann, H., Widmer, J., & Sulser, U. (2000). Electrosteric Repulsion Induced By Superplasticizers between Cement Particles-An Overlooked Mechanism?. *ACI SPECIAL PUBLICATIONS*, *195*, 29-42.

Ghezal, A., & Khayat, K. H. (2002). Optimizing self-consolidating concrete with limestone filler by using statistical factorial design methods. *Materials Journal*, *99*(3), 264-272.

Ghoddousi, P., Javid, A. A. S., & Sobhani, J. (2014). Effects of particle packing density on the stability and rheology of self-consolidating concrete containing mineral admixtures. *Construction and Building Materials*, *53*, 102-109.

Kennedy, C. T. (1940). The design of concrete mixes. In *Journal Proceedings* (Vol. 36, No. 2, pp. 373-400).

Khayat, K. H., Ghezal, A., & Hadriche, M. S. (1999). Factorial design model for proportioning self-consolidating concrete. *Materials and Structures*, *32*(9), 679-686.

Khayat, K., Assaad, J., Mesbah, H., & Lessard, M. (2005). Effect of section width and casting rate on variations of formwork pressure of self-consolidating concrete. *Materials and structures*, *38*(1), 73-78.

Khayat, K. H., Bickley, J., & Lessard, M. (2000). Performance of self-consolidating concrete for casting basement and foundation walls. *Materials Journal*, *97*(3), 374-380.

Koehler, E.P., Fowler, D.W. (2007). "ICAR Mixture Proportioning Procedure for SCC" International Center for Aggregates Research, Austin, TX.

Li, L. G., & Kwan, A. K. (2013). Concrete mix design based on water film thickness and paste film thickness. *Cement and Concrete Composites*, *39*, 33-42.

Mebrouki, A., Bendani, K., Bouhamou, N., & Belas, N. (2014). Excess paste method to formulate a self-compacting concrete. *Journal of Building Materials and Structures*, *1*(1), 23-29.

Mewis, J. (1979). Thixotropy-a general review. *Journal of Non-Newtonian Fluid Mechanics*, *6*(1), 1-20.

Nagamoto, N., & Ozawa, K. (1999). Mixture properties of self-compacting, high-performance concrete. *Special Publication*, *172*, 623-636.

Nanthagopalan, P., & Santhanam, M. (2012). An empirical approach for the optimisation of aggregate combinations for self-compacting concrete. *Materials and structures*, *45*(8), 1167-1179.

Nehdi, M., & Rahman, M. A. (2004). Effect of geometry and surface friction of test accessory on oscillatory rheological properties of cement pastes. *Materials Journal*, *101*(5), 416-424.

Nielsson, I., & Wallevik, O. H. (2003). Rheological evaluation of some empirical test methods–preliminary results. In *Third international RILEM symposium, RILEM Pub. PRO* (Vol. 33, pp. 59-68).

Ovarlez, G., & Roussel, N. (2006). A physical model for the prediction of lateral stress exerted by self-compacting concrete on formwork. *Materials and Structures*, *39*(2), 269-279.

Petkova, V., & Samichkov, V. (2007). Some influences on the thixotropy of composite slag Portland cement suspensions with secondary industrial waste. *Construction and Building Materials*, *21*(7), 1520-1527.

Phan, T. H., Chaouche, M., & Moranville, M. (2006). Influence of organic admixtures on the rheological behaviour of cement pastes. *Cement and Concrete Research*, *36*(10), 1807-1813.

Shi, Y., Matsui, I., & Feng, N. (2002). Effect of compound mineral powders on workability and rheological property of HPC. *Cement and Concrete Research*, *32*(1), 71-78.

Smeplass, S. (1994). Applicability of the Bingham model to high strength concrete. In *RILEM PROCEEDINGS* (pp. 145-145). CHAPMAN & HALL.

Tattersall, G. H. (2003). *Workability and quality control of concrete*. CRC Press.

Uchikawa, H., Hanehara, S., & Sawaki, D. (1997). The role of steric repulsive force in the dispersion of cement particles in fresh paste prepared with organic admixture. *Cement and Concrete Research*, *27*(1), 37-50.

Ur'ev, N. B., Baru, R. L., Izhik, A. P., Choi, S. V., & Saskovets, V. V. (1997). Rheology and thixotropy of cement-water suspensions in the presence of superplasticizers. *Colloid journal of the Russian Academy of Sciences*, *59*(6), 773-779.

Wallevik, J. E. (2003). *Rheology of particle suspensions: fresh concrete, mortar and cement paste with various types of lignosulfonates*. Fakultet for ingeniørvitenskap og teknologi.

Wong, H. H. C., & Kwan, A. K. H. (2008). Packing density of cementitious materials: measurement and modelling. *Magazine of Concrete Research*.

APPENDIX A- Flow Curves and Breakdown/Buildup Area

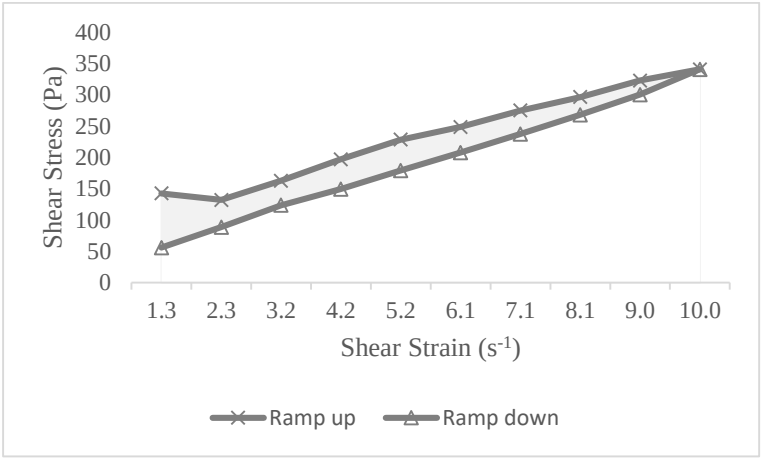

Figure B.1: Flow curve for mix #1

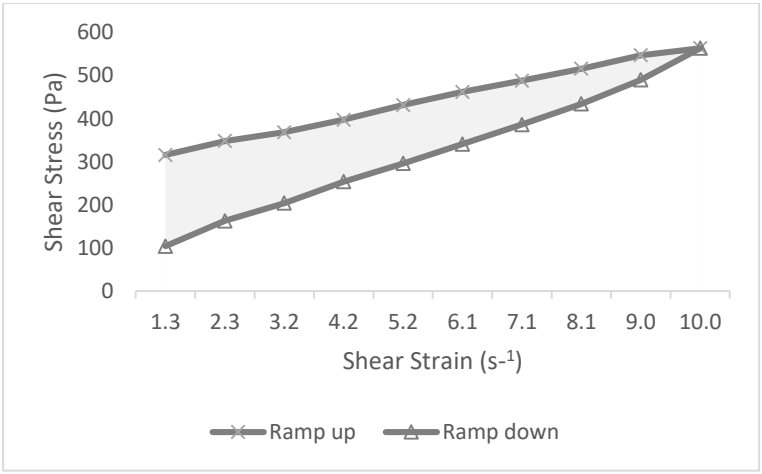

Figure B.2: Flow curve for mix #2

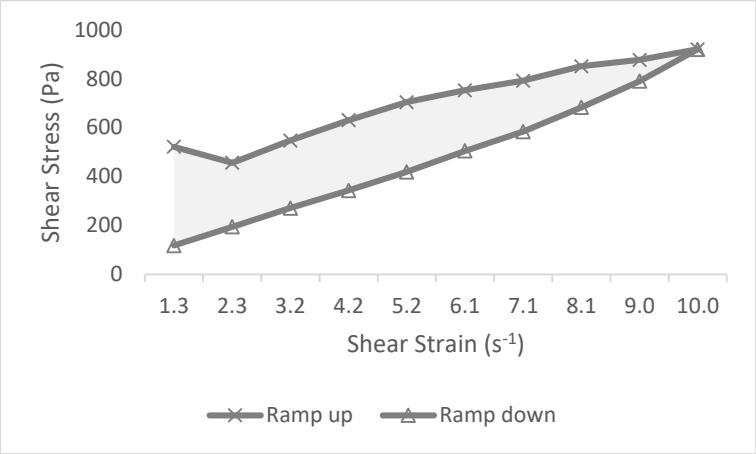

Figure B.3: Flow curve for mix #3

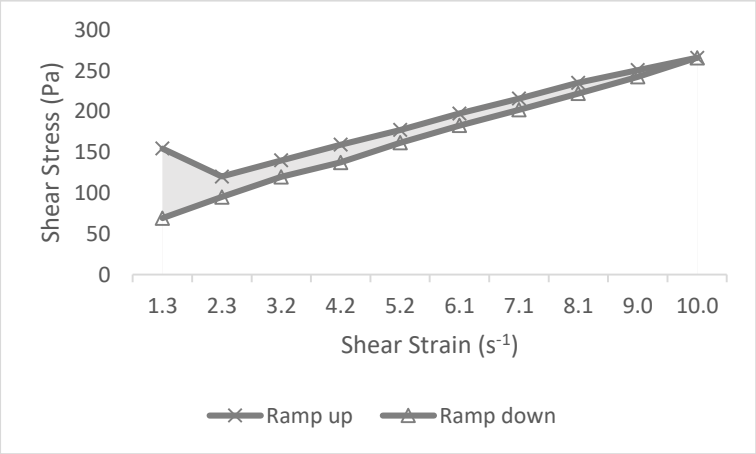

Figure B.4: Flow curve for mix #4

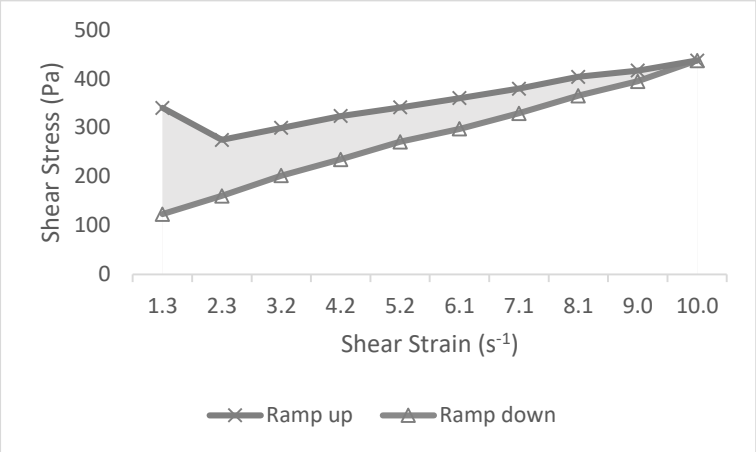

Figure B.5: Flow curve for mix #5

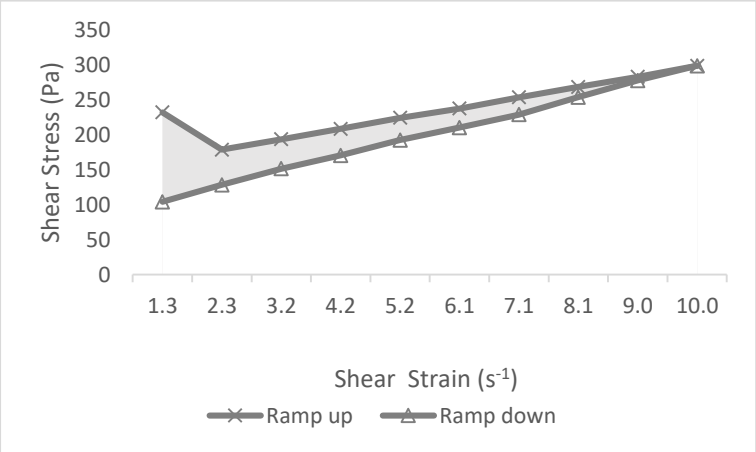

Figure B.6: Flow curve for mix #6

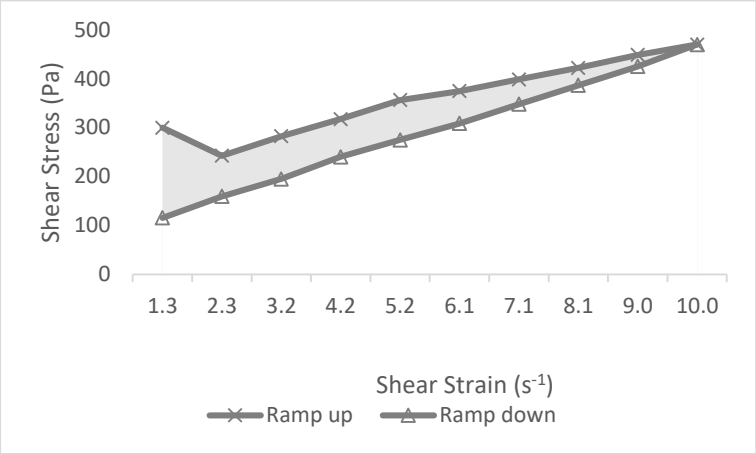

Figure B.7: Flow curve for mix #7

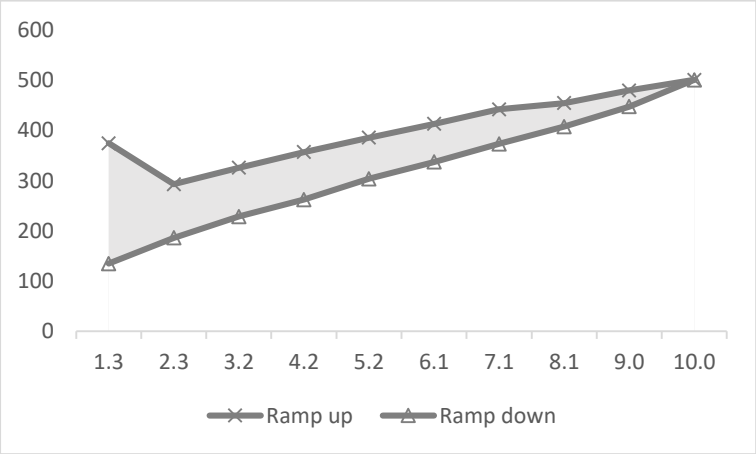

Figure B.8: Flow curve for mix #8

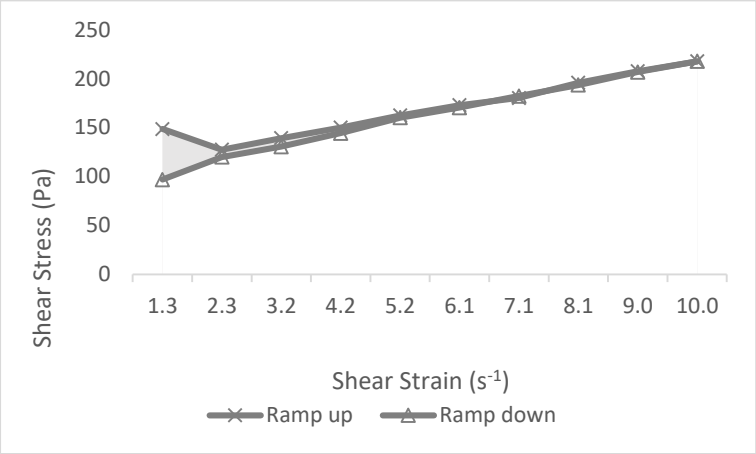

Figure B.9: Flow curve for mix #9

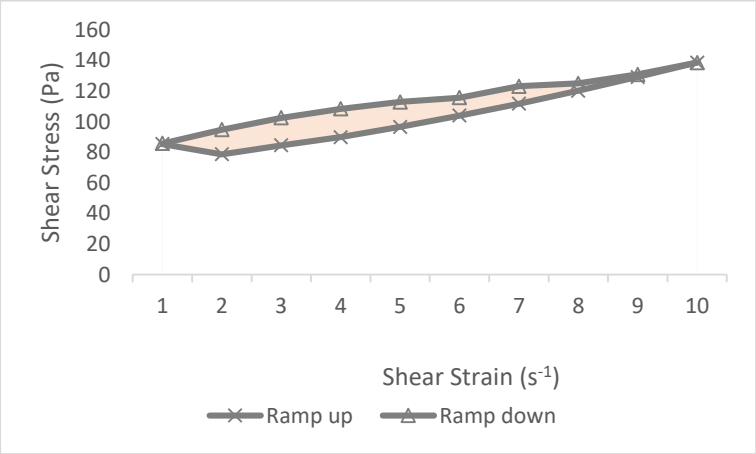

Figure B.10: Flow curve for mix #10

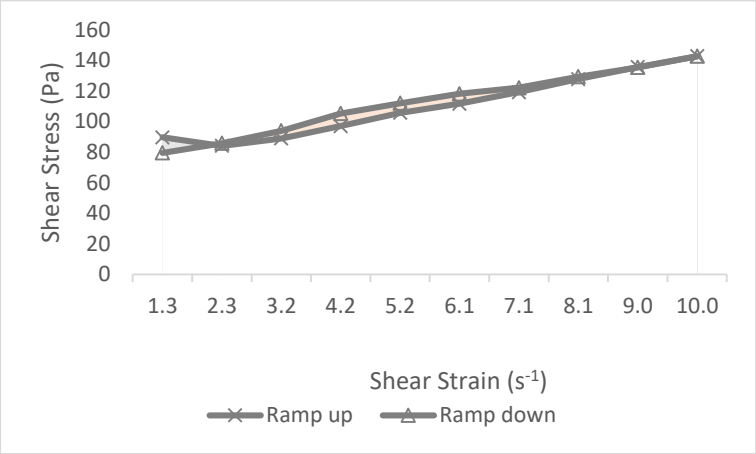

Figure B.11: Flow curve for mix #11

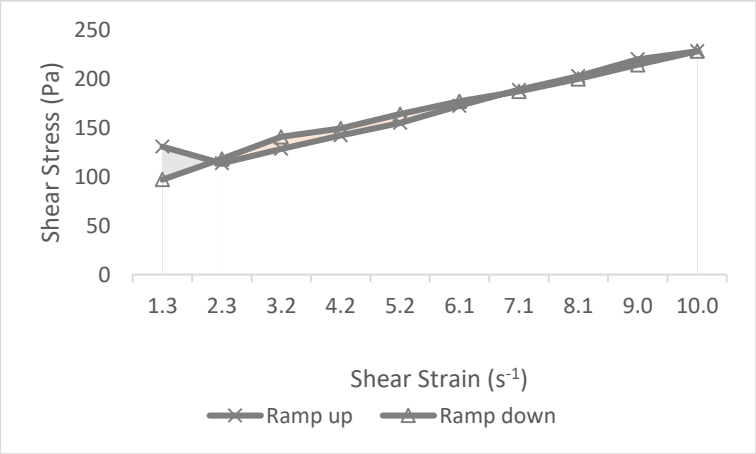

Figure B.12: Flow curve for mix #12

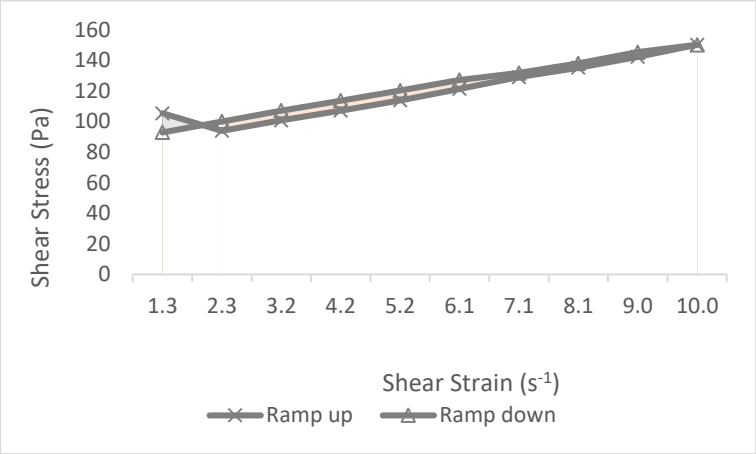

Figure B.13: Flow curve for mix #13

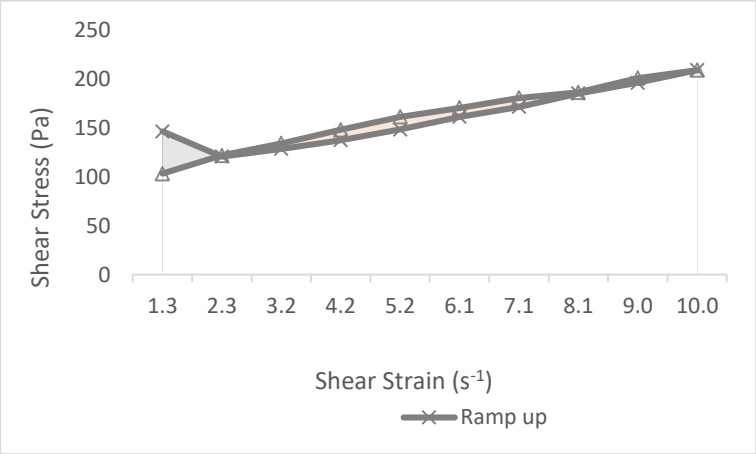

Figure B.14: Flow curve for mix #14

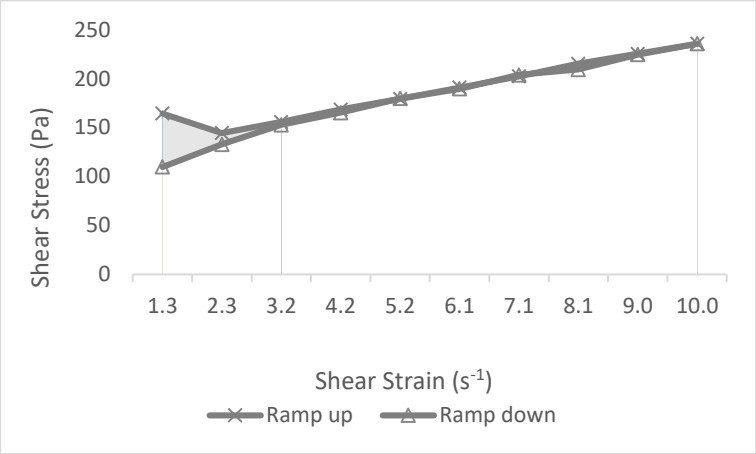

Figure B.15: Flow curve for mix #15

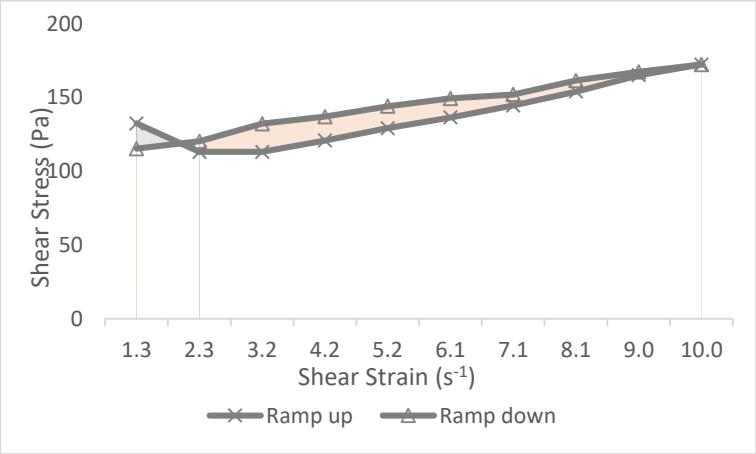

Figure B.16: Flow curve for mix #16

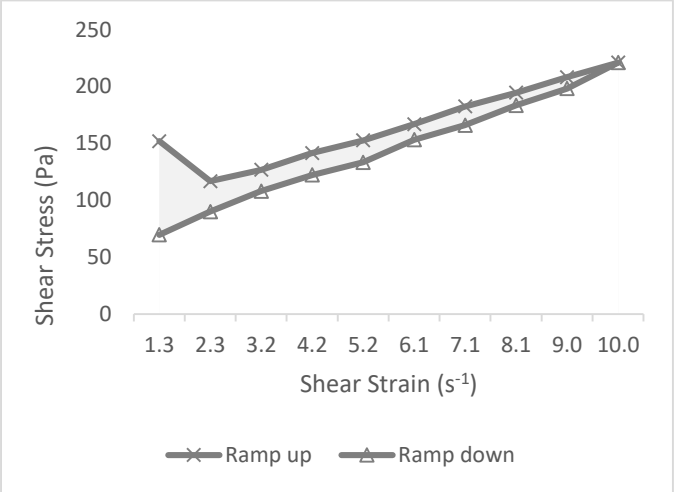

Figure B.17: Flow curve for mix #17